DESIGN, SIMULATION, AND STABILITY OF A HEXAPEDAL RUNNING ROBOT

A DISSERTATION
SUBMITTED TO THE DEPARTMENT OF MECHANICAL ENGINEERING
AND THE COMMITTEE ON GRADUATE STUDIES
OF STANFORD UNIVERSITY
IN PARTIAL FULFILLMENT OF THE REQUIREMENTS
FOR THE DEGREE OF
DOCTOR OF PHILOSOPHY

Jonathan E. Clark
August 2004

© Copyright by Jonathan E. Clark 2004
All Rights Reserved

I certify that I have read this dissertation and that, in my opinion, it is fully adequate in scope and quality as a dissertation for the degree of Doctor of Philosophy.

Mark R. Cutkosky
(Principal Adviser)

I certify that I have read this dissertation and that, in my opinion, it is fully adequate in scope and quality as a dissertation for the degree of Doctor of Philosophy.

Scott L. Delp

I certify that I have read this dissertation and that, in my opinion, it is fully adequate in scope and quality as a dissertation for the degree of Doctor of Philosophy.

Kenneth J. Waldron

Approved for the University Committee on Graduate Studies.

Abstract

Animals are the current gold standard of locomotion ability. Their ability to navigate rough terrain is unmatched by their man-made counterparts. Recent studies by biologists have begun to demonstrate some of the principles behind their remarkable capabilities. In particular, studies of cockroaches have shown that they use a feed-forward motor actuation pattern that is virtually unchanged, even when running over very rough terrain. It appears that their considerable structural compliance contributes significantly to their stability when running. Their sprawled posture and tuned impedance in their musculoskeletal system enable an instantaneous or preflex response to disturbances. This allows for rapid response to the large perturbations experienced when interacting with irregular terrain.

Consideration of these principles has led to the design of the *Sprawl* family of robots, which features one active thruster and one entirely passive rotary joint on each leg. Without these spring elements the robots would not be able to run. With them, they can easily overcome hip-height obstacles without any alteration of their open-loop controller. The robots function as tuned oscillating systems and small changes in their physical parameters (e.g. leg stiffness and damping) can produce large changes in their speed and stability.

Simple conceptual models of hopping have been used to analyze the effects of modifying the open-loop control system on system performance. These simple one-legged models have proven effective in helping to tune the actuation dynamics of the robot, but their simplicity precludes their use in tuning the sprawled self-stabilizing posture of the robot.

This thesis describes the development, calibration, and analysis of a three-dimensional

dynamic simulation of the *Sprawl* robots. This simulation was developed as a design tool to investigate the effects of parameter variation, and to gain understanding about how to tune the leg configuration and hip impedance which constitute the self-stabilizing posture of the robot.

The simulation is used to characterize the sensitivity of the system's performance to changes in the robots' physical parameters. The key parameters that influence speed and stability are identified, and their effects and the nature of their coupling are investigated. In particular, the coupling between actuation and environmental parameters is evaluated. The simulation results suggest that for changing slopes and surface friction altering the leg configuration and (to a lesser degree) the actuation frequency of the robot may dramatically increase performance.

While speed is easy to measure, no universal metric for running stability exists. This thesis discusses four distinct steady-state measures of stability that are applicable to a simulated running robot. The effect of modifying the posture of the robot on stability is investigated for each of these measures. These results delineate the nature of the trade off between speed and stability, and indicate advantageous design points to maximize both.

As a demonstration of its utility as a design tool, the simulation is used to tune the performance of one of the *Sprawl* robots. The mass distribution, hip impedance, and leg postures of the model are adjusted to improve speed while preserving stability. The resulting design was implemented on the physical robot. The simulation-based design was compared to the empirically tuned robot settings and the modified design resulted in a two-fold increase of the robot's speed.

Dedicated to ...

Contents

List of Tables

List of Figures

Chapter 1

Introduction

For most of the history of the world legs have been mankind's primary means of transportation. While wheels have been incredibly useful in innumerable tasks, it is only with the advent of the steam engine that self-powered wheeled vehicles came into their own. Up until that time terrestrial locomotion was legged locomotion. And legged locomotion meant a muscle based power source. We walked, we rode horses, we pulled wagons, but we always used legs.

With the advent of the railway and the automobile the mechanical engineer came into his own. Thousands of miles of track were laid, and later millions of miles of roads were paved. The automobile has so permeated our culture that 'walking' and 'running' are considered recreational pastimes!

Nevertheless there are a lot of places that cars can not go. Consequently researchers have, despite the difficulties, attempted to create artificial or robotic walkers and runners. Over the past quarter century substantial progress has been made in robotics in general. Many of these advances have carried over to legged locomotion, but some inherent properties of legged motion have limited the successes in utilizing the traditional position and force base control techniques used in other areas of robotics.

The purpose of this thesis is to put forward the design, simulation, and analysis of a class of biologically inspired running robots. This analysis argues that the ease of design and control, as well as the performance of running robots can be dramatically

improved with an appropriately designed self-stabilizing structure. While the robots described in this thesis do not yet qualify as the "greatest thing since the wheel" for the field of locomotion, I believe that the principles examined represent one step toward making a viable artificial running machine.

1.1 Motivation

There are a number of advantages inherent to legged systems, the foremost of which is their flexibility in dealing with rough terrain. They can step over pits or obstacles, they can turn rapidly, and they lend themselves to climbing, swimming, burrowing, and a host of other activities. These are all activities that we humans and many other animals do relatively effortlessly. The challenge now for roboticists is to create machines that duplicate the mobility and agility of living creatures.

A large percentage of earth's surface is unavailable to wheeled vehicles. Much of this area is, perhaps consequently, unpopulated. Nevertheless there are often compelling reasons to send autonomous vehicles into these areas. Volcanos, surf zones, densely wooded areas, caves, and mountainous regions are all possibly off-limits to a wheeled or tracked vehicle. Nevertheless for exploration purposes it would be ideal to have a class of vehicle that did not need (or make) its own road. One example of an early commercial interests is in the logging industry where a legged harvester is being developed by Plustech, a John Deere company.

In addition to wilderness areas, there are environments made hostile due to man-made effects such as mine fields and urban disaster sites. In these situations, sending in humans is dangerous, yet their locomotive flexibility is required. One can also imagine a number of scenarios involving surveillance, security, or planetary exploration where having a vehicle with animal like invariance to terrain would be ideal.

1.2 Challenges

To solve the problem of getting from here to there (locomotion), engineering and technology have favored solutions such as the wheel that have radically departed

from biological examples. In doing so they have exploited the strengths of their discipline including the ability to produce accurate, repeatable, uniform geometric parts, smooth bearing surfaces, and rotary actuators.

Creating effective legged robots, however, requires moving more directly into the domain of motion that is favored by animals. Some inherent difficulties with legged systems include: intermittent contact with the ground, interaction with an unknown environment, unexpected environmental disturbances, and more complicated mechanical dynamics. Relative to these demands, most mechanical attempts to created legged robots have resulted in slow, fragile, or unstable systems.

Animals mitigate these difficulties in a number of ways including: a sophisticated vision system for obstacle detection, a vestibular system to sense balance, a central controller or brain to perform path planning, a distributed reflex system to regulate gaits, and passive compliance in the legs to help in stabilization.

Researchers have worked for years to create artificial vision systems, inertial sensors, and controllers for planning and gait generation. Determining the role of passive compliance in augmenting stability has, however, been comparatively underdeveloped. This thesis argues that by understanding and utilizing the way in which animals use the passive compliance and energy dissipation in their leg structures the overall task of achieving fast and stable running can be greatly simplified.

1.3 Contributions

The main contribution of this thesis is to characterize under what conditions an appropriately tuned passive physical system can allow legged robots to run over rough terrain with purely open loop control. The development and analysis of the *Sprawl* family of robots demonstrates that a proper mechanical structure is not only necessary, but can in fact be sufficient for robust outdoor locomotion.

The construction and use of a detailed dynamic simulation of the robot has allowed the passive dynamic stabilizing properties of the legs or "preflexes" [18] to be tuned to double the robots speed. For robust operation however, stability as well as speed needs to be improved. Characterizing stability over rough terrain is a difficult task, and

there is currently no universal metric for measuring it in such situations. Consequently in this thesis a number of measures for gauging the impact of design changes on stability are put forward and compared.

Specific contributions of this thesis include:

- Design and construction of the first monolithic multi-material compliant SDM legs for the *Sprawl* robots.
- Development and calibration of a three-dimensional multi-body dynamic simulation of the *Sprawl* family of robots, and demonstration that the simulation can be used to dramatically improve the design.
- Characterization of the parameter space for self-stabilizing leg posture.
- Evidence that a sprawled for-aft leg posture and differential leg use, increase the range of fast and stable operation.
- Demonstration of how increasing hip impedance increases stability and characterization of its effect on the velocity of the robot.
- First direct comparison of the effect of varying robot parameters for multiple stability measures (including perturbation response rate and a dynamic stability margin) on a running robot.

1.4 Thesis Overview

Chapter 2 gives an overview of previous work in walking and running robots. Special attention is paid to the approaches taken to measure and generate stable gaits. The concept of stability margins for walking robots is discussed, as is return-map analysis for simplified hopping and walking systems. The context for the present work is given in terms of the most recent developments in building and controlling running robots.

Chapter 3 describes the design of the *Sprawl* family of running robots developed and analyzed in this thesis. The biological findings that motivated their construction are reviewed, and the manufacturing process that enabled the construction of the

multi-material complaint legs is briefly summarized. The chapter concludes with a discussion of initial results from a parameter variation design of experiments, which indicate the relative importance of actuation and stance parameters on performance, and how strongly these parameters are coupled.

Chapter 4 describes the construction and calibration of a three dimensional dynamic simulation of the robot used to evaluate design changes. The model was designed to be as simple as possible while maintaining sufficient fidelity to the robots for predictive purposes. The experimental tests used to characterize the model components are described as are comparisons between the behavior of the robot and model.

Chapter 5 describes how the simulation was used to investigate the parameter space and tune the performance of the robot. The robot's energetics and sensitivity to parameter variation are described, as are the effect of varying environmental parameters on speed and efficiency. Critical leg parameters and couplings are identified. The chapter concludes with a description of how the simulation was used to redesign the robot's legs, doubling the robot's speed.

Chapter 6 investigates the shape of the parameter space that results in self-stabilizing running, and how changing these parameters affects the robot's performance. Four distinct measures for running 'stability' over rough terrain are presented. The effects of changing the leg posture and hip impedance on each of these criteria are compared.

Chapter 7 gives some conclusions and suggestions for future work.

Chapter 2

Previous Work

This chapter gives an overview of some of the previous research on legged robots, with an emphasis on the efforts that have led toward fast, stable locomotion, especially over rough terrain. The first section describes some significant walking robots and the designs and controllers they have used to achieved motion. Difficulties with rough terrain have led to a number of approaches to generating and coordinating leg trajectories. Robots have implemented a variety of strategies, from centralized force-control algorithms to decentralized, reflexive controllers to rule-based and adaptive controllers. The overview of walking robots concludes with a discussion of the measures or "margins" that have been developed to quantify stability, and to help avoid configurations and motions that would lead to falls.

The next section discusses dynamic and running systems, including simple hopping robots and passive dynamic bipeds. These simple systems are designed so that their inherent dynamics can be utilized to help stabilize themselves or to develop energetically efficient controllers. Additionally, these simple systems allow for the use of reasonably simple and tractable models to guide their design and analyze their stability. Included is a very brief overview of the return-map stability analysis technique used on these systems.

The concluding section looks at multi-legged running systems, most of which have been developed concurrently with the research described in this thesis. These fast and stable runners have come the closest to achieving performance levels necessary

for practical application in areas such as de-mining, planetary exploration, forestry, surveillance, and search and rescue.

Since these robots are generally too complex to allow an analytic analysis of their dynamics and stability, a number of approaches have been used to achieve stable locomotion. These methods are discussed, giving context to the approach described in this thesis.

2.1 Walking Robots

2.1.1 Early Walkers

In the days before microprocessors were powerful enough to implement sophisticated control systems, a number of techniques were used to stabilize walking machines. These techniques relied on human feedback, clever mechanical design, or simple feed-forward trajectories. The principles embodied in these machines are of particular interest due to their renaissance (in modified form) in some of the most recent and successful running robots.

Teleoperation

An ingenuous approach to controlling a walking machine was taken by the *GE Electric Walking Truck* built in 1967 [75]. It used human teleoperation to control and stabilize itself. Built to extend the functional reach and power of a human, it was, in effect, a quadrupedal mechanical exoskeleton. While the *Walking Truck* was functional, researches quickly found that coordinating and controlling so many degrees of freedom was a difficult and demanding task which quickly exhausted the operator. Although GE abandoned the project, it did demonstrate impressive performance by leveraging properties of the human body.

Simple Trajectories

In the 1970s and early 1980s, the level of computational power available was insufficient to implement intricate behaviors on complex geometries. Consequently, the first

generation of computer controlled walking machines including the *Phoney Pony* and the *OSU Hexapod* had two and three degrees of freedom per leg and were able to follow only very simple, pre-programmed trajectories [89]. These simple motions were sufficient to generate forward movement, but the rigid legs fared poorly on rough terrain. The proliferation of walking toys and 'robotic hobby kits' based on these principles, demonstrates the success of this approach and its limitation to smooth surfaces and slow speeds.

Beam Walkers

A less biological, but simpler approach to building stable legged robots was taken by *Ambler* [62] and the *Walking Beam* [26]. Structurally, both of these machines moved like two nested tables where one set of legs could translate while the other was in contact with the ground. Thus one set of legs could support the body, while the retracted set could be positioned for the next step. Designed to go to Mars, their size and wight proved to be prohibitive. A smaller version of a frame walker, *Dante II*, did succeed in climbing into a volcanic crater on Mt. Spurr in 1994 [10]. Its fragility, however, proved to be its undoing as it had to be pulled out with its tether after breaking on the rough terrain.

Despite their limitations, these robots could handle some pretty rough terrain. Though these robot designs are now outdated, some of the principles they embodied, such as the use of simple trajectories and alternating tripod gaits have been recently revisited by a number of running robots.

2.1.2 Centralized Controller

As computational power and the sophistication of controllers increased during the 1980s, so did the complexity of the structures they were asked to direct. One excellent example of a sophisticated walker is the *Adaptive Suspension Vehicle* (ASV) [97], which had six legs each with three degrees of freedom. It was powered by a motorcycle engine and was able to carry its operator.

The ASV was able to walk outdoors, up and down shallow slopes and even over

railroad ties. It used a variety of techniques including a primitive vision system and a 'follow the leader' gait to implement obstacle avoidance behaviors [74]. Drawbacks to the ASV included its noise, rough ride, extreme cost, and complex control requirements.

The clever use of a pantograph mechanism in the leg decoupled the control of the leg degrees of freedom. This deviation from a biological leg design allowed the height, extension, and rotation of the leg to be independently controlled, greatly simplifying the control problem. The computational burden was further reduced by the implementation of a control scheme based on "zero foot interaction forces" [102]. Despite using these techniques the control of the ASV remained a computationally intensive task.

2.1.3 Gait Generation Via Distributed Control

The experience with the ASV and other robots with complex structures and many degrees of freedom in the legs, demonstrated the difficulty in developing robust control systems to coordinate multi-leg motions.

Brooks and his students at MIT have argued that implementing a distributed control system is the answer, and supported this claim by building a series of small robots including *Attila* [5], *Gengis* [6], and *Boadecia* [14].

As a source of inspiration for designing distributed control systems, Brooks and other researchers have turned to biology. Due to their relatively simple physiology, investigation into insect locomotion, particularly the stick insect, has been very fruitful in developing simple, distributed controllers which generate natural gaits. Cruse in particular has identified a number of low-level reflexes that work together to coordinate the timing of the thrust and retraction of insects legs [28].

Some examples of robots that have used these principles include *CWRU robot I* [31] and *II* [30], and the *TUM Robot* [81]. These small (0.3 to 0.6 m long) hexapedal robots are capable of slowly walking over rough terrain and even a slotted surface. They use foot contact sensors and simple microprocessors to implement their reflex coordination and foot placement algorithms.

Despite these advances, the generation of smooth and natural walking motions has still proven difficult to achieve through discrete rules. Several researches have attempted to mimic nature or the brain in a more centralized manner. One approach, attempted with the hexapod *Lauron*, was to implement a motion controller based on neural networks [12], another approach attempted by Galagher was to use genetic algorithms to evolve the controllers [38].

Most recently Klaasen *et al.* have used "Basic Motion Patterns" derived from reflexes and neural networks to generate gaits for their octapedal robot *Scorpion*. They found that its walking patterns were comparable to those found in real scorpions [56]. In a similar vein, the robot *Tekken* has augmented a central pattern generator (CPG) and reflex based controller with legs equipped with virtual spring-dampers designed to mimic the viscoelastic properties of muscle. This autonomous quadruped can walk over terrains with "medium degrees of irregularity" [32].

The generation of smooth and stable walking trajectories has developed gradually over time. The use of biological principles in the design of the robots and controllers has helped considerably. We are just now beginning to be able to create fluid walking gaits over rough terrain. In addition to being smooth, these gaits need to guarantee stability. To aid in this a number of stability measures or "margins" have been developed over the years.

2.1.4 Static Stability Margins

Slow moving or quasi-static robots are stable as long as the ground projection of the center of mass (GCOM) of the robot lies within the polygon of support defined by the stance legs. A measure of stability called "Static Stability Margin" (SSM) has been defined by McGhee [66] to be the minimum distance from the GCOM to an edge of the support polygon. This is shown schematically on figure 2.1.a.

A variant of SSM, the "Longitudinal Stability Margin" (LSM) is given by the distance along the ground in the sagittal plane from projections of the center of mass to the front edge of the support polygon [106].

These stability margins, however, do not account for slopes or other irregularities

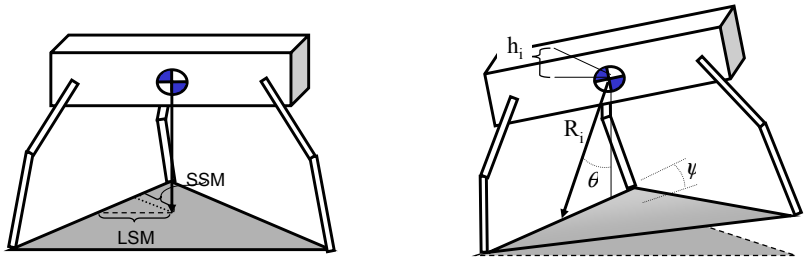

Static Stability Margin (SSM) Energy Stability Margin (ESM)

Figure 2.1: Static Stability Margin (SSM) and Energy Stability Margin (ESM) Illustrated. The polygon of support is depicted as a gray triangle. The SSM is the distance from the ground projection of the center of mass of the robot to the nearest edge of the support polygon. The LSM is the sagittal projection of the SSM. The ESM indicates the amount of potential energy (proportional to h_i) that needs to be overcome before tipping occurs. Thus slope and body height are explicitly considered.

of terrain or the height of the center of mass of the robot. An improved and more practical measure called the "Energy Stability Measure" (ESM) was proposed by Messuri [71], and is shown schematically in figure 2.1b. The ESM measures how much potential energy needs to be overcome before the robot tips. Essentially, this measures how much the center of mass must rise during tipping before it exits the support polygon. Mathematically this is given by:

$$S_{ESM} = min_i^{ls} \left(mgh_i\right) \quad where\ h_i = R_i \left(1 - cos\theta_i\right) cos\psi_i \tag{2.1}$$

Where m is the mass of the robot, g is the gravitational constant and h_i is the height the center of mass can rise before the robot tips along the i^{th} edge of the support polygon. R is the distance between the COM and the i^{th} edge of the support polygon, and θ is the angle between R_i and the gravity vector. ψ_i indicates inclination of the i^{th} edge of the support polygon with respect to its projection onto the plane normal to the gravity vector.

A version of this measure (scaled by mg), called the "Normalized Energy Stability Margin" (NESM) [46] was successfully implemented by Hirose on *Titan VII* [47]. This robot utilized a controller that modified its stance posture to maximize the NESM

and was able to negotiate slopes of up to 30 degrees.

2.1.5 Dynamic Stability Margins

The static stability margins described in section 2.1.4 are only valid for robots traveling very slowly, typically using a wave or crawl gait. To incorporate the effect of the dynamics on the stability of robots moving at more than 'quasi-static' speeds, a number of alternative stability margins have been proposed.

Center of Pressure

By tracking the distance from the instantaneous center of pressure (COP) instead of the GCOM of a robot, a more accurate stability margin can be generated. The COP is the location of the resultant ground reaction force in the contact plane, (as shown in figure 2.2) and can be expressed mathematically as:

$$\vec{OP} = \frac{\sum_{i=1}^{n} q_i f_{ni}}{\sum_{i=1}^{n} f_{ni}} \tag{2.2}$$

Where OP is the position vector from the origin to the COP, f_{ni} is the normal component of the ground reaction force at the i^{th} foot, and q_i is the position vector from the origin of the coordinate system to the point of contact of the i^{th} foot. The distance from the nearest edge of the polygon of support to the COP has been termed both the "Dynamic Stability Margin" [79], and the "Effective Mass Center" [54] as it takes into account some of the dynamics of the mechanism as well as its kinematics.

Comparison

Over the years a number of other stability margins have been proposed. Only recently has a study been undertaken by Garcia to analyze the relative merits of these definitions [39]. She compared six different margins for six cases of a simulated quadruped walking in various conditions and found that each measure can give a different instant of maximum stability depending on the test condition; no single criterion gives the optimal or most reliable results for all of the test conditions. Nevertheless this

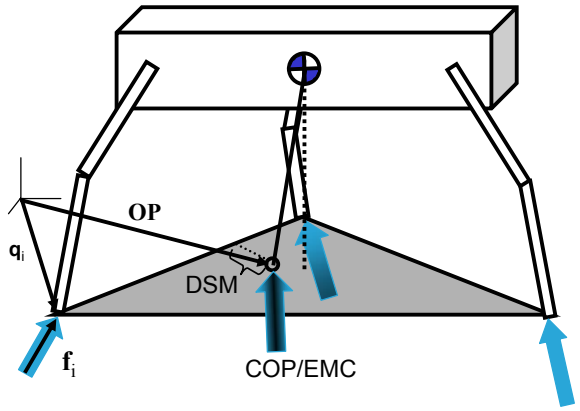

Figure 2.2: The dynamic stability measure is the distance from the center of pressure (COP) or "Effective Mass Center" (EMC) to the nearest edge of the support polygon (shown in gray).

investigation was the first to shed some light on differences between these measures. One shortcoming of this study for the present work was that all of the tests only considered four-legged walking gaits.

2.1.6 Bipedal Walking Stability

All of the walkers discussed thus far have been multi-legged, which allows gaits with relatively large stability margins. While this eases the stability problem, people have continued to pursue the dream of an anthropomorphic robot. In fact, the increased difficulty of getting a two legged machine to walk has spurred the development of more sophisticated and sensitive controllers.

In 1970 Vukobratovic proposed using what he called the "Zero Moment Point" (ZMP) to help stabilize a biped [101]. Schematically the location of the ZMP with respect to an arbitrary origin is shown in figure 2.3. Mathematically the ZMP is defined as:

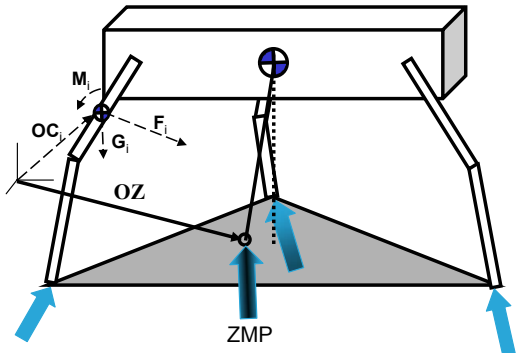

OZ = position vector from the origin to the ZMP
OCi = direction vector from the origin to the mass center of the i-th link
M_i = moment of the inertial force of the i-th link about its mass center
F_i = inertial force of the i-th link about its mass center
G_i = gravitational force of the i-th link about its mass center

Figure 2.3: The Zero Moment Point is the point in the support plane where the resultant inertial force must act so that the magnitude of the out-of-plane resultant moments are zero. If the robot is not tipping, then this is the same point as the center of pressure.

$$\left(\mathbf{OZ} \times \sum_{i=1}^{n} (F_i + G_i)\right)_h = \left(\sum_{i=1}^{n} \mathbf{OC}_i \times (F_i + G_i) + \sum_{i=1}^{n} M_i\right)_h \tag{2.3}$$

Where **OZ** is the position vector from the origin to the ZMP and $\mathbf{OC}_i$ is the position vector from the origin to the mass center of the i^{th} link. M_i is the moment of the inertial force, F_i is the inertial force, and G_i is the gravitational force. Each of these is computed about the corresponding mass center for each link.

As long as the ZMP is within the polygon of support then it is coincident with the COP. The difference is that the ZMP is computed from the link accelerations rather than the ground reaction forces (GRF). This allows the use of centeralized proprioceptive sensors to compute the robot's stability.

Recently Goswami reformulated the ZMP in terms of the forces acting on the ankle of the stance foot (for a biped) and called the distance from the edge of the support polygon to this point the "Foot Rotation Index" (FRI) [43]. He also suggested that when this point is outside of the polygon, it serves as a measure of instability.

A number of walking robots have used the ZMP, or a variant of it, in their control

scheme include Honda's *Asimo* [45, 107]. However, none of these robots have been able to demonstrate good performance over rough terrain. This is partially due to the fact that when having a single rigid foot in contact with a rough surface a small pressure shift may dramatically change the ground-foot interaction mid-stride, instantly destabilizing the robot.

Other approaches to walking controllers have included an 'intuitive' approach attempted by G. Pratt and J. Pratt at MIT. They specified specific aspects of walking that needed to be achieved with each stride and wrote simple controllers to ensure that each of these happened. This control scheme was successfully implemented on *Spring Flamingo* [84].

They have also used a neural net to stabilize a biped in simulation. The neural net helps to account for the unmodeled dynamics and has demonstrated Lyapunov stability [51]. They continued this work with the development of a "Virtual Model Control" to allow a planar biped to walk on unknown slopes (and by extension) rough terrain with minimal sensing [83]. The implementation of these control schemes has increased the robustness of the biped on unstructured terrain, but they are still constrained to slow motions.

2.1.7 Walking Constraints

Most of the robots described up to this point have been composed of rigid links articulated by motor-encoder feed-back loops. Consequently, they are precise, repeatable and have large workspaces, but are slow. To go faster requires understanding and accounting for the dynamics of the system as well as for the significant and sometimes unpredictable impulses from foot contact. Robots in general are therefore limited not only by the computational power available, but more fundamentally by their sensor and actuator bandwidths. For many motions this constraint is not significant, but for fast legged locomotion, which is characterized by large and unpredictable impacts, this limitation is critical.

2.2 Dynamic Locomotion

Running involves more than simply moving faster than walking. It usually involves a change of gait and aerial phases during which no feet are on the ground. A more rigorous definition of running can be formed by looking at the relative phase of the kinetic and potential energy during a gait [20]. McMahon [67] describes two simple models that have been widely used to capture walking and running. The stance leg in walking is modeled as an inverted pendulum, with the potential energy being the greatest at the top of the swing, and the kinetic energy greatest just before the stride transition. Running is modeled as a spring-loaded inverted pendulum (SLIP) where potential energy is stored in the axial leg spring during stance. This model also allows for the possibility of flight phases between steps. These models have been found to have good correlation with a wide range of observed human and animal ground reaction forces [15, 68].

Full *et. al* [35] have hypothesized that the SLIP model constitutes a fundamental template for dynamic locomotion. They suggests that this pogo-stick type hopping motion captures some of the essential dynamics found in all running systems. Alexander has suggested that the use of mechanical springs in running helps reject disturbances, return energy to the system, and can help ease control [2].

2.2.1 Hopping Robots

The earliest successful dynamic running robots were built by Raibert and his students at CMU and later at MIT [87]. The first planar hopping monopod created in 1980 [87] was a pneumatic air piston/spring that was controlled by three simple control laws. Raibert assumed that hopping height, forward velocity, and pitch could be controlled independently. Simple laws were put forth to correlate hopping height to the magnitude of thrust, velocity to the touch-down angle of the leg, and body pitch to the hip servoing during stance. Though these motions are, in fact, coupled, the decoupled controllers were elegantly simple and turned out to be 'close enough'. The robot was able to run at speeds up to 2.3 m/s, hop up stairs and a biped version could even do a flip [48]. One limitation was that the initial planar runner required complete

and accurate state information acquired by seven sensors in order to implement this control scheme.

The remarkable success of these hoppers spawned an analytic study of simple hopping robots and their stability. Koditschek found that their dynamics were very similar to those of juggling robots [57], and both systems can be analyzed in closed-form using return maps and the eigenvalue analysis described in section 2.2.3 [19] [95]. Mombaur [72] extended this analysis to the case of planar hopper, and Cham [21] furthered this work by removing the assumptions of low damping and no gravity during stance.

Variants of hopping robots that have been built include an energy efficient variant of a hopping monopod, called the *Bow-legged Hopper*, developed at CMU. This hopper used a very efficient compliant leg which could store and return 70% of the energy from each bounce [17]. An alternative approach taken by Ahmaid and Buehler involved using both the hip and leg actuator to stabilize the trajectory while preserving the passive motion. This approach dramatically reduced the required actuation energy at the hip [1].

In addition to increasing the efficiency of hoppers, work has been done to increase their stability. Ringrose, for example, built an entirely open-loop self-stabilizing hopping robot based on curved feet and a feed-forward actuation scheme [88].

The relatively simple dynamics of hopping and promising early experimental successes have led to the development of a remarkable set of robots that have been the first to achieve fast and stable motion.

2.2.2 Passive Dynamic Bipeds

In parallel to the research on hopping robots, work has been done investigating the passive dynamics of simple bipedal walkers. McGeer has demonstrated analytically and experimentally that a completely passive set of rigid links can walk down a gentle slope, powered only by gravity [65]. This remarkable achievement demonstrates the importance of understanding and utilizing the inherent dynamics of a legged system. Others including Garcia [40], Goswami [42], and Kuo [61] have followed this with

studies of these simple bipeds utilizing a stability analysis similar to that used for hopping robots (as described in section 2.2.3).

More recently several groups of researchers have exploited the concept that utilizing the natural dynamics of walking can lead to energy efficient and stable gaits with minimal control effort. These attempts at "passivity-mimicking" have included work by Asano [7], Ohta [77], and Ono [78].

2.2.3 Stability Analysis for Simple Dynamic Systems

The simple hopping and walking models described in sections 2.2.1 and 2.2.2 have allowed for the analytical (or at least numerical) computation of system stability by means of an eigenvalue analysis of return maps.

Return maps are functions that describe how an oscillatory or repeating function changes from one cycle to the next. For walking these have also been called "step functions" [65], since they describe the how state of the system (q) changes from step to step, i.e. $q_{n+1} = f(q_n)$. In nonlinear dynamics language, a steady-state gait is seen as a stable limit cycle or "fixed point" (q^*) on the return map. This implies that all of the elements of the state vector (except forward position) are the same from one step to the next, i.e. $q^* = f(q^*)$. When a return map can be found, either analytically or numerically, and evaluated at fixed points, an analysis of the eigenvalues and eigenvectors of its Jacobian indicates the shape of the local basin of attraction for the trajectory.

$$J_f(q^*) = \left.\frac{\partial f}{\partial q_n}\right|_{q^*} = \left.\frac{\partial q_{n+1}}{\partial q_n}\right|_{q^*} \tag{2.4}$$

Where $J_f(q^*)$ is the Jacobian of the return map evaluated at the fixed point (q^*). Since each step or cycle is discrete event, if absolute values of all of the eigenvalues are less than one, the trajectory is stable. The magnitude of each eigenvalue indicates the slope in its corresponding direction (eigenvector), or the percentage decay from one step to the next. This is a local measure of the slope for the basin of attraction. An advantage of this technique is that it incorporates the effect of perturbations from all directions and on all state variables in a single measure [94].

This analysis technique is general and can be applied to a number of non-linear systems including running [36], but thus far has only been successfully used on simple models. The most applicable of these to this work is Chams's analysis of planar hoppers. The results of this study inspired a scheme to tune the valve actuation pattern of *Sprawlita* [23].

2.3 Multi-legged Runners

Most recently a number of researchers have shown that fast locomotion over rough terrain can be achieved by building platforms combining the advantages of a springy hopper with the stability of a multi-legged platform.

There are a number of potential biological models for designing a compliant multi-legged runner. The two most popular classes are mammalian runners, such as dogs or horses, which generally have four long vertical legs and narrow posture, and arthropods which tend to be smaller, have low centers of gravity, six legs, and a sprawled postures.

2.3.1 Mammalian Runners

Recent studies of mammal-like running include the work done by Berkemeier [11] who looked at a 2-DOF quadruped hopping in place with bound and pronk like gaits. He found that a dimensionless inertia of 1 was essential for a stability of the bound. (Any roughly mammalian multi-legged structure will have the requisite inertial properties.)

Buehler *et al.* have developed *Scout*, a quadruped that utilizes compliant legs and actuated hips. The platform has been used to analyze a number of control schemes and gaits from a "Walking Bound" with constant hip velocities during stance [29], to a trot, and even to gaits with gallop-like footfall patterns [82].

Currently under development is a galloping machine designed to have kinematics inspired by the Nubian goat. This robot is designed to run with an asymmetric foot fall pattern to investigate high speed galloping gaits. It features electric actuation, distributed controllers, and low inertia complaint legs [76]

2.3.2 Arthropod Runners

Developed concurrently with the *Sprawl* robots described in the next chapter, *RHex* [92] is a half meter long autonomous hexapedal running robot built on biological principles similar to the ones described in this thesis. It demonstrates the possibility of simple, robust dynamic running machines that rely heavily on passive dynamics and an open-loop gait. It can run at more than 5.0 *bodylengths/second* and over rough terrain. Its controller has been modified to allow it to pronk and go up steep slopes [58], climb stairs [73], right itself [93], and even swim. It has come closer than any robot to date to achieving autonomous mobility in unstructured terrain.

2.4 Stability in Multi-legged Runners

Stable running is inherently different and in many ways more difficult than stable walking. The increase in speed and the gait patterns used in running result in dynamic effects that cannot be ignored: larger momentum, shorter response times, and large impacts at ground contact.

At first glance it appears that achieving a stable gait in a multi-legged runner is simpler than for a hopping monopod since statically stable configurations are possible. However, the additional complexity of the multi-limbed structure makes the direct application of the closed form control solutions and the functional approximations that worked well for monopods impossible except for a small class of physical designs.

Despite the fact that statically stable configurations are possible during running, none of the stability margins described in sections 2.1.4 and 2.1.5 is applicable for fast dynamic running systems, since even robots with wide postures have airborne phases and can violate the 'dynamic' stability margin with each stride. The return map stability analysis methods described in section 2.2.3 has only been succesfully applied to simple systems, such as one-legged hoppers, and even then they only give the slope of the basin of attraction around the fixed point.

In short, there is no universal measure for the dynamic stability of a complex system running over rough terrain. An effort to begin to remedy this situation is

described in chapter 6.

Even without the ability to directly analyze or measure the stability of a system it is still possible to build controllers and robots that run well on rough terrain. It appears that outside of the body of research with which this thesis is associated, there are two main approaches that have been used to build fast and stable robots, implementing complex controllers and mapping to simple models.

2.4.1 Complex Controllers

The first approach to dealing with the difficulties associated with controlling complex, multi-legged running machines is to use "intelligent" or "adaptive" controllers. This is the approach taken by the OSU/Stanford hopping leg and galloping goat. They use a direct adaptive fuzzy controller to deal with the non-linearities, plant errors, and disturbances experienced by the robot. This system does not require a good model of the plant or extensive system identification, but instead uses heuristics (105 rules) as the basis for the controller. Thus the system can make use of the natural dynamics of the system and can generate gait characteristics comparable to their biological inspiration [63]. The downside to this method is that is something of a 'black box' type approach and it is difficult to know exactly what the controller is doing to ensure stability.

2.4.2 Mapping to Simple Models

Raibert has extended his three part control scheme for hopping robots to bipedal and quadrupedal running by means of controlling a "virtual leg" [87]. By exploiting symmetry, the structure of the biped and quadruped are essentially simplified to that of a monopod. The two or four legs are constrained to act together and are treated for control purposes as a single leg operating at the center of the robot. The three-part control scheme that worked for the hoppers is applied to the virtual leg and the biped or quadruped is able to trot, pace, and bound [86].

Although it does not explicitly use symmetry in its design and control, *RHex* has been shown (when loaded) to achieve center of mass trajectories which match the

predictions of the SLIP model [3]. Furthermore, control strategies for mapping the six-legged behavior to a single-legged hopper have been developed [90]. These allow controllers developed for the known dynamics of the simple model to be mapped to those of a more complex robot.

Grizzle *et al.* have developed a technique similar to Saranli [90] for a multi-link bipedal system using a control system to force the dynamics to map to those of 2D system that allows the application of linear tools for evaluating stability. These include two basic ideas: "Virtual Constraints" and "Hybrid Zero Dynamics" [25, 44]. These techniques allow the development of provably asymptotic and exponential controllers [103, 104].

In each of these cases a complex robot morphology has been reduced to a simple dynamic walking or running model for which direct and provably stable controllers can be written.

2.4.3 Passive Dynamic Self-stabilization

The methods listed in the previous section, however, inherently rely on feedback stabilization loops which are sensitive to bandwidth constraints for sudden impacts. They can also only give insight into how to tune the passive dynamics in the dimensions and directions captured in the simple model. Each of these systems relies on passive leg springs for stability, but by using a black-box like controller or a simplified model, the ability to gain insight into how to tune these properties is limited. The SLIP model can be used to give some idea how to tune the vertical compliance, as has been done in *Rhex* [4] and *iSprawl* [55], but leaves unaddressed the rest of the whole-body effective stiffness matrix. The reliance upon these control techniques leaves an impoverished repertoire from which to design the passive dynamics of the system.

A third approach to designing a stable runner is to carefully tune the 3D structure to exploit both the natural rigid dynamics (like passive walkers), and the impedances of the individual passive strain elements. This is the approach taken with the *Sprawl* family of runners and described in this thesis.

While the mapping of complex systems to simple systems allows the development

of good controllers, the mapping reduces the design space. This thesis argues that it is exactly in that space where the passive dynamics of the system exist that make high-performance and self-stabilization even over rough terrain possible–with only feed-forward control.

2.5 Summary

A large number of walking and running robots have been developed over the years. In the process, a great variety of controllers have been created in order to generate stable gaits, and a number of measures and methods have been designed to analyze their stability. Nevertheless, until the recent development of biologically inspired compliant multi-legged runners, no robot has been built that can run well on rough as well as smooth terrain. These recent robots have demonstrated that a tuned physical structure is fundamental to achieving this capability. As detailed in chapter 3, the *Sprawl* family of robots shows that this is not only a necessary condition, but if tuned properly, can be a sufficient condition for fast stable running.

Chapter 3

Biomimetic Design and Fabrication of *Sprawlita*

This chapter outlines the design, construction, and initial testing of *Sprawlita*, a small hexapedal running robot based on biological principles. These principles of locomotion, taken from the study of small invertebrates, especially cockroaches, include the use of thrusting legs, passive hip compliance, and a sprawled posture. Their application has resulted in a robot that can run at over 5 *bodylengths/second*, and over hip-height terrain. It accomplishes this with an open-loop control scheme, and heavy reliance upon the stabilizing properties of its passive dynamic structure. The prototype robot was fabricated using a manufacturing process that allows many of these principles to be integrated into the structure of the robot itself, much like the biological systems that inspired it (Figure 3.1). The chapter concludes by presenting some initial experiments investigating the effects of changing the structure of the robot and the open-loop control scheme on the performance of the robot.

3.1 Design Inspiration from Biology

For quick and robust traversal over uneven and uncertain terrain, design inspiration is drawn from small arthropods. In particular, cockroaches are capable of remarkable speed and stability. For example, it has been shown that *Periplaneta americana* can

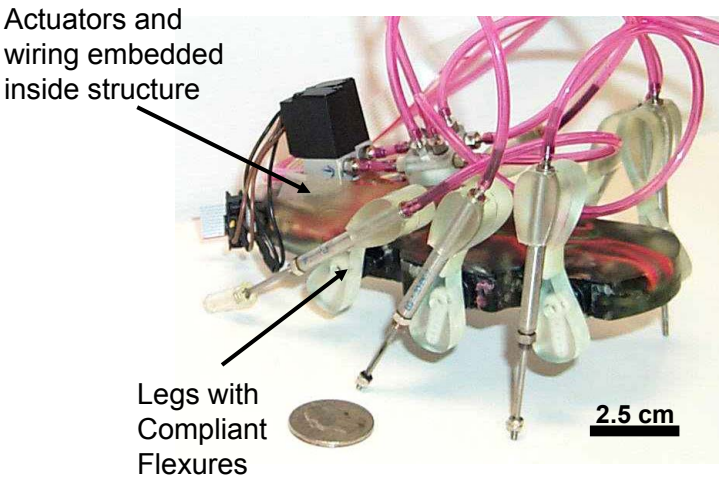

Figure 3.1: *Sprawlita* a dynamically-stable running hexapod based on functional principles from biomechanical studies of the cockroach. *Sprawlita* was the first prototype fabricated using Shape Deposition Manufacturing and is capable of running at 3 body-lengths per second.

achieve speeds of up to 50 *bodylengths/second* [37]. *Blaberus discoidalis* is capable of traversing uneven terrain with obstacles of up to three times the height of its center of mass without appreciably slowing down [33]. Studies of these cockroaches suggest the following design principles for fast, stable, running hexapods:

- self-stabilizing posture
- thrusting and stabilizing leg function
- integrated construction
- passive viscoelastic structure
- timed, open-loop/feedforward control.

The following sections describe these principles and how they are implemented in the design and fabrication of the *Sprawl* robots.

3.1.1 Self-stabilizing Posture

The use of a sprawled hexapedal posture has many advantages. Many robots have been designed with six legs so that they can walk with an alternating tripod gait. By walking with three non-adjacent legs on the ground at one time, the robot can constantly ensure static stability. The use of this approach, however, has limited many of these robots to slow, near-static speeds.

Observations of cockroaches running at high speeds, on the other hand, show that while they also run with an alternating tripod gait, their centers of mass approach and exceed the bounds of the triangle of support within a stride [99]. Cockroaches achieve a form of dynamic stability in rapid locomotion while maintaining a wide base of support on the ground.

In addition, Kubow and Full [35] suggest a further advantage to an appropriately sprawled posture with large lateral forces. Their studies show that for such a system, horizontal perturbations to a steady running cycle are rejected by the resulting changes in the body's position relative to the location of the feet.

Sprawlita, the first-generation Shape Deposition Manufacturing (SDM) prototype robot is approximately 16 *cm* in length, and was built for the simple task of fast straight-ahead running over rough terrain. Thus, it was designed with a similar, but not identical, sprawled morphology in the sagittal plane. The sprawl, or inclination, angle between the legs is limited by foot traction; for larger animals (or robots), it becomes progressively harder to sustain the necessary tangential forces. As shown in Figure 3.2, the center of mass was placed behind and slightly below the location of the hips, but still within the wide base of support provided by the sprawled posture.

3.1.2 Thrusting and Stabilizing Leg Function

Using the stability provided by a tripod of support formed by at least three legs, many robotic walkers actuate the legs to move the robot's center of mass forward while minimizing internal forces in order to increase efficiency [60]. Furthermore, a common leg design places a vertically-oriented joint at the hip to avoid costly torques for gravity compensation. The resulting rowing action minimizes internal forces, but

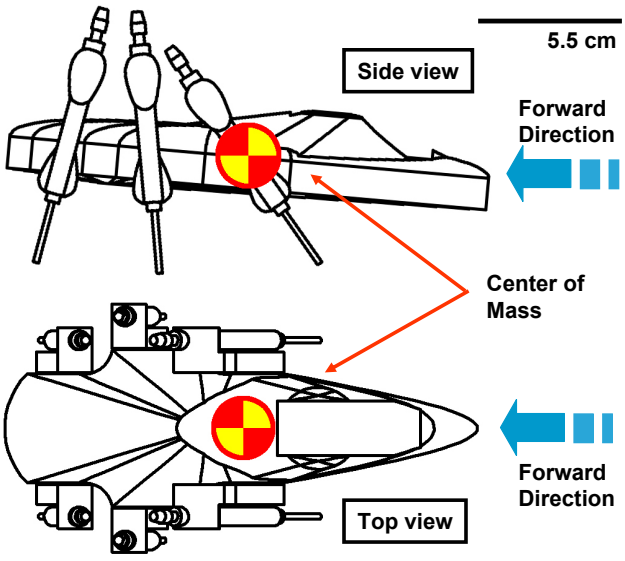

Figure 3.2: Self-stabilizing posture: A rear and low center of mass and wide base of support contribute to the over-all stability of locomotion

contradicts what is observed in the cockroach and other running animals.

Studies of the cockroach's ground-reaction forces during running indicate that its legs act mainly as thrusters. Throughout the stride the ground reaction forces for each leg point roughly in the direction of the leg's hip [34]. In the cockroach's wide sprawled posture, the front legs apply this thrusting mainly for deceleration, while the hind legs act as powerful accelerators. Middle legs both accelerate and decelerate during the stride. The creation of large internal forces may be inefficient for smooth, steady-state running, but there is evidence that this contributes to dynamic robustness to perturbations [59], and to rapid turning [52].

A similar leg function has been designed in the *Sprawl* robots as shown in Figure 3.3. The primary thrusting action is performed by a prismatic actuator, here implemented as a pneumatic piston. This piston is attached to the body through a compliant rotary joint at the hip. This unactuated rotary joint is based on studies of the cockroach's compliant trochanter-femur joint, which is believed to be largely passive. In the prototypes, the compliant hip joint allows rotation mainly in the sagittal plane, as shown in Figure 3.3.

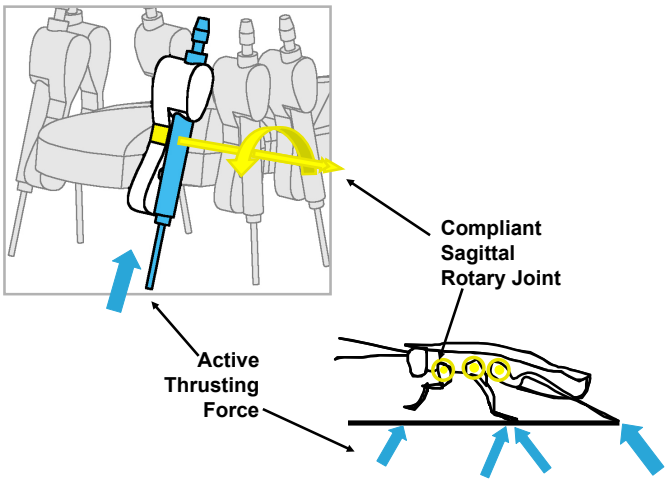

Figure 3.3: Leg Function Studies of ground reaction forces in cockroach locomotion show that forces are directed towards the hip joints, essentially acting as thrusters. In addition, each leg performs a different function: front legs act as decelerators while hind legs act as accelerators; middle legs act as both.

These active-prismatic, passive-rotary legs are sprawled in the sagittal plane to provide specialized leg function. Servo motors rotate the base of the hip with respect to the body, thus setting the nominal, or equilibrium, angle about which the leg will rotate. By changing this angle, the function that the leg performs is altered by aiming the thrusting action toward the back (to accelerate) or toward the front (to decelerate).

3.1.3 Integrated Construction

Bailey *et al.* argue that biomimetic design must also be accompanied by biomimetic fabrication [8]. A common mode of failure for today's robots lies in the numerous fasteners and connectors that hold them together. This is especially problematic in smaller robots, where much of the design space is dominated by fasteners. Fundamentally, a mechanism designed to be assembled can also disassemble itself.

Nature, on the other hand, composes its designs in a different manner. Actuators, sensors and structural members are compactly packaged in an integrated fashion and

are protected from the environment. In addition, nature's compliant materials are capable of large strains without failure [100]. Material properties are varied to meet local loading requirements; for example, bone is hard and dense at the joints, but porous in between.

Of course, we may never be able to achieve the complexity and elegance of biological structures; however, the emerging manufacturing technology adopted to fabricate the prototype robots does allow building integrated assemblies with embedded components and material variations. This yields a structure that is rugged enough to withstand the collisions and falls that are inevitable in running through an unstructured environment.

3.1.4 Passive Viscoelastic Structure

The advantages of compliance, or low impedance, for interaction with an unknown environment have long been recognized [49]. A popular approach, even in locomoting robots, has been active impedance control of rigidly-built robot appendages. Even with active control, the high transient forces due to impacts involving stiff links cannot be precluded because of limitations in servo bandwidth.

Animals, on the other hand, are commonly anything but rigid. In particular, studies of the cockroach *Blaberus discoidalis* are revealing the role of the viscoelastic properties of its muscles and exoskeleton in locomotion [41, 69, 105].

The prototype's leg design contains a passive compliant and damped rotary hip joint fabricated as a flexure of soft viscoelastic polymer urethane embedded in a leg structure of stiffer plastic. This is an initial attempt at integrating desired impedance properties passively through the structure of the robot itself. Although it primarily allows rotation in the sagittal plane, the joint provides some compliance in the other directions as well.

The construction of the multi-material compliant leg used in the robot, shown in Figure 3.4, is made possible by a process called Shape Deposition Manufacturing (SDM) [70] [13]. This process has the capability to vary the material properties during construction of the part. Each layer can be built up of a different material, each with

its own characteristics. The deposition of a layer of soft viscoelastic polyurethane creates the compliant, damped hip flexure joint. A stiffer grade of polyurethane was used for the structural members, which encase the piston and servo mounting.

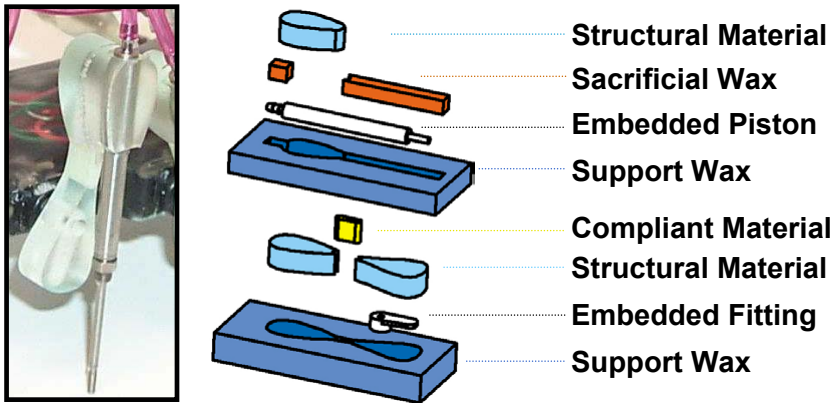

Figure 3.4: Shape Deposition Manufacturing process plan for *Sprawlita's* legs. The alternating layers of hard and soft materials, as well as the embedded components that make up the compliant legs, are shown.

As shown in Figure 3.5, this rotational viscoelastic compliance in the legs is essential for the locomotion mechanism. At the beginning of the half-stride (a), the tripod has just made contact with the ground and the hip deflections are small. Near the end of the half-stride (b), the pistons are at full stroke and the compliant hips are significantly deflected. Once the tripod is retracted, the legs passively return to their equilibrium positions.

Consequently, the actual path taken by the feet with respect to the body is determined by the dynamics of the body interacting with the compliance of the legs during running. This is in sharp contrast to most robots whose legs are commanded to follow a prescribed nominal trajectory.

Modeling has been done to compare the properties of these polyurethanes with the material characteristics found in the exoskeleton of cockroaches. It was found that simple viscoelastic material models can be fitted to both the biological materials and the polyurethanes [105].

Other, more sophisticated, leg designs for *Sprawlita* have also been experimented

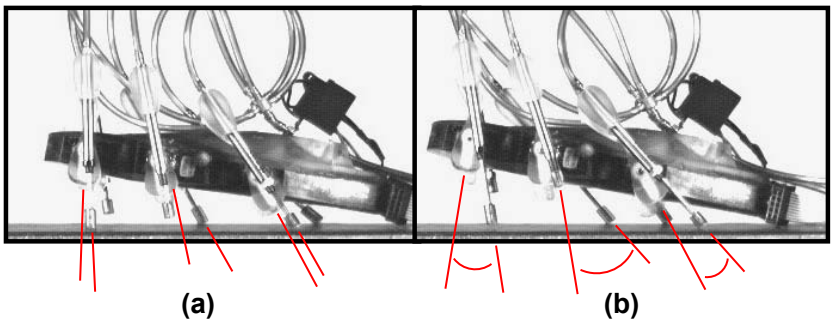

Figure 3.5: Leg deflection as shown by high-speed video

with. Figure 3.6 shows a prototype leg that was designed to have axial compliance in series with the piston as well as rotational compliance. A spatial fourbar mechanism was chosen to allow for only those two degrees of freedom. The geometry of the five compliant segments on the fourbar allows independent control of the stiffness in the rotational and axial directions. This leg was fabricated before an understanding of how to properly tune the compliance of the legs was achieved. Consequently, it is much too stiff, and produces slower running than the earlier one degree of freedom legs.

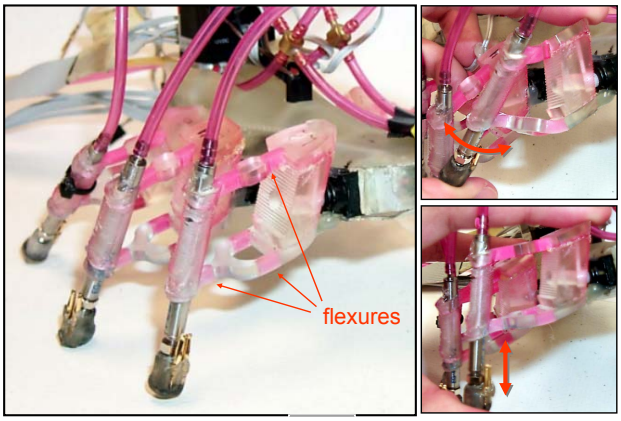

Figure 3.6: An alternative leg design allowing deflection in one rotational and one axial direction. The leg is a spatial fourbar with compliant segments that allow the stiffness in each direction to be tuned independently.

While other robots such as Raibert's hoppers [87], the *Bow-legged Hopper* [17] and *Rhex* [92] have made use of complaint legs, the legs described in this section are the first monolithic multi-material compliant legs built for a running robot. They are also the first to rely upon compliance for their rotational displacement. Tuning their stiffness properly is the key to *Sprawlita's* locomotion, and this is made possible by use of SDM as a fabrication tool.

3.1.5 Open-loop/Feedforward Control

The self-stabilizing properties of the viscoelastic mechanical system and functional morphology mentioned above have been termed 'preflexes' [18]. These preflexes provide an immediate, or 'zero-order' response to perturbations without the delays of neural reflexes. Studies of the cockroach running over uneven terrain suggest that these preflexes play a dominant role in the task of locomotion. It has been shown that there are only minor changes in the cockroach's muscle activation pattern as it rapidly transitions from smooth to uneven terrain [33]; there is no carefully controlled foot placement or noticeable changes in gait, period, or pattern. These findings suggest a control hierarchy as shown in Figure 3.7 [35].

In this scheme, the basic task of locomotion is accomplished by a properly tuned mechanical system activated by a feedforward, or open-loop, control input. This combination effectively provides a mechanical 'closed-loop' that is sufficient to maintain stability in the face of sudden perturbations or terrain changes [22]. Sensory information is then used to modify the feedforward pattern to change the animal's behavior in order to adapt to changing conditions. For example, rapid turning may be effected simply by changing the location of feet touchdown locations [52].

The *Sprawl* robots are controlled by alternately activating each of the leg tripods, where a leg tripod is made up of a front and rear leg on the same side and a middle leg on the opposing side. Each of these tripods is pressurized by a separate three-way solenoid valve, which connects the pistons either to a pressurized reservoir or to the atmosphere. These valves are operated at a frequency and duration determined respectively by the stride period and duty cycle.

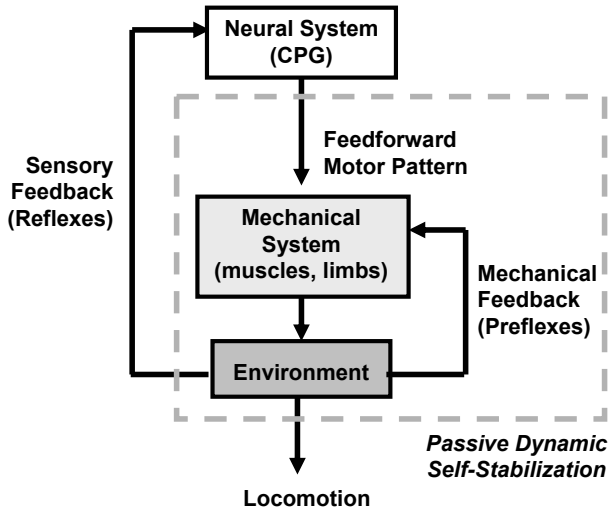

Figure 3.7: Suggested roles of a feedforward motor pattern, preflexes, and sensory feedback. Here, disturbance rejection is the result of the mechanical system and not an active neural control loop. (Adapted from [35].)

The feedforward controller also commands the nominal angle for each hip, which determines foot placement and thrust direction. However, these angles are not changed within each stride, but are instead servoed in response to changes in the desired task. For example, forward and backward velocity, as well as turning radius, are functions of the relative nominal angles of each hip.

Running over rough terrain utilizes the stabilizing properties of the passive viscoelastic leg structures rather than adjusting the nominal gait or adjusting feedback gains as has been done in most legged robots. The result is a simple basic control strategy that sidesteps most of the issues and complexity associated with generating a stable gait and trajectory.

3.2 Performance Results

As *Sprawlita* scurries across the floor and over obstacles, the combination of the preflexes and control scheme mentioned above appear to result in locomotion similar to

the animal it is mimicking. Nevertheless, a closer examination of ground reaction forces and center-of-mass trajectory reveal subtle differences from the cockroach's locomotion. This comparison is detailed by Bailey *et al.* [9] and suggests possible improvements to this particular mapping of the biological principles. This section presents results of performance tests in terms of maximum forward velocity and discusses initial attempts to understand the role of the robot's design parameters on this performance metric.

3.2.1 Parameter Design Studies

Variations in stride period, tripod duty cycle and nominal leg angles have been found to have a significant effect on the speed of locomotion. Moreover, the optimal parameter settings vary as a function of the slope and condition of the terrain. A number of parameter design studies have been undertaken to investigate these relationships. An example of which, shown in figure 3.8, shows how the velocity varies as a function of the slope for two different gait periods. As indicated, the shorter period gives faster performance on level ground. But for slopes of greater than 12 degrees the longer period is preferable.

3.2.2 Design of Experiments

To better understand the relative importance and coupling of the factors influencing the speed of locomotion, a full factorial binary design of experiments (DOE) was performed [16]. For these tests the robot was started from rest and time required to traverse a fixed distance was recorded. For each configuration 3 trials were made, for a total of 384 runs. The order of the trials was randomized in order to block unwanted effects such as wear on the robot or variation in the timing due to human fatigue. While first and second order interaction effects could have been determined from a partial factorial array, the large number of runs from the full factorial improved the statistical significance of the results.

As shown in table 3.1, the robot parameters selected for the study were stride period, duty cycle, front hip angle, middle hip angle, rear hip angle, and flexure

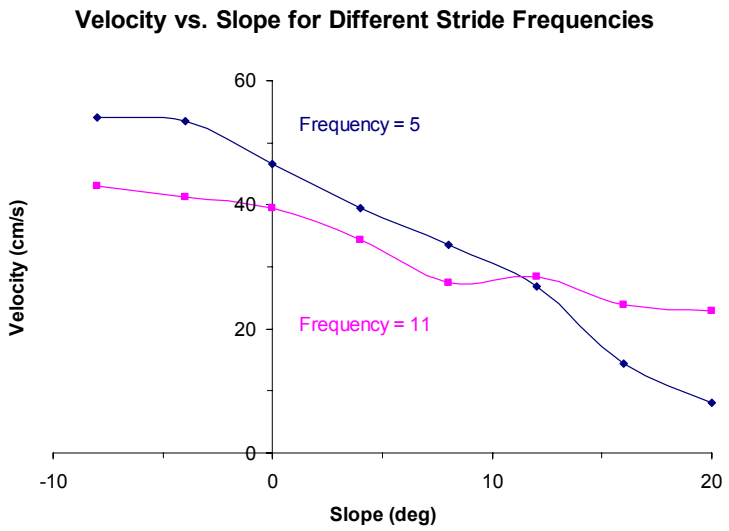

Figure 3.8: Robot performance test results for slopes ranging from -8 degrees downhill to 20 degrees uphill for two different stride periods. These tests indicate the need to adapt variables of the locomotion scheme to environmental conditions.

compliance. The first two of these parameters define the open-loop motor patten. The next three parameters, the nominal leg angles, can also be varied during run time via the hip servos. While not actuated during normal running they could be altered on a stride-to-stride basis to steer the robot, or to adapt the robot's posture to changing environmental conditions. One such environmental condition that was tested in this set of experiments was ground slope.

Parameter	**High Value**	**Low Value**
Valve Duty Cycle	40%	25%
Stride Period	180 ms	120 ms
Ground Slope	8°	0°
Compliance	.084 Nm	.026 Nm
Front Leg Angle	10°	$-10°$
Middle Leg Angle	$-10°$	$-30°$
Rear Leg Angle	$-30°$	$-50°$

Table 3.1: Parameters and their high and low values used in the design of experiments.

These five robot parameters span the portion of the robot's configuration space for which run-time variation is possible. Despite the difficulties associated with varying the physical aspects of the robot design, it is important to understand how they affect the performance of the robot. Initial exploration has indicated that the robot performance is particularly sensitive to the amount of passive impedance at the hips. Consequently, hip flexure impedance was included as one of the factors in this study. Due to the difficulty of replacing the robot legs between trials, this factor was not randomized when generating the test sequence.

The high and low values for the experiment were chosen empirically based on reasonable values for level ground and hill climbing. It should be noted that for all of the tested conditions the robot converged from an initial rest position to steady running gait. This indicates that reasonable values were selected, and that the parameter space that results in acceptable running is at least as large at the six-dimensional box defined by the high and low values of this DOE.

DOE Results

Under the experiments conditions, the maximum speed on smooth level ground was 43 cm/s, or approximately 2.5 $bodylengths/second$. The most significant factor affecting running speed was the change in ground slope. As shown in Table 3.2, the most significant robot parameters affecting the speed of locomotion were, in decreasing order of significance, hip compliance, rear leg angles, front leg angles, and stride period. These results indicate that while changing both the open-loop actuation pattern (stride period and duty cycle) and the stance parameters (leg angles and hip impedance) affect the performance of the robot, properly tuning the impedance and stance properties is particularly important.

Slopes

The results of the DOE also indicate that for running up hill the most significant parameters to vary, again in decreasing order of significance, were stride period, rear leg

Parameter	P-Value
Compliance	$2.98 * 10^{-11}$
Rear Leg Angle	$3.51 * 10^{-7}$
Front Leg Angle	$3.81 * 10^{-4}$
Stride Period	$7.49 * 10^{-4}$

Table 3.2: Most significant parameters on robot velocity

angles, and front leg angles. Although these interaction effects were not quite statistically significant to the 95% confidence level (P-values of: .059, .117, and .177), the results agree with the parameter study shown in figure 3.8 and suggest the importance of adaptation of the basic feedforward pattern to match changes in the environment.

Cham *et al.* [24] have made use of these findings to implement an elegant adaptation scheme for *Sprawlita* which takes data from a binary contact sensor in a foot, and adjusts the stride period to maximize the amount of work performed by the actuators. Other potential adaptation schemes are explored in section 5.4.

Interaction Effects

Three other first-order interaction effects were found to be statistically significant. These are, as shown in table 3.3, stride period and hip compliance, rear-leg angle and compliance, and front leg angle and duty cycle. The coupling of each of these parameter changes has a significant effect on locomotion speed. In the case of front leg angle and duty cycle, the interaction had a greater effect than duty cycle alone!

Parameter	P-Value
Stride Period and Compliance	0.0022
Rear Leg Angle and Compliance	0.0276
Front Leg Angle and Duty Cycle	0.0456

Table 3.3: Significant parameter interaction effects

While these results only indicate an effect, and do not specify a specific root cause, plausible physical reasoning exists to explain why each of these couplings would be significant. If the robot does bounce as the SLIP model [35] suggests, then it is

reasonable that leg stiffness and damping, which define the system's natural frequency, would be coupled with the stride period–the frequency at which the system is being driven.

Regarding leg angles and compliance, the rear legs are designed to provide the main forward thrust for the robot, and if their angle becomes too steep with respect to the ground, significant foot slippage will occur. As the rear hip stiffness decreases the amount of flexion, and hence slipping, during stance will increase. Careful consideration as to the shape of the friction cone for the rear legs is called for. This may be particularly important as the frictional properties of the substrate change.

It appears that the front legs are more sensitive than the other legs to the duration of the stance phase as defined by the valve duty cycle. With a nearly vertical posture, the front legs stabilize and lift the body with each stride. It appears that this stabilization is more sensitive to timing than the propulsion provided by the middle and rear legs.

The fact that a number of interaction effects were found to be significant underscores the coupled nature of *Sprawlita's* locomotion, and the importance of looking at multiple parameters simultaneously.

3.2.3 Unstructured Terrain

On flat, even terrain, the robot is able to clear obstacles 3.5 *cm* high corresponding to its ground clearance, or one 'belly-height'. As slope increases, the height of the maximum obstacles the robot can traverse decreases. With the development of a computationally autonomous version of the *Sprawl* robots, the ability to move across various ground conditions was also tested. The robot is capable of running at speed across a variety of terrain such as dirt, brick, and rough asphalt. It can manage some types of rougher terrain, such as grass, bark, and sand, but high-centering becomes a problem as the obstacles become larger than the stroke length of the legs. For deformable surfaces such as sand, appropriate foot design is critical to prevent miring.

3.3 Conclusions

The design and construction of the *Sprawl* family of hexapedal runners has shown that the adoption of appropriate functional biomimetic principles can enable robots to begin to mimic some of the agility, versatility and speed of legged animals. The heavy reliance on the self-stabilizing posture utilizing passive impedance has enabled impressive performance with only simple open-loop control.

The experimental results from the DOE (described in section 3.2.2) are encouraging, as they show that there is a wide set of control and configuration parameters for *Sprawlita* which result in fast and stable running. Finding an optimal configuration is, however, somewhat more challenging. Traditionally, this optimization becomes a controller design problem. In the *Sprawl* robots however, tuning the open-loop control system alone is not sufficient to maximize the potential of the robot. The results of the DOE, as well as the attempt to improve performance by implementing the (slow) 2 DOF spatial-fourbar legs, demonstrate that the proper tuning of the physical impedance and stance parameters is critical.

Exploring any region of the parameter space through experimentation alone is slow and difficult. Investigating changes to structural parameters such as leg lengths or hip stiffness is particularly tedious. Yet, having a clear understanding of the mechanisms behind the locomotion is essential. Simple models of running can be very useful in this respect, but critical elements of *Sprawlita's* design, such as the antagonistic leg postures and the distributed rotational hip impedance are difficult to capture in a simple model. In order to be able to understand how changing the physical design of the robot affects its ability to run quickly and stably, a computer simulation of the robot is needed. The development of this model, and its comparison to the physical robot is outlined in the next chapter.

Chapter 4

Modeling and Verification

With the construction of the *Sprawl* family of hexapedal running robots [27], it has been demonstrated that a carefully designed mechanical structure can enable fast and stable locomotion over a variety of terrain without feed-back control. The tuning of the mechanical design, especially the compliant legs, has allowed the robots to run over hip-height obstacles at speeds of over 5.0 *bodylengths/second*.

With this approach, the emphasis is shifted from the design of the control system to the design of the structure of the robot. It therefore becomes increasingly important to understand the effect of varying design parameters on performance. Some parameters, such as actuation frequency and the nominal leg angles, are easily adjusted at run time. Others, such as the location of the center of mass, leg lengths, and hip flexure stiffnesses, require time-consuming design modifications. Nevertheless, it is critical for the designer to understand how these quantities affect the dynamics of locomotion.

Both simple and complex models have been used to understand and refine the design of the *Sprawl* robots. The simplified models have consisted of spring-based, clock-driven hoppers derived from the pioneering work of Raibert and Koditschek [87, 57]. Subsequent investigations of open-loop vertical hopping [88, 24, 21] have provided important insights regarding thrust timing, ground contact, hop height, and stability. However, the real robots reveal other behaviors that cannot be captured by such idealized models.

The more complex models described in this chapter consist of multi-body dynamic simulations of the running platform which include design parameters describing the system's geometry, mechanical characteristics and actuation. Other investigators have used similar approaches to design control systems for complex, multi-legged robots [91, 56, 80]; however the emphasis in the current study was on using complex models to determine the range of design parameters that will lead to fast, stable hexapedal locomotion using only open-loop control.

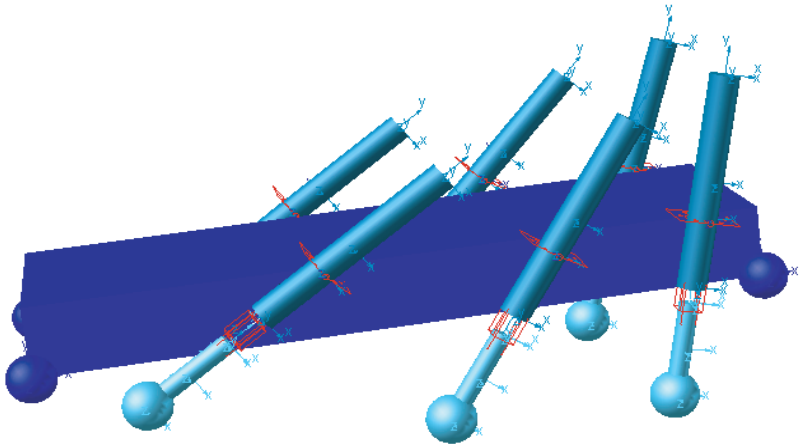

Figure 4.1: Overview of simulation of *Sprawlita* featuring passively compliant hips and pneumatic thrusting legs

4.1 Modeling and System Identification

Due to the complexity of the model that is required to answer the above questions, the $MSC.ADAMS^{TM}$ commercial dynamic simulation package was chosen as the modeling environment. $ADAMS^{TM}$ offers an appropriate combination of integrator accuracy and stability, ease of building and parameterizing a design, and convenient display and analysis tools.

Care was taken to establish the parameters defining the passive self-stabilizing structure of the robot. As shown in figure 4.1, the model consists of a rigid body

supported by six identical legs. The center of mass of the robot is located slightly behind the middle legs, as in many insects [52], and as shown by Schmitt *et al.* [96], to promote lateral stability. Each leg has one active and one passive degree of freedom: a prismatic pneumatic actuator thrusts along the axis of the leg, and a flexure provides rotational stiffness and damping at the hip where the leg attaches to the body. The robot also has servo motors at the hips, but these are used only to establish the equilibrium positions of the legs. Thus, as in insects, propulsion is due mainly to thrust forces directed along the legs, with elastic hip rotations being responsible for swinging the legs forward at the end of each stride. Each foot, as well as the corners of the body, has a contact model for collisions with the floor, and can drag and bounce. The various subsystems, and the system identification processes used in their development, are described in the following sections.

4.1.1 Legs - passive rotational elements

Each leg, as shown in figure 4.2a and described in section 3.1.4, is fabricated using SDM, and consists of two different grades of urethane. The clear structural material is approximately 13 times more rigid than the translucent white grade. The soft material was designed to act like the primarily passive tarsus-femur joint of a cockroach [105]. The flexure was designed so that the bending stiffness in the fore-aft and medio-lateral directions could be independently controlled by varying its dimensions.

The short length of the flexible section of the material compared to the length of the leg suggests modeling it as a small-length flexural pivot [50]. If one assumes that a pure moment is applied, then the rotation of a flexible beam can be described by the Bernoulli-Euler equation as $\Theta_0 = \frac{M_0\, l}{EI}$. Where M_0 is the applied moment, E is the modulus of elasticity of the bending material, and I is the mass moment of inertia of the flexure. For a Hookian spring described by $M_0 = K\Theta_0$ and a rectangular cross-sectional geometry (w, h) the stiffness K is simply:

$$K = \frac{E(wh^3)}{12\, l} \tag{4.1}$$

Based on the geometry of the flexures, the rotational stiffness should be 0.05 Nm

in the fore-aft direction and 7.9 times stiffer (or 0.39 Nm) in the lateral direction. The effective spring constant in the fore-aft direction was measured experimentally and found to be 0.05 Nm. The softer, primary mode of bending is in the direction of travel. Therefore, only a single degree of freedom was allowed in the initial version of the model. Later simulations indicated that during turning the lateral mode of bending becomes important. This addition, however, did not noticeably affect the straight-ahead motion of the simulation [64].

The urethane used in the leg flexures is viscoelastic, and as shown by Xu *et al.* [105] it dissipates energy in a way not unlike that observed in cockroach legs. To simulate the observed energy loss at running speeds, a viscous rotational damper was added in parallel to the hip spring on each leg. The effective damping was experimentally determined to be $2.3E-4\ Nms$ (see Appendix A.1).

The simulated response of the leg model to non-zero initial conditions was similar to the motion of the real leg as measured by high speed video. Figure 4.2b shows the results of a step disturbance for the robot leg as captured by high-speed video and the output from the ADAMS leg model. The thin solid line shows the average of several experimental step responses and dotted lines show the variability corresponding to one standard deviation. The heavy solid line is the simulated response, which produces similar energy dissipation for excursions corresponding to a standard step size, but faster decay for small excursions. This method of fitting a second-order system model to the real non-linear system attempts to minimizes the error during the stance phase, which has the largest impact on the locomotion dynamics.

4.1.2 Legs - active translational elements

Each SDM leg has a spring-loaded, normally retracted, piston embedded in it (as shown in figure 4.2a). Consequently, each leg is modeled with an active prismatic degree of freedom. The pistons are actuated by pneumatic valves and the associated pressure rise times are shown in figure 4.3a.

The geometry, spring stiffness, and pre-load for the piston are all specified by the manufacturer and are given in table 4.1. Note that these pistons have a 20 mm stroke

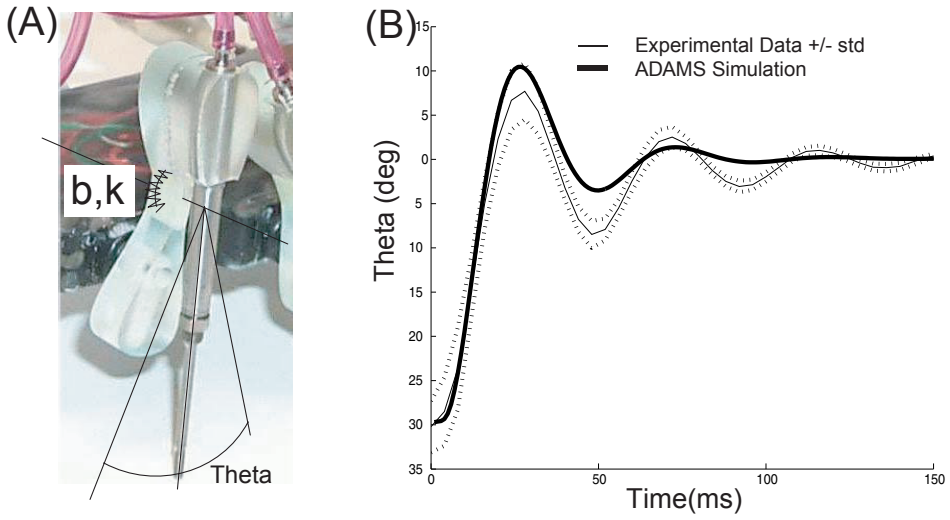

Figure 4.2: (a) Overview of hip model and (b) the step deflection response for both the robot leg and the model

with hard stops at either end. The stops were modeled by stiff spring-dampers that engage at prismatic translations corresponding to the ends of the piston stroke.

Festo Pistons	**Values**
Length	.058 m
Outer Diameter	.005 m
Inner Diameter	.004 m
Mass	.006 kg
Stiffness	55.0 N/m
Spring Preload	1.50 N
Damping	.002 $\frac{N}{m/s}$

Table 4.1: Festo Piston Values

The damping in the piston was modeled as pure viscous damping for simplicity. The value of the effective damping for the pistons was calculated experimentally.

Each of the pneumatic valves is given a square wave signal as a control input. The frequency and duty cycle (% on) of the square wave determine the stride period and amount of thrust applied to the legs.

Tests have shown that the pressure rise in the robots is approximately exponential

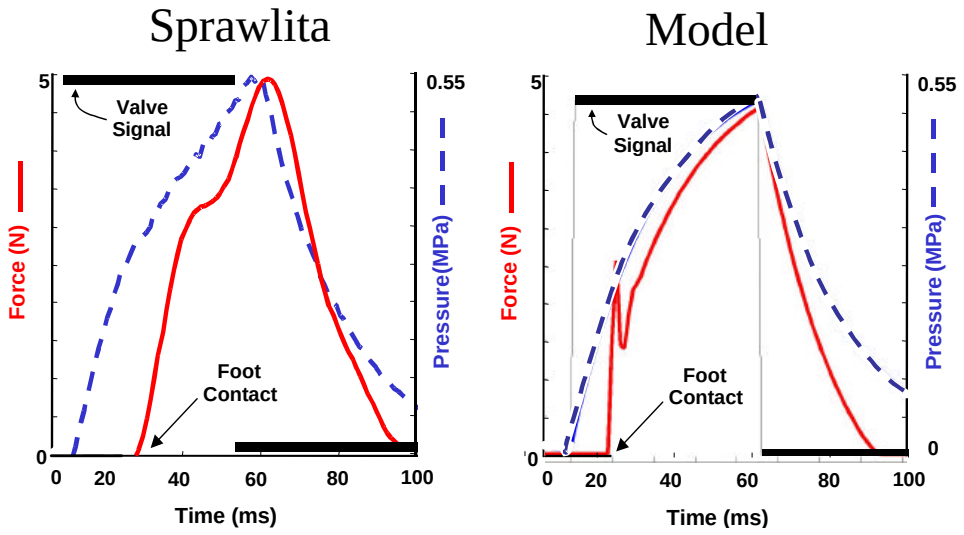

Figure 4.3: A comparison of the pressure rise and ground reaction force for the robot and the model

in nature, as shown in figure 4.3. Consequently, the first modeling efforts used a simple first-order ODE to calculate the pressure acting on the piston:

$$\tau \dot{p(t)} + p(t) = p_0 \quad where \quad p_0 = \begin{cases} p_{max} & \text{if valve on} \\ 0 & \text{if valve off} \end{cases} \tag{4.2}$$

An advantage of this simple model is that it requires only a single parameter (τ) to characterize the rate at which the pressure rises to the supply limit (P_{max}).

Pneumatic model

Simulations of the robot running indicate that there are large ground reaction force spikes at the beginning of each foot's contact (see figure 4.3). These are partially due to the penetration/penalty based contact code used by the modeling software, but could also be caused by the failure of the simple model to capture the compliance of the pneumatics. Consequently, a slightly more sophisticated model was introduced that models the air flow through the piston.

For this model, the mass flow through the valve is given by:

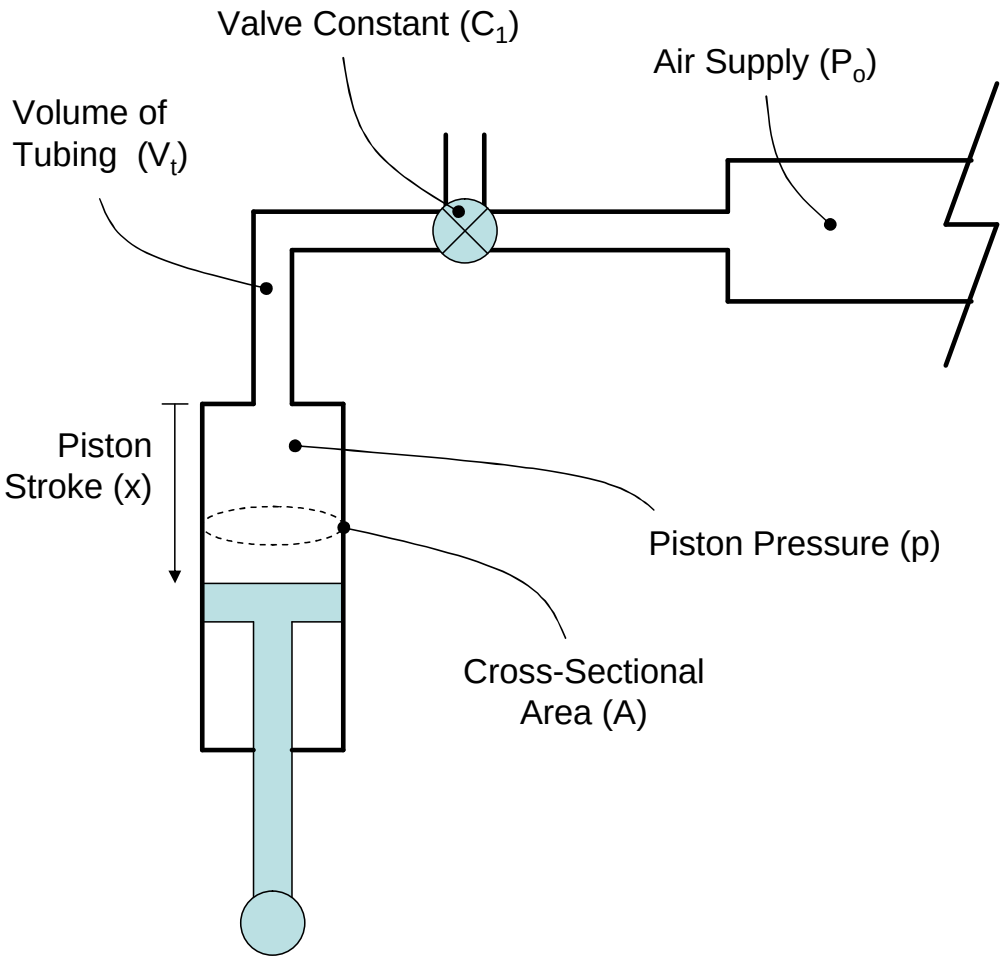

Figure 4.4: Schematic for the ideal gas pneumatic pressure model. The mass of the air m_{air}, extension of the piston x and pressure in the piston p are all states of the system and are computed at each time step of the simulation.

$$\dot{m}_{air} = C_1 \left(P_0 - p\right) \tag{4.3}$$

The pressure in the piston is then given by equation by:

$$p = \frac{m_{air} RT}{v} = \frac{m_{air} C_2}{Ax + V_t} \tag{4.4}$$

Figure 4.4 shows a schematic of the model in which air is allowed to flow into the piston/tubing chamber from a constant pressure source. The air is assumed to be an adiabatic ideal gas. As the mass of air in the chamber increases the pressure on the piston increases. When the piston strikes the ground the air in the piston is compressed and the volume can momentarily decrease. As equations 4.3 and 4.4 and figure 4.4 indicate, the use of this model introduces two new physical parameters, the volume of the piston/tube chamber (V_t), and the flow rate through the valve (C_1). The volume was calculated and the flow rate was estimated from a best fit of the experimental pressure rise data from the robot, an example of which is shown in figure 4.3a.

Parameter	**Values**
Supply Pressure (P_0)	.040 MPa
Valve Constant(C_1)	$7.5e-6$
Volume of Tubing (V_t)	$8.3e-7$ m^3
Cross-sectional Area (A)	$1.6e-5$ m^2
Gas Constant(R)	0.287 $kJ/(Kg\ K)$
Temperature (T)	300 K

Table 4.2: Table of values for the Ideal Gas model of pneumatics

Once calibrated, the pressure rise for both models is similar for normal running with ground contact, as shown in Figure 4.5a. As shown in figure 4.5b, the use of the ideal gas pneumatic model (case 2) mitigates the impact spike due to ground contact. In addition, the ideal gas model generates a slightly larger thrust and more drag more than the exponential model (case 1). The net result is locomotion at similar forward velocities (0.595 m/s for the exponential model and 0.604 m/s for the ideal gas model).

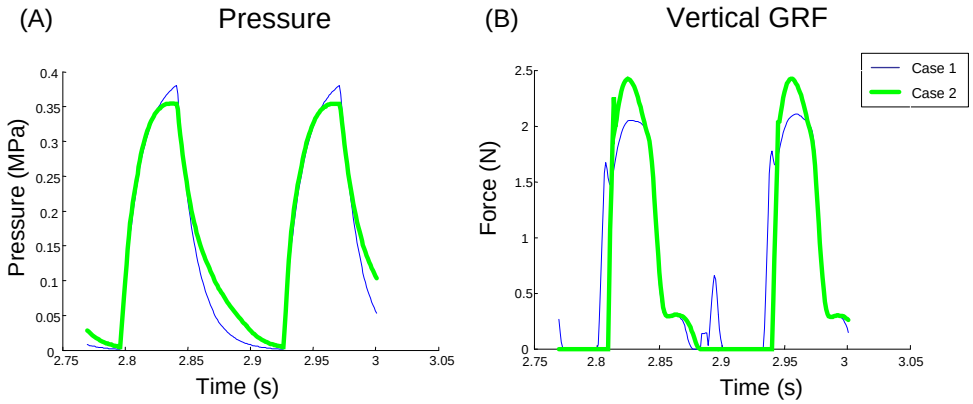

Figure 4.5: A comparison of the exponential (case 1) and ideal gas (case 2) models of *Sprawlita's* pneumatics. Figure (a) compares the pressure profiles for two strides, and (b) shows the front leg vertical ground reaction force for the same strides

4.1.3 Contacts - Modeling (Robot/World Interaction)

Foot/Ground Model

During running, ground contact is intermittent and its initiation and duration are based on the open-loop clock timing, the piston pressure model, and the position and orientation of the body. The foot-floor contact in the vertical direction was modeled by a stiff nonlinear spring damper:

$$F_n = k(x)^n + b\dot{x} \ for \ x > 0 \tag{4.5}$$

The ground characteristic parameters k, n, and b are the ground stiffness, exponential, and damping. These were experimentally measured for the foot and treadmill interaction and found to be $62,600\ Nm$, 2, and $10\ Nm/s$, respectively (see Appendix A.3).

The damping constant, b, ramps up from zero to full damping during a brief initial contact period in order to avoid numerical problems associated with discontinuous forces that can occur with intermittent contact. Horizontal foot forces were computed based on a Coulomb friction model. Static and dynamic friction coefficients were experimentally determined to be $\mu_s = 1.2$ and $\mu_d = 1.08$ for the rubber feet on the

textured rubber treadmill (see Appendix A.2). Friction coefficients also ramped up from zero to full friction over a brief initial contact period to avoid discontinuities in the horizontal forces.

The geometry of contact between *Sprawlita's* rounded feet and the flat treadmill was modeled as a sphere on a plane. This approximation allows $ADAMS^{TM}$ to use an efficient closed-form model to compute the initiation and penetration between the feet and ground.

Body and Tether drag

High speed video and simulations show that during normal running the rear of the robot as well as the feet make contact with the ground. When running over obstacles, or when poorly configured, the front or 'nose' of the robot will, at times, also make contact with the ground. To account for these phenomena, spherical contacts were added at the four lower corners of the box that represents the body of the robot (see figure 4.1). These contacts are treated in the same way as the foot contacts. During normal running the rear corners of the robot will sometimes drag and support about 20% of the model's weight, producing up to 0.9 N of drag force due to friction.

Although efforts were taken to minimize the size and weight of the connecting electrical cable, it still has a large impact on the running dynamics of the robot. It creates a drag force and affects the turning dynamics. The effect of these changes depends on how the tether is mounted and whether the robot is running on the treadmill or on the lab floor [64].

Initially, no account was taken for the effect of the tether. This resulted in the model predicting speeds much higher than those demonstrated by the robot. The addition of a viscous drag force, proportional to the filtered velocity of the robot and located at the center rear of the robot, accounts fairly well for the observed cable drag. During normal running this simulated tether produces 0.42 N of drag force, which is equivalent to about 14% of the weight of the robot.

4.2 Model Verification

While some care has been taken to match each model component to experimental data there is a limit to the accuracy that can achieved from a simulation with so many simplifications and approximations. To verify that sufficient fidelity has been preserved in the model a number of comparisons between the model and robot behaviors were made. These comparisons include the kinematics during running, as recorded by high-speed video, and the ground reaction forces. The predictive power of the model was tested by looking at the effect of varying valve actuation frequency on velocity.

4.2.1 Kinematic Comparison

A comparison of the animation of the dynamic model versus high-speed video of the robot on a treadmill shows that the motions are quite similar, with nearly identical velocity, body orientation, actuator frequency, thrust duration, leg bend angles, and duration of airborne phases. [1]

A quantitative analysis of the difference between the robot and simulation was performed by comparing high-speed marker data from the robot running to simulation results. A summary of the numerical comparison of the kinematics is shown in table 4.3. As the table reveals, the leg flexing angles and the actuator duty cycles are quite similar. However, the model runs somewhat more smoothly than the real robot with smaller vertical and angular motions of the body.

4.2.2 Sensitivity to Actuation Frequency

For purposes of design, the sensitivity of the running behavior to variations in the robot parameters is of interest. Consequently, the simulation should be able to reproduce the parameter sensitivities that we have observed experimentally. Experiments

[1] The interested reader can view a clip of the high-speed video ($250 frames/second$) superimposed on the animated model at the following URL: `http://dart.stanford.edu:88/Get/File-442/blend3_light.mov` .

Value per Stride	Model	Robot
ΔY Body COM	.0019 m	$.0054 \pm .0012$ m
$\Delta\theta$ Front Legs	40.4 deg	35.6 ± 1.2 deg
$\Delta\theta$ Middle Legs	30.6 deg	26.1 ± 4.4 deg
$\Delta\theta$ Rear Legs	15.5 deg	14.4 ± 2.1 deg
Δ Body Pitch	1.3 deg	2.9 ± 1.0 deg
Mean Body Pitch	9.6 deg	8.8 ± 0.2 deg

Table 4.3: Visual Verification Table

have shown that the stride period used in the open-loop robot controller has a significant and non-linear effect on the speed of the robot [24]. As shown in figure 4.6, adjusting the stride period of the model has a similar effect on running speed and shows an optimum at the same period (approximately 130 ms) as observed for the robot. Thus the model should be useful for evaluating the effects of design changes when tuning the robot for speed. The curve for the model in Figure 4.6 is consistently somewhat above that of real robot on a treadmill, likely due to imperfect modeling of the tether and ground friction. As discussed in section 4.2.3, if the model is tuned to provide comparable ground reaction forces and tether force as measured for the robot, the model consistently runs faster, but with the same sensitivity to stride period and leg angles.

4.2.3 Ground Reaction Forces

Ground reaction forces dictate the acceleration of the body; hence verifying the accuracy of the ground forces predicted during a simulation is an essential test of the veracity of the model. The legs of the robot were designed to function like those of a cockroach, with the rear legs primarily propelling the robot forward, the front legs primarily braking, and the middle legs performing both functions [27]. A comparison of the measured and simulated ground reactions demonstrates that the specialization of the legs is captured by the model (Figure 4.7). The middle and rear legs create less drag in the model than on the robot. This may be due to the absence of the pneumatic tubes on the model, which serve to stiffen the robot's legs for large excursions.

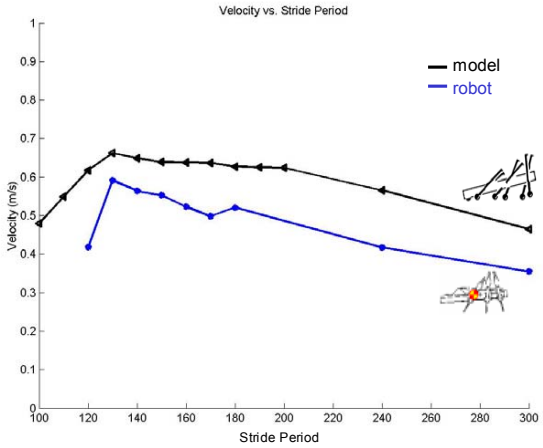

Figure 4.6: Velocity vs. stride period for model and robot

Consequently, the rear corners of the model make a larger contribution to supporting the body and produce more drag than on the robot. This would also explain the reduced vertical forces from the rear legs of the model.

4.3 Conclusions

This chapter has described how the simulation of *Sprawlita* has been built and calibrated. Particular attention has been paid to experimentally tuning the passive dynamics of the hips and the pneumatic actuation system–to a reasonable degree considering the number of simplifications involved in the modeling. While sacrificing accuracy, these approximations have kept the number of parameters that describe the physical system to a manageable level.

To determine how well the model's behavior mimics the robot a number of comparisons have been made. The system's kinematics, parameter sensitivity, and ground reaction forces have all been simulated and tested. While the model is clearly not an exact match, the simulation's behavior is sufficiently close to the robot's to justify its use in studying the robot's behavior and investigating potential design changes and adaptation schemes.

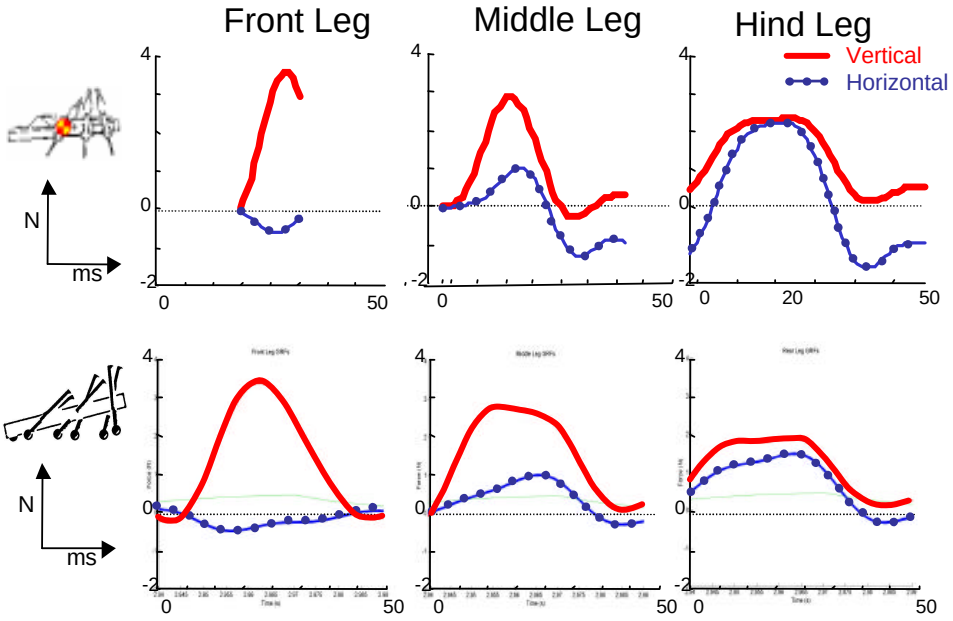

Figure 4.7: Ground reaction forces for each leg of robot and model

The next chapter begins with an exploration of the performance and energetics of the nominal configuration of the simulation. A sensitivity analysis of this base configuration highlights the factors that have the largest impact on the robot's performance. The model is also used to explore the effects of operating the robot over various terrain and tuning the robot for peak performance.

Chapter 5

Parameter Variation and Tuning

The expressed purpose of building a simulation of the robot is to have a platform to investigate the effects of introducing changes into the robot design and controller. Initially, the simulation is used to look at the nominal configuration of the robot. This provides a baseline for comparison of parameter variation studies, and it allows for investigation into how well the robot runs in terms of efficiency and what design changes could improve its performance.

Next, an individual parameter sensitivity test is performed. Three classes of parameters are examined: the run-time control parameters, the leg and body settings, and the environmental variables. The initial analysis tests how much small changes in each individual parameter affect the locomotion speed of the model. A comparison of the sensitivities gives some indication as to the relative importance of various design considerations.

This linear and uncoupled study is followed by more detailed investigation into how various important factors are coupled. Particular attention is paid to the effect of changing the leg angles on performance and the effect of altering terrain variables. As the robot moves on different terrains, the corresponding simulation parameters that model the robot/world interaction should vary. The simulation is used to determine how altering the run-time control variables can be used mitigate the effects of these changes. This understanding can provide the basis for developing potential run-time 'adaptations' of the open-loop controller.

The chapter concludes with a design exercise in which the simulation is used to tune the performance of a version of the robot designed to operate outdoors carrying a significant payload. The robot is then reconfigured according to the predictions of the simulation, and the performance increase is measured.

5.1 Analysis: Nominal Configuration

Looking at how the model runs in its nominal configuration can serve as a basis for perturbation studies, and can give insight into the type of motion the model and robot are using. This baseline configuration was chosen to match the hand-tuned settings used on the robot, and was used in the verification tests in chapter 4.

For the physical robot the running speed is the most straightforward performance criterion to measure. For the simulation, however, it is just as easy to measure the energetics of the system. An analysis of the energetics helps shed light on the relative contribution of design elements to inefficiencies in running. These losses may come from a number of possible sources including:

- Excessive foot drag
- Body drag
- Pneumatic losses
- Antagonistic leg function
- Shortened strides

Each of these aspects of *Sprawlita's* gait result from design decisions that lead to a fast stable robot. The passive hip flexures use stored energy to reposition the legs between strides, but also cause the middle and rear legs to drag. The use of pneumatics gives a compact and powerful linear thruster with compliance, but uses the compressed air inefficiently. The sprawled posture helps stabilize the robot, but the front legs do negative work during part of the stride. The high stride frequency increases speed, but is not optimized for efficiency. An analysis of the energetics

indicates how each of these design decisions contributes to the trade offs between speed, stability, and efficiency.

Table 5.1 summarizes the performance and energetics of the simulation at its nominal configuration. The following sections described how each of these values were computed, and what they tell about the relative impact of each of the design decisions discussed above.

	Value
Speed	0.7 m/s
Energy Consumed per stride	1.86 J
Efficiency	0.049 m/J
Specific Resistance	7.24
Positive Work per stride	0.58 J
% KE exchange per stride	21.7
% KE stored in PE	5.8

Table 5.1: Nominal Case Energy and Performance Values

Speed

With a nominal stride period of 130 ms and a forward velocity of 0.7 m/s, the robot travels 0.091 $meters/stride$. With a piston stroke of 20 mm and a mean leg angle displacement of about 30 $degrees$, the body center of mass can travel at most .032 m per stance phase. With two stance phases per stride, this indicates that each airborne phase covers at least 0.015 m. Although these flight phases are not large, they reduce the dragging of the rear feet and increase the ability of the robot to clear obstacles.

5.1.1 Energy per Stride

For releasing compressed gas as an energy source, and assuming an adiabatic expansion, the equation for the energy per stride is given by:

$$Energy/Stride = \sum_{i=1}^{6} \left| \frac{h_{air}\ stroke_i\ force_i}{R\,T} \right|_{Stride} \tag{5.1}$$

Where the enthalpy of air h_{air} is $(300.19kJ/Kg)$, the $stroke_i$ is the maximum stroke excursion for each leg, $force_i$ is the maximum force generated by each piston, R is the gas constant for air $(287\frac{J}{kg\ K})$, and T is the temperature $(300K)$.

This calculates the power consumed by looking at the maximum force applied over the maximum stroke length for each piston per stride. Measuring the maximum extension of each piston is necessary, since during normal operation, the full stroke is not utilized by all of the legs. When applied with the ideal gas model of pneumatics, this measure includes the significant amount of air used to fill the tubes, and gives a conservative estimate.

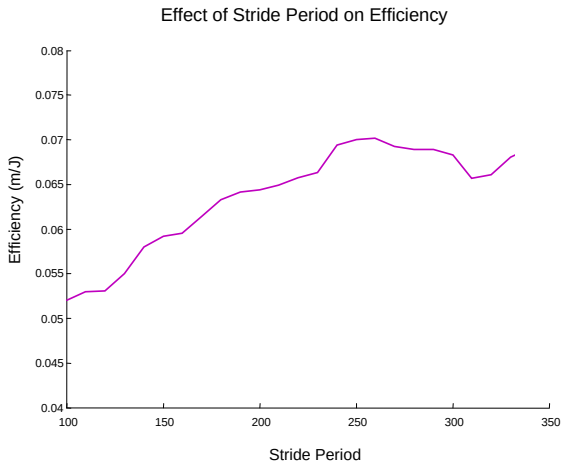

Figure 5.1: The effect of altering the valve stride period on locomotion efficiency.

This measure is used to calculate the effect of altering the valve activation period on running efficiency, as shown in figure 5.1. Significant is the fact that the maximum locomotion efficiency for *Sprawlita* occurs at a stride period of about 260ms, as opposed to 130ms stride period which is optimal for speed (as shown in figure 4.6). This difference between optimal speed and efficiency was also found for the one-legged planer hopper investigated by Cham [21].

As with the simple model, the optimal efficiency comes with the maximization of stride length, which occurs with longer stride periods. Longer stance phases result in greater flexion at the hip, allowing the body to rock further forward during stance.

The actual increase is a function of body mass, linkage kinematics, and hip stiffness. Past a certain equilibrium position, for very long strides, the body begins to rock backwards decreasing stride length and efficiency.

For normal running the natural period of the body translation and rotation during stance is longer than the duration of actuation. This reduces the efficiency at the nominal operation point, but alterations to the body dynamics to make it 'fall' faster (e.g. by changing the mean leg angles or hip compliance) impact the system's stability. This is one way in which changing the system's physical parameters trades efficiency for speed and stability.

5.1.2 Specific Resistance

A common measure for locomoting efficiency in running animals and robots is 'specific resistance.' This is a scalable measure of how much power is required to run at a given speed. For robots both total electric power or mechanical power delivered by the actuators have been used to determine their specific resistance.

The equation for specific resistance is given by:

$$\epsilon = \frac{P}{mgv} \tag{5.2}$$

Where P is the power consumed, mg is the weight, and v is the velocity of the robot. In table 5.2 the value for power consumed by *Sprawlita* is based on the volume of compressed air used. Some systems have reported specific resistances based on mechanical work done by the actuators. For the simulation of *Sprawlita*, using this value would result in $\epsilon = 2.19$. This large difference highlights the inefficiencies in *Sprawlita's* method of converting stored energy into useful work done by the actuators.

As table 5.2 shows, *Sprawlita* is relatively inefficient in terms of energy use. This is not surprising considering the large amount of compressed air that is vented without being used each stride. The replacement of the pneumatic drive system with an onboard electromechanical system in *iSprawl*, however, results in a specific resistance of 1.7 [55]. This rather more impressive value indicates that the cost of the sprawled posture and open-looping timing frequency (which are preserved on *iSprawl*) is not

	Value
Scout II	1.0
ASV	1.3
Rhex	2.5
MIT Quadruped	5.0
Sprawlita	7.2
iSprawl	1.7

Table 5.2: Reported specific resistance for running robots

nearly so high as the pneumatic losses and foot drag (which have been removed).

5.1.3 Mechanical Work

An examination of the mechanical work performed by each leg highlights their distinct functional roles. The equation for mechanical work done by the pistons per stride is given by:

$$\frac{W}{Stride} = \int \sum_{i=1}^{6} F_i \cdot V_{com} \tag{5.3}$$

Where F_i is the thrust vector for each leg and V_{com} is the instantaneous velocity of the center of mass of the body. Although each leg is structurally identical, the different leg angles dramatically change the function of each leg. The front legs, which primarily stabilize and lift the robot only contribute 19% of the actual work done on the body. The front legs actually do a small amount (about 2.8% of the total) of negative work. This active deceleration of the robot occurs at the beginning of the stride, and is highly dependent on the nominal leg angle. The middle legs contribute 33%, and the rear legs are the primary thrusters, adding 48% of the work done.

A significant amount of energy is expended in lifting the robot and in lateral oscillations. In fact only 30% of the energy consumed by the robot actually propels it forward, countering the effects of drag and impact losses.

The asymmetric or sprawled leg posture of *Sprawlita* results in different functional roles for each leg. The front legs actually do a small amount of negative work, but the

braking and lifting forces they provide are essential for the whole-body stabilization.

5.1.4 Kinetic Energy Exchange

As part of their locomotion cycle most walking and running systems transfer energy between kinetic and potential forms during locomotion. For walking systems a significant percentage of energy is stored as gravitational potential during the middle of a stride. Runners often store the energy from impact in tendons or springs. The amount of energy exchanged between kinetic and gravitational potential forms gives an indication of the nature of locomotion (run vs. walk) and gives an upper limit on the amount of energy recycled through structural elastic elements.

The percentage of kinetic and potential energy exchanged and stored each stride as given in table 5.1 is calculated based on the body of the robot, neglecting the relatively light legs. Just over 85% of the kinetic energy of the robot is represented by the average forward velocity of the robot. Only 5.8% of the total energy of the system is represented by the vertical oscillations of the body. This ratio indicates a running gait, with very little energy being exchanged between kinetic and gravitational forms.

Over a stride, the kinetic energy only changes by 22%. This is indicative of a smooth running gait. The geometry of *Sprawlita's* leg flexures precludes their use in returning the energy they absorb during stance. They do however use their stored energy to return the legs to their nominal position removing the necessity of actuating the hip joint. Consequently there is no effective vertical spring, only a damper. Therefore at least 22% of the system kinetic energy has to be added by the actuators each stride. Thus it is less efficient than a pure SLIP runner, which could ideally recycle the energy from impact. The advantage of *Sprawlita's* leg design is in simplicity, having only one actuator, and stability–the heavy damping quickly stabilizes perturbations.

5.1.5 Summary

In its current configuration *Sprawlita* is relatively inefficient compared to other running robots. The analysis of the energetics of *Sprawlita* described in this section

indicates that of the potential sources of inefficiency described in section 5.1, the losses due to pneumatics and leg drag are the most significant and least productive.

The other sources of loss, including the negative work done by the front legs and the shortened strides from the high valve actuation frequency, are less significant and serve to stabilize and increase the speed of the robot. The addition of vertical springs in the legs should increase efficiency, but their effect on stability should be monitored.

By using a sprawled posture and running at high frequency, *Sprawlita* trades energetic efficiency for speed and stability. As the electromechanical *iSprawl* indicates these trades are very effective, and their cost is small compared to the waste in the pneumatic system and from leg drag.

5.2 Parameter Sensitivity

The experimental design of experiments performed on *Sprawlita* (section 3.2.2) investigated the effects of varying a easily changed physical aspects of the robot on performance. Since the physical design, rather than a software controller, is responsible for the stability and performance of the robot it is essential to understand how all of the physical parameters affect performance, not just those that are easy to change at run time. This section investigates this and identifies the key parameters for further study.

The parameters that influence the behavior of the robot are divided into three categories as shown in table 5.3. The first set has to do with the actuation of the robot, and can be varied at run time. These include three parameters for controlling the timing of the pistons, and three settings for the servos attached to the legs. This set represents the basis for any adaptive behaviors with which to imbue the robot. Additionally, these simulation results can be compared to the experimental data from section 3.2.2 as a further check.

The second category defines the dynamics of the body and legs. There is a parameter for the inertia, stiffness and damping for each degree of freedom of the legs. These define the passive rotational and linear retraction dynamics. Any changes to these parameters on the robot requires a redesign of the legs or replacement of components

and are consequently expensive to implement, but important to understand.

The third set of parameters define the interaction with the surface on which the robot is running. These can be considered as uncontrolled parameters, since the robot when running outside has little choice as to the character of the surface on which it runs.

The sensitivity of the robot's straight-ahead velocity is calculated with respect to each of the parameters discussed above according to equation 5.4.

$$Sensitivity = \frac{\left|\frac{\Delta V}{V}\right|}{\left|\frac{\Delta X}{X}\right|} \tag{5.4}$$

Where (V) is the robot's nominal steady-state velocity and (X) is the parameter being modified. Each parameter was altered by +/- 1,5, and 10 percent of the nominal values, and the results were averaged. For the angular cases, indicated with a (*), the nominal values were modified by +/- 1,5, and 10 degrees rather than a percentage of the nominal.

The third column in table 5.3 shows a measure of the stable range of operation for each parameter. This range was calculated by varying the parameter from 50% to 150% of its nominal value and evaluating its performance. The range that results in 'felicitous' running (i.e. stable, period-1, running at speeds of greater than half of the nominal velocity) is shown. The large range for each of these variables indicates the enormous design space available, and the relative insensitivity of the robot's stability to small parameter changes or model discrepancies. The fundamentally stable nature of the locomotion scheme reduces the effects of modeling errors and accentuates the applicability and utility of the model. The heavy reliance on passive compliance may largely be responsible for this fortuitous result.

Figures 5.2, 5.3, and 5.4 show graphically the effect on performance caused by varying each parameter over this range. A dashed line is drawn for configurations resulting in non-felicitous running. In addition, the nominal setting and +/- 10 percent levels used for calculating the sensitivity are shown.

	Nominal	**Vel. Sens.**	**Stable Range**
Stride Period	0.130 s	0.160	-40 to +50
Duty Cycle	35 %	0.830	-20 to +50
Front Leg Angle	-6.0 deg	0.780*	-5 to +40*
Mid Leg Angle	-30.0 deg	0.143*	-50 to +20*
Rear Leg Angle	-58.0 deg	2.015*	-10 to +20*
Hip Stiffness	.052 Nm	0.153	-10 to +50
Hip Damping	2.3E-4 Nms	0.024	-50 to +50
Supply Pressure	.40 MPa	2.435	-10 to +50
Piston Stiffness	55 Nm	0.318	-50 to +50
Piston Damping	2.1 Ns/m	0.704	-40 to +50
Stroke Length	.020 m	0.161	-50 to +50
Body Mass	.215 kg	0.601	-50 to +50
Upper Leg Mass	0.009 kg	0.076	-50 to +50
Foot Mass	.001 kg	0.016	-50 to +50
Surface Friction (μ_s, μ_d)	1.2/1.08	0.331	-40 to +50
Ground Stiffness	62.6 kN/m	0.046	-50 to +50
Ground Damping	10 Ns/m	0.057	-50 to +50
Tether Drag	0.53 Ns/m	0.181	-50 to +40
Slope	0.0 deg	5.12*	-40 to +10*

Table 5.3: Nominal case parameter variation sensitivity

5.2.1 Actuated Parameters

Figure 5.2 shows the variation for the parameters in the first section of table 5.3. These five parameters describe the system configuration that can be altered during run-time. The stride period and duty cycle determine the valve actuation, and the three nominal leg angles can be altered by small 'shape changing' servo motors at each hip.

Among these factors, the rear leg angle has the greatest sensitivity. As discussed in section 5.1.3, the rear legs produce almost 50% of the positive work on the robot. Decreased performance occurs when the rear leg angle becomes too large causing foot slippage, and when the angle becomes too small, resulting in less force pushing the robot forward. The front legs also show a high sensitivity. They only produce a small amount of net work, but they are particularly important for stabilizing the robot. As

shown in figure 5.2(c) small decreases in the angle results in unstable running.

The stride period and the duty cycle combine to determine the duration of the thrust phase. Varying either of these will increase or decrease the net thrust from each stance phase. Although duty cycle has a higher sensitivity, figures 5.2(a and b) have essentially the same shape. Additionally, by adjusting the stride period, the frequency as well as the magnitude of each thrust phase can be altered, and the actuation frequency can be tuned to match the natural dynamics of the body.

It is also worth noting that all of the curves in figure 5.2 have a parabolic shape, with the nominal condition very near or at the maximum configuration. While the global velocity maximum for the actuation parameters may be at some other setting than those selected as the nominal, only by looking at leg angle and valve parameter interactions will further tuning be possible.

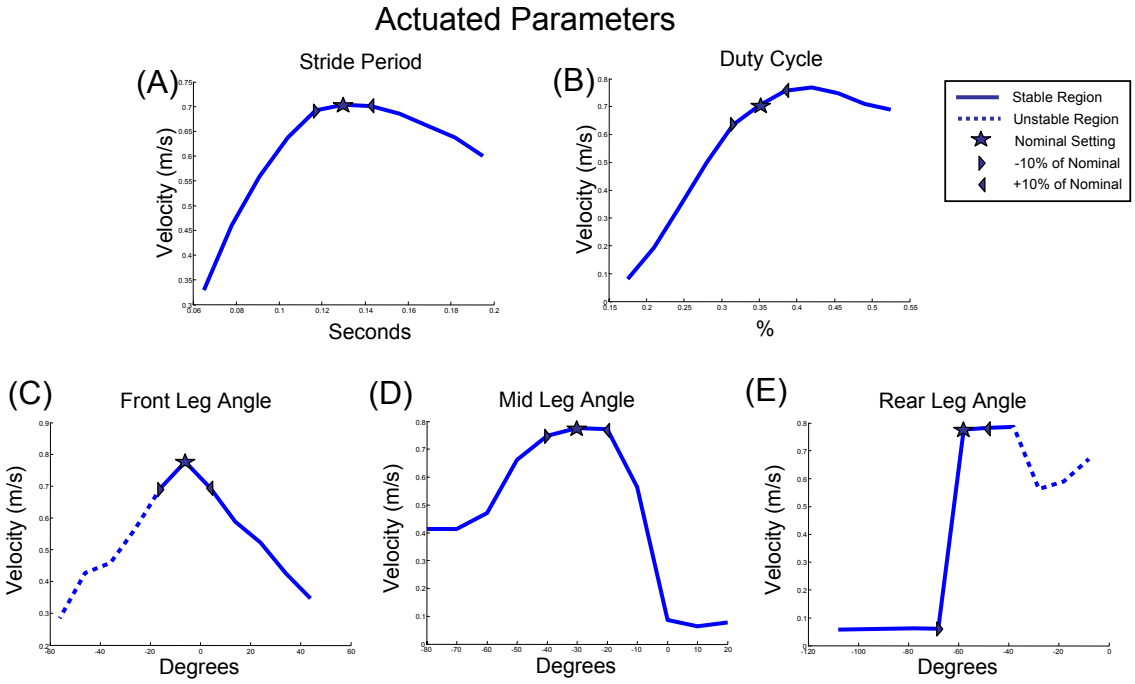

Figure 5.2: Velocity Profiles for Actuation Parameter Variations

5.2.2 Body and Leg Parameters

The greatest sensitivity in the second section of table 5.3 is associated with the pneumatic supply pressure. Not surprisingly increasing the available pressure to the legs dramatically increases the robot's speed. If a simple mechanism were in place to regulate the pressure, it would serve as an effective method of controlling the robot's speed. As shown in figure 5.3(c), within the range of values physically achievable, simply maximizing the pressure is desired.

Hip stiffness and damping are physically linked by the nature of the polyurethane used in the hip flexures. Figure 5.3(b) indicates that minimizing the damping is desirable, but the stiffness, as shown in figure 5.3(a), is already near the limit of stable operation. Since the hip stiffness can be arbitrarily specified, and has a large impact on stability, correctly tailoring the compliance to its local maximum is critical to tuning the overall performance of the robot.

As shown in figure 5.3(d-f) each of the piston parameters has a straightforward effect on performance. A long, compliant, and low friction piston would be ideal. According to table 5.3, the damping is the most significant of these three parameters. This fact motivated the search and replacement of the Festo pistons with pistons of the same size produced by SMC corporation. These new pistons had a slightly higher stiffness (76.5 vs. 55.0 N/m), but had a considerably lower effective viscous friction (1.76 Ns/m vs. 2.1 Ns/m). No commercially available pistons with longer stroke lengths (at similar diameters) or lower effective damping were found. Any further refinement of these parameters would require custom fabrication or an alternative actuation scheme. Some attempts at devising linkages and coupling pistons to double the stroke length were attempted, but without great success.

As expected, the mass of the robot's body and legs has a large effect on the robot's performance. As shown in figure 5.3(g-i), the effects of increasing the body and the leg mass are monotonic and nearly linear over the range of values tested. Clearly shaving weight is advantageous, but this is naturally limited by structural and performance requirements. The parameters that fully define the moments and products of inertia of the body and legs were considered of secondary importance, and were not examined in this investigation.

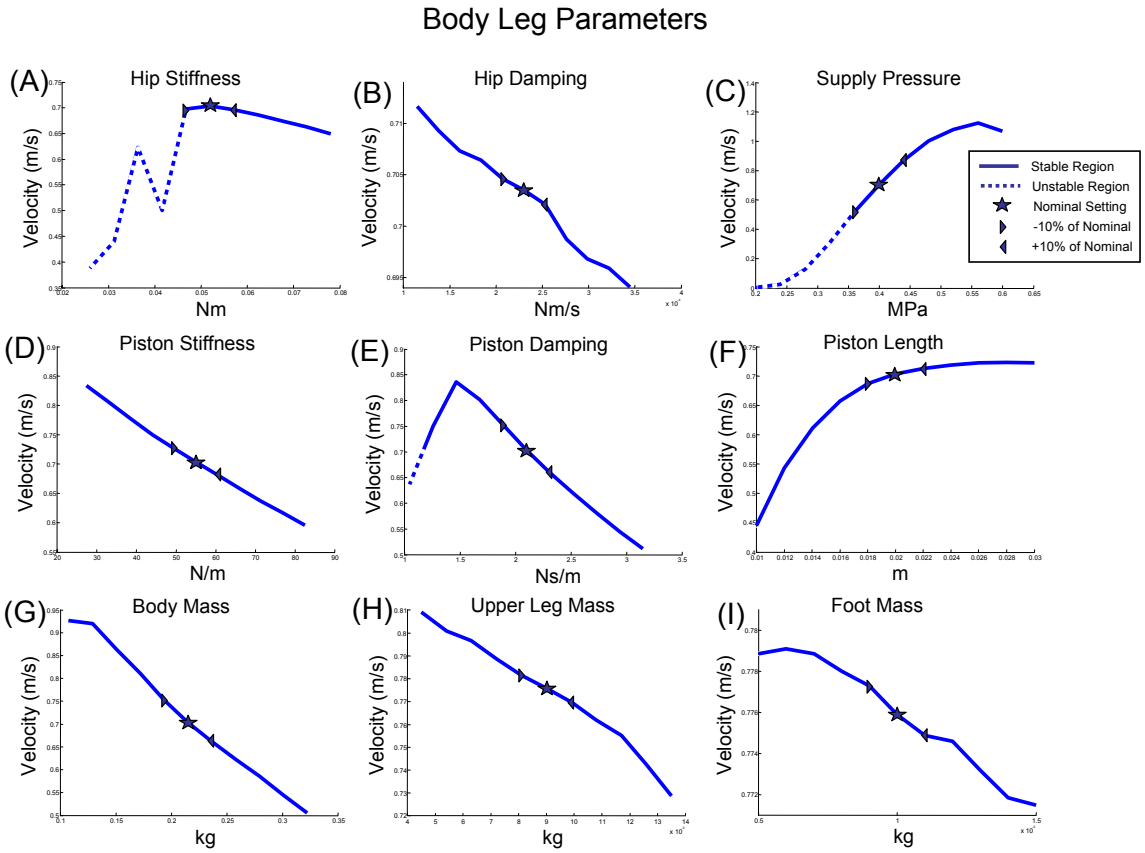

Figure 5.3: Velocity Profiles for Body Parameter Variations

5.2.3 Environmental Parameters

The sensitivity analysis shown in table 5.3 indicates that ground slope and surface friction have the greatest effects on the robot's velocity. Clearly, the removal of the tether connecting the robot to the computer and air-supply would be advantageous. To a lesser degree increasing the ground stiffness and damping would also be profitable. At first glance, it may seem surprising that increasing ground damping would increase velocity, however the decrease in bouncing and skittering from increasing damping result in a net gain in speed. Since one cannot always choose the conditions of the terrain, direct manipulation of these parameters outside of the lab being impossible, the best one can do is alter the actuation parameters to attempt to compensate. A more detailed analysis of the coupling of these two sets of parameters is undertaken in section 5.4.

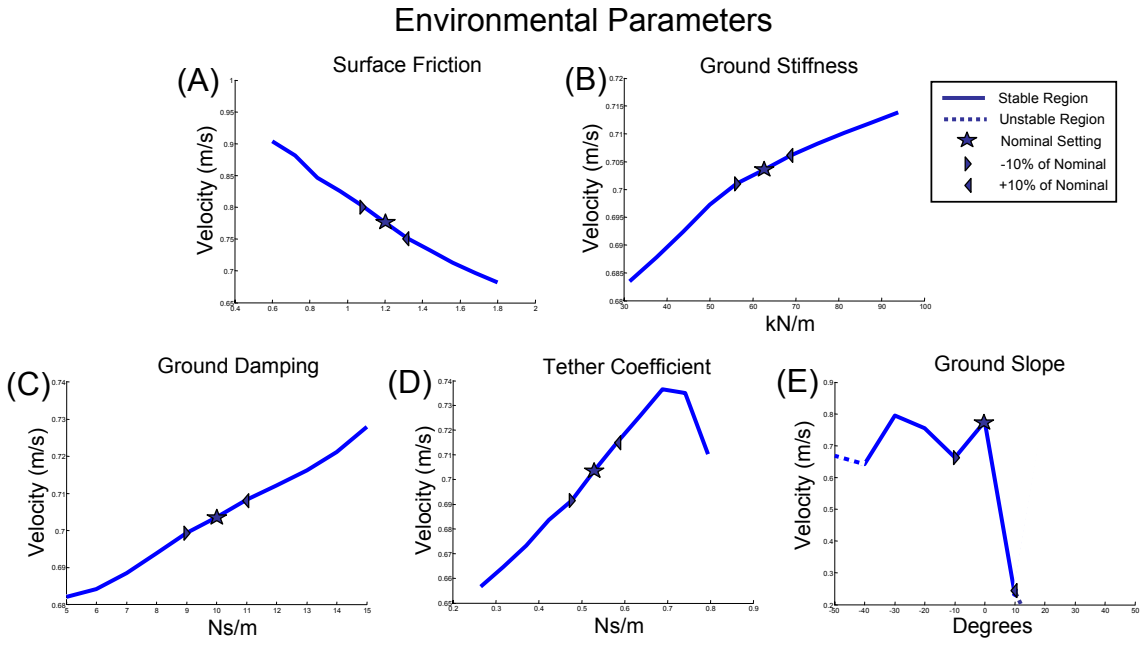

Figure 5.4: Velocity Profiles for Environmental Parameter Variations

5.2.4 Comparison to Experimental DOE

The sensitivity analysis performed on the simulation agrees well with the results of the design of experiments discussed in section 3.2.2. Both studies indicate the significant effect of ground slope, hip compliance, rear and front leg angle, and stride period in almost exactly the same order! The only exception was that in the experimental results, the hip compliance was found to be more significant than the leg angles and stride period. In the simulation results, this order was switched, but this may largely be due to the greater range of hip stiffness tested experimentally. As figure 5.3(A) shows, a slightly larger range of hip stiffness results in dramatically changed performance, which exactly matches the experimental findings.

5.2.5 Parameter Variation Conclusion

This linear perturbation analysis provides initial insights into the parameters to be focused on when considering means of improving the speed of the robot. Future studies will consider the potentially significant and non-linear coupling that arise while simultaneously varying multiple parameters.

Leg angles, stride period, and hip stiffness and damping are the best candidates for tuning the operation of *Sprawlita*. Clearly, one wants to reduce parameters such as piston friction, tether drag and mass, but there is a physical limit on how much these can be reduced. Both the actuation parameters and the hip stiffnesses are easy to change, and a full range of values is open for investigation.

As shown in figures 5.2 and 5.3, leg angles, stride period, and hip stiffness all have parabolic velocity profiles, indicating that these parameters need to be tuned to a specific target, not just maximized or minimized. This and their coupled nature make their tuning complex. The use of these five variables to tune performance will be investigated in the remainder of this chapter, and they will be revisited in chapter 6 to tune for stability.

5.3 Leg Angle Variation

One of the unique features of the *Sprawl* robots is the distinct function role for the front, middle, and rear legs. Although currently all of the legs are identical in structure, their orientation with respect to the body dramatically affects their behavior. When constructing the robots we hypothesized that the introduction of a 'sprawl angle' into their design would increase their stability.

Experimental testing has shown that the effects of changing *Sprawlita's* nominal leg angles are coupled, and have a large impact on the locomotion dynamics. To investigate the nature of this coupling, a series of simulation trials were run. In order to allow for visualization of the results, and to reduce the number of tests necessary it is desirable to intelligently constrain these parameters. Consequently, contralateral pairs of legs are fixed to have the same orientation. All three leg pairs were further constrained such that the line of action of each piston intersected at a common point, as shown in figure 5.5. With these constraints, the orientation of all of the legs can be specified with two parameters. Plotting the location of this intersection point relative to the body of the robot allows for a geometric interpretation of the results.

Figure 5.5 shows the effect of varying this leg intersection point. 121 different configurations which span the reasonable configuration space were selected. The nominal configuration is shown by the dotted lines. For each of these configurations two circles are drawn with the radius of the outer circle being proportional to the maximum steady-state velocity of the robot, and the size of the smaller being proportional to the minimum steady-state velocity. If both circles are visible, it is indicative of non-period-1 running. The circles with x's inside represent configurations that resulted in the robot nose-diving. This mapping allows one to see the effect of the coupling of the leg angles that could not be seen by the sensitivity analysis alone (as in figure 5.2).

Earlier work with simple one-legged models of *Sprawlita* has shown that optimal speeds are usually achieved with configurations that lie on the boundary of instability [21]. These simulation results indicate that this also holds for the more complex six-legged robot morphology. This is an important verification of the applicability of the

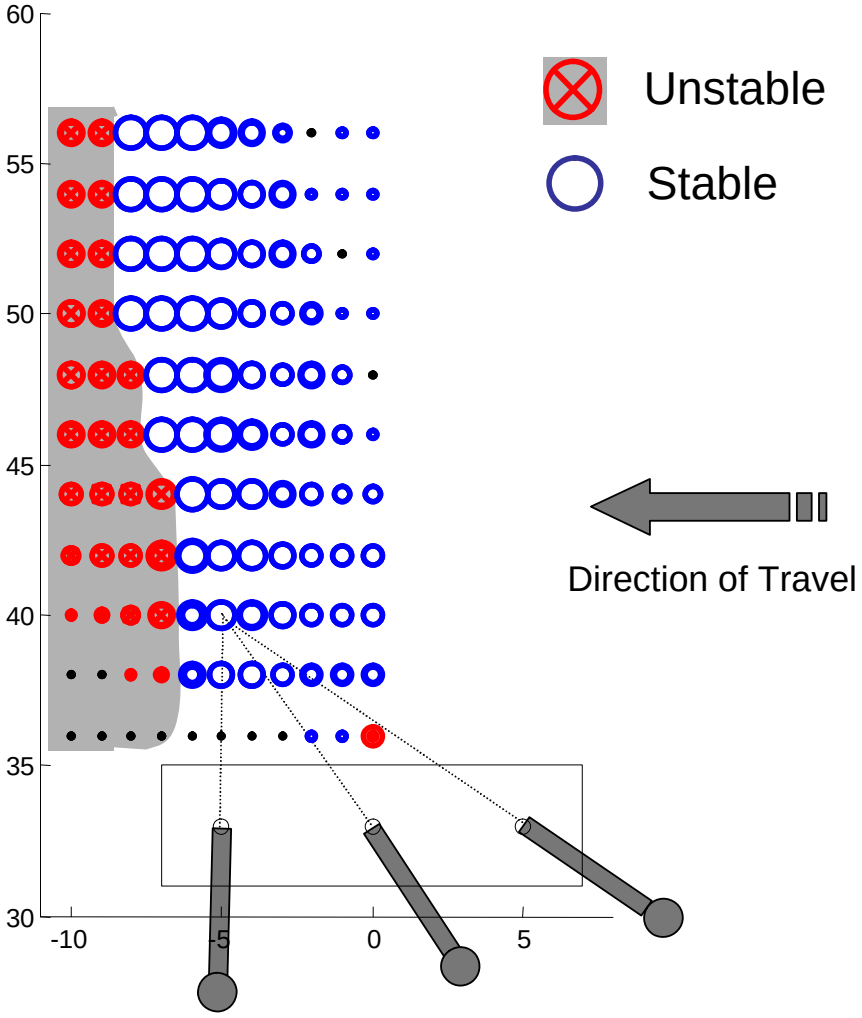

Figure 5.5: Speed and stability as a function of leg orientation

simple template models to anchored robot designs.

In addition to supporting the findings of single-leg models of running, the simulation highlights aspects of the robot design that cannot be captured by such simple models. Specifically, figure 5.5 shows how increasing the sprawl angle of the legs decreases speed slightly, but increases the range of leg settings that produces moderately fast and stable locomotion. This increase is evident for a range of mean leg angles, but the amount of sprawl is limited by frictional constraints.

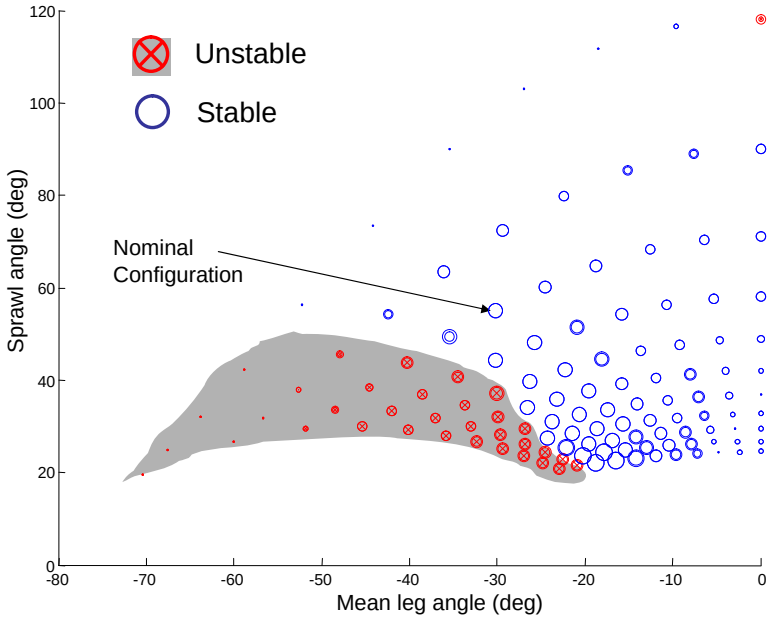

Figure 5.6: Speed and Stability as a function of leg orientation

By looking at the same data replotted in terms of mean leg angle and sprawl angle, as shown in figure 5.6, we can more clearly see the effect of deviation from a parallel leg orientation (0° sprawl angle). The maximum speed occurs at lower sprawl angles, but there is a narrow range of mean angles that achieves this performance, and it is very close to the range of unstable configurations. As the sprawl angle increases, the speed decreases, but so does the sensitivity to the mean leg angle. At the nominal configuration (as shown) there is a fair amount of room for leg misalignment while still producing fast and stable motion.

5.4 Ground Properties and Adaptation

While it is desirable to have a robot that can run well over just about any terrain, a distinction can be made between dealing with obstacles and dealing with different types of otherwise smooth ground.

The difficult tasks of obstacle avoidance and climbing are areas of active research interest. As discussed in section 3.2.3 *Sprawlita* has demonstrated that it has no problem clearing objects of hip/belly height or lower. For larger obstacles, detection and maneuverability are required and are being considered separately. Some discussion of this is found in [64].

While smooth terrain is comparatively easy to traverse, running well on it depends greatly on the physical properties of the ground. As shown in section 5.2.3, running over slippery or soft ground or running uphill make it more difficult to move quickly. Changes in the control scheme may be necessary to minimize the resulting performance deteriation. This section describes the effects of different substrate conditions on forward running, and how changing actuation parameters is linked to these conditions.

5.4.1 Motivation: Adaptation

Although there is a great range of ground conditions and slopes in nature, the character of the environment often changes gradually. Even when there are abrupt changes, the frequency of such events is low compared to the robot's stride frequency. Consequently, robots, as well biological systems, can afford to modify their basic running pattern over a number of strides when the terrain changes. Thus, using a slower, high-level, adaptation scheme to tune the fast, low-level, open-loop control to compensate for a changing environment is a promising approach [23].

Cham *et al.* have demonstrated that a method based on ground contact timing of the feet can be use to regulate the robot's leg firing frequency in order to maximize ground speed over a level surface [24]. This approach was motivated by the analysis of simple one DOF hoppers. It was found that maximum efficiency and hopping heights could be achieved for long-thrust hoppers when the end of their leg thrusts

were timed to correspond to lift off. A simple contact switch on one foot of *Sprawlita* was instrumented to measure takeoff and landing events, and this information was then used to increase or decrease the leg firing frequency.

This delightfully simple method worked well on a flat treadmill. When the same scheme was used on a robot running uphill, the speed improved, but to a sub-optimal level. How this adaptation scheme fares for soft or slippery ground has not yet been tested.

The fundamental information required to evaluate the need or usefulness of an adaptation scheme is the effect that varying the ground properties has on the performance of the robot. As discussed in section 3.2.1, while running uphill always slows the robot down, increasing the open-loop stride period of the robot can help mitigate the effect. For each slope a different stride period becomes optimal.

What happens as the ground becomes softer or slicker? Can we quantify the changes in the control scheme that will give the best performance for these conditions? Should something other than stride period be altered to improve performance? Is it desirable to have auxiliary sensors to detect slope, ground stiffness, etc.? To answer these questions a study of the interaction effects of the environmental and actuation parameters is undertaken.

5.4.2 Environmental Simulation Studies

In the dynamic simulation there are four environmental parameters that can be varied. These are ground slope, surface friction (comprising both static and dynamic terms), ground/foot interaction stiffness and ground/foot damping.

It is straightforward to measure the effect of changing the terrain and the actuation parameters in terms of the robot's velocity and efficiency. Efficiency is of interest as the stride period changes, as it is the primary parameter that affects the rate of energy consumption.

Simulations can show for each possible environment what control strategy would result in optimal running, and whether ground sensing would give enough information for the adaptation scheme to reach this ideal operation point. In addition to varying

the robot's valve actuation period, as done in [24] the mean leg angle was chosen as a second potential adaptation variable to investigate.

Configuration of Environmental Studies

Simulations were run while varying the four environmental parameters, as shown in table 5.4.

Parameter	Test Values	Units
Slope	(**0**, 3, 6, 9, 12)	degrees
Friction	(0.3, 0.6, 0.9, **1.2**, 1.5)	
Stiffness	(37.5, 75, 150, 300, **600**)	KN/m
Damping	(5, **10**, 20, 40, 80)	N/(m/s)

Table 5.4: Environmental parameter values

The bold values indicate the nominal values that were held fixed while varying each parameter individually. Each configuration was run over 16 different stride periods varying from 50 ms to 200 ms, and eleven different mean leg angles ranging from -33 *degrees* to vertical. For each test the velocity and efficiency were calculated.

5.4.3 Stride Period Variation

This section describes the effects of varying the open loop stride period as the environmental parameters are changed. This indicates the degree to which altering the valve actuation frequency can be used to adapt to changes in damping, stiffness, friction, and slope. The effect of changing stride period is measured in terms of robot velocity and efficiency.

Figure 5.7 shows how the robot velocity varies as a function of changing terrain conditions. Figure 5.7(a) shows that for the range of ground contact damping tested there was very little change in the robot's velocity. Higher values of contact damping reduced the amount of bouncing and skittering from contact, and resulted in faster running. Altering the open-loop stride frequency had no effect on the robot's variation in performance over the tested range of values.

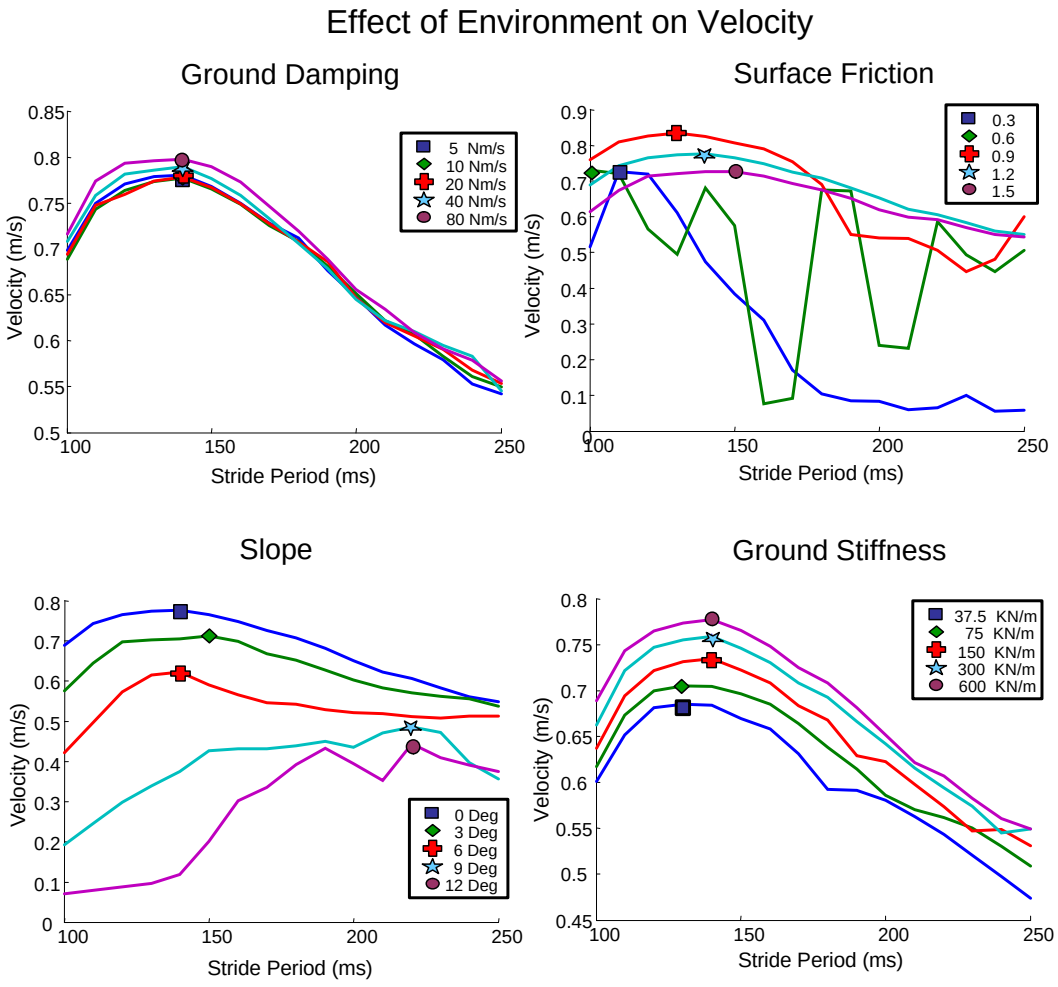

Figure 5.7: Effect of ground contact stiffness on the velocity for various stride periods

The range of values tested for surface friction captured a more interesting range of behaviors. As shown in figure 5.7(b), the smallest coefficients of friction (0.3 and 0.6) resulted in large variations in performance for a range of stride periods. The shortest stride frequencies tended to mitigate the amount of slipping, especially for the slipperiest surface. As the level of friction increased beyond 0.9, the performance of the robot decreased, due to an increase in drag forces. This decrease can be slightly reduced by slowing the stride frequency. Thus, it appears that a run-time adaptation scheme which alters the open-loop stride period for changing surface friction may be desirable.

The most significant environmental parameter tested, as shown in Figure 5.7(c), is clearly ground slope. For slopes of 9 *degrees* or more, the robot should run at a significantly higher stride period in order to minimize the decrease in performance. Slope and open loop running frequency are clearly correlated, and an adaptation scheme is called for.

Increasing the stiffness of the surface resulted in an increase in running speed for the robot, as shown in Figure 5.7(d). Altering the stride period, however, had a negligible effect on the variation.

Efficiency

As noted in section 5.1, increasing the valve actuation frequency directly changes the energy consumption of the robot, as well as affecting the performance. Consequently, incorporating the stride period into an adaptation scheme to improve velocity will also have an impact on the robot's energetic efficiency. Alternatively, a different adaptation scheme may be called for to optimize efficiency for changing terrain conditions. To investigate this, the environmental trials described in section 5.4.3 were also evaluated in terms of efficiency. In this case the optimal stride period occurs at about 260 ms (as shown in figure 5.1), the same trends were found for efficiency as for velocity. There may be some evidence for increasing the stride period as stiffness increases, and less evidence for slope, but otherwise the results are identical.

Interaction effects

In order to determine if there were any significant parameter interaction effects a partial factorial design of experiments was run. Each environmental parameter, as well as stride period, was assigned a high and low value as shown in table 5.5.

Parameter	Low value	High value	Units
Slope	0	8	deg
Friction	0.9	1.5	
Stiffness	37.5	600	KN/m
Damping	5	80	N/(m/s)
Stride Period	130	200	ms

Table 5.5: Stride Period Interaction Effect Parameters

The values for the design of experiments correspond to the ranges tested for the individual parameter studies. A total of thirty-two trials were run, and the steady-state velocity for each was recorded. Table 5.6 shows the statistical significance of each of the interaction effects. Each of the primary factors except stiffness and friction were found to be statistically significant, with a p-value of less than 0.05. This indicates that each of these factors substantially influences the velocity and efficiency of the model. There was only one stride period interaction effect that was significant, slope, with a p-value of 4.28e-7. These results agree with the individual parameter interaction study of section 5.4.3.

Parameter	P-Value
Slope and Friction	2.16e-11
Slope and Stride Period	4.28e-7
Slope and Damping	.0036
Stiffness and Damping	.0058

Table 5.6: Results of Stride Period DOE

The three other interactions that were significant were the slope and friction interaction (p-value = 2.16e-11), the slope and damping interaction (p-value = 0.0036), and the stiffness and damping interaction (p-value = 0.0058).

This set of simulation results indicate that the interaction of slope and friction does make a statistically significant impact on the robot's locomotion. The results, however, also suggest that while stride period adaptation is beneficial for changing slopes, the secondary effects of slope and friction or slope and stiffness are not susceptible to mitigation by changing the robot's open loop running frequency.

5.4.4 Leg Angle Variation

As an alternative to varying stride period, modifying the robots leg configuration could serve as the basis for a terrain adaptation scheme. Changing the robot's leg angles may reduce the slipping on a low friction surface, or make the robot less likely to stumble on a very soft surface. To investigate this the parameter variation study performed in section 5.4.3 was repeated with the leg angles being varied instead of the stride period. For each surface variation the mean leg angles were altered over the range of values shown in figure 5.8.

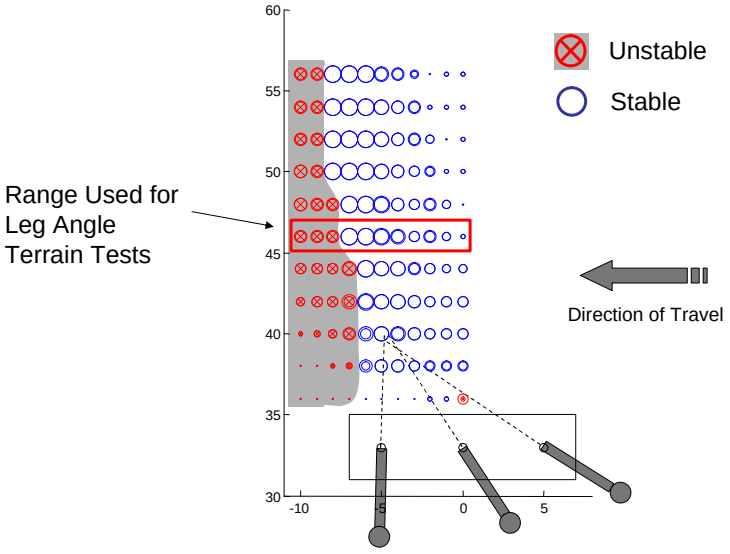

Figure 5.8: Range of leg angles chosen for terrain adaptation tests

As shown in figure 5.9, altering the mean leg angle for changing stiffness and damping seems to have little effect. For high or low friction there appears to be

some advantage to reducing the mean leg angle (making the legs more upright). For low friction this reduces slipping, and for high friction, it reduces drag. The most interesting effect comes from ground slope. As figure 5.9(c) clearly shows, there is a huge advantage to tilting the legs forward for increasing slope, even into a range that would result in unstable running on flat terrain. Adjusting the mean leg angle from $-26°$ to $-36°$ almost double the robots speed on a $12°$ slope.

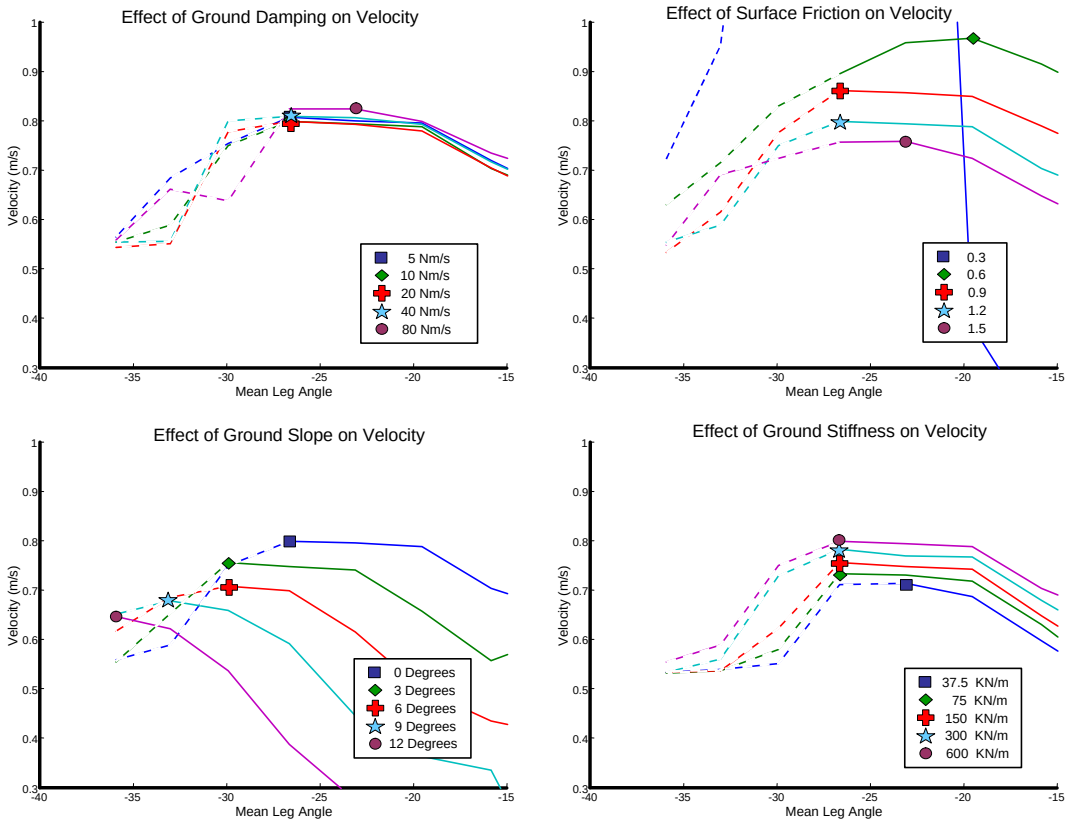

Figure 5.9: Effect of varying the mean leg angle on the velocity of the model for various terrain conditions

5.4.5 Conclusions of Environmental Studies

For the range of values examined in the parameter study, it is clear that changes to the surface friction and ground slope have a greater effect on locomotion speed and

efficiency than do changes in the stiffness and damping of the surface.

From the results of the parameter variation studies and the design of experiments it appears that changing the stiffness or damping of the surface over which the model runs does not require significantly changing the stride period adaptation scheme based on foot-contact timing previously developed. As suggested by earlier experiments, a change in slope requires a different stride period to optimize the robots running. This study indicates that changes in surface friction, as well as ground slope may benefit from a stride period alteration scheme: slower frequencies for climbing hills, and higher frequencies for slippery surfaces.

As with stride period, changing leg angles appears to have little effect on peak performance for changing ground stiffness, damping, and friction. Altering the leg angles, however does have a significant effect when running on slopes. When running up hill the robot should shift its mean leg angle forward to compensate, even though these configurations would cause it to crash when running on flat terrain. Altering the stance parameters appears to be more effective than altering the stride frequency. For example on a 12 *degree* slope altering the leg angles results in stable running at speeds over 50% higher than can be achieved by modifying the timing of the stride period.

5.5 Application of Model in Design Process

Up until the adaptations described in this section, all of the *Sprawl* hexapods were confined to running indoors. Each platform was connected to an air supply and to a off-board microprocessor.

In order to free the robot from the lab, the microprocessor interface was replaced by on-board circuitry and a battery. Together these weighed about 100 g (about 1/3 of the body mass) and were attached to the back of the *Sprawl* body. A portable compressed air supply was provided by a small tank that could be easily carried by the operator. The difficulty with this setup was that after adding the battery pack and a new set of stiffer legs the robot ran at a top speed of less than 0.40 m/s. (As compared to the tethered versions that could run at speeds over 0.80 m/s.)

This section describes how the dynamic simulation was used to determine quantitatively what changes needed to be made to the robot in order to make its performance similar to its tethered cousins.

5.5.1 Approach

The simulation model was adapted to match the new robot's configuration by changing the valve pneumatics, adding mass for a battery and six valves, and changing the stiffness and damping of leg flexures. Parameter variation tests were then run to investigate the effect on the model of these changes.

5.5.2 Leg stiffness

Prior to the simulation studies, the new robot's hip flexures were initially scaled up from *Sprawlita's* 2.76 mm to 4.3 mm in order account for the larger mass of the reconfigured robot. The initial experiments with the simulation indicated that these hips were probably too stiff, therefore tests were run for stiffnesses from 0.05 Nm (the value used for *Sprawlita*) to 0.25 Nm evaluating the model's velocity.

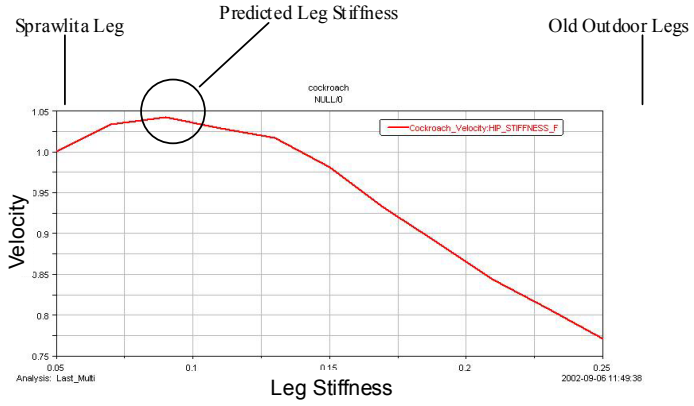

Figure 5.10: Effect of Leg Hip Stiffness on Velocity for Outdoor Sprawl

As shown in figure 5.10, there was a clear maximum with a hip stiffness of 0.094 Nm. Using the equations from section 4.1.1, the desired flexure width was

calculated to be 3.1 mm. The step response of a leg with the predicted stiffness was computed. For a leg with these properties, the maximum overshoot occurs at 55 ms, which is the nominal duration of the swing phase. It appears that as long as stability is preserved, the legs operate best when tuned to oscillate at the robot's natural running frequency.

5.5.3 Leg Orientation

In order to tune the robot's leg configuration, the leg angles are constrained, as in section 5.3, such that their lines of action in the nominal configuration intersect at a single point. Figure 5.11 shows the results of running the legs at 121 different configurations chosen to span a reasonable region of this space. The grey region indicates the configurations for which the model 'nose dived' or crashed. As before, for each stable configuration, two circles are drawn, where the size of each circle is proportional to the minimum and maximum velocity at steady state. If two circles are visible, it is an indication of non-period-1 running.

The set of leg configurations that result in 'felicitous' running (the region enclosed by the dashed lines) is smaller than for the original *Sprawlita*, and contains those settings corresponding to a mean angle closer to vertical, and with a larger amount of leg sprawl. This is presumably due to *Outdoor Sprawl's* smaller thrust to weight ratio.

The physical robot was tested at the initial configuration (as labeled on figure 5.11) which corresponds to the maximum predicted stable speed. The robot, however, tripped after a few strides due to small disturbances on the treadmill. Consequently, the second configuration (also labeled on figure 5.11) was chosen to increase stability while minimizing the loss in predicted speed. True to the simulation's predictions, the robot ran slightly slower, but much more stably.

5.5.4 Battery Pack Mass and Location

The effect of varying the location and mass of the battery pack was also investigated. Believing that these parameters were likely to be coupled, a simple DOE was tested.

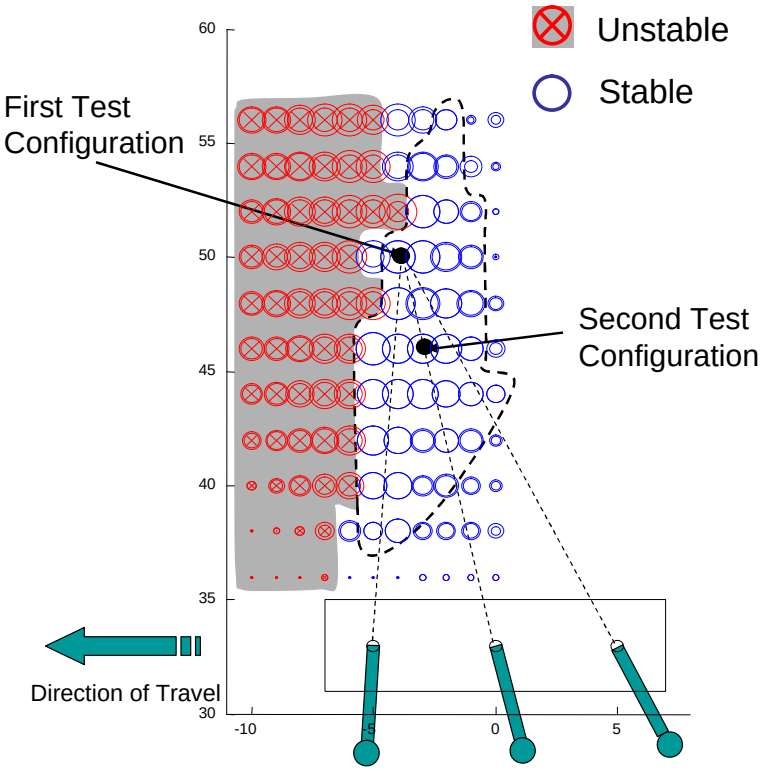

Figure 5.11: Effect of Leg Angle on Velocity for Outdoor Sprawl. Each grid location represents a different nominal configuration of the robot. Each point is where the lines of action of the leg pistons intersect. The circle's radius at each point is proportional to the robot's velocity at that configuration. The shaded area represents the unstable region.

Masses of 20, 60, and 100 g and locations between 0.03 and -0.10 m (fore and aft of the center of mass) were evaluated. The DOE results indicate that the coupling was, in fact, not strong, and that the added mass should be located at the robot's center of mass–suggesting that the leg angles were already properly aligned for balancing impulses. Changing the mass from 20 g to 100 g nearly linearly decreased the speed by 0.20 m/s.

5.5.5 Results

After implementing the changes, the robot ran at 0.80 m/s, over twice as fast as it had run before the changes were made. This demonstrates that the simulation developed and described in this thesis can be effectively used as a design tool. The fact that the first leg configuration resulted in unstable running for the robot on real terrain suggests two possibilities. The first is that the mapping of the boundary of instability from the simulation to the robot was not exact. The second possibility is that moving the leg configuration point within the predicted 'stable' region influences the robot's ability to deal with real world terrain variations and disturbances. While both effects are probably real, the second raises some interesting questions. How do these open-loop stable gaits compare in the face of perturbations and irregularities found in the real world? What is the optimal configuration for different types of terrain? How does changing the leg properties change the robots ability to self-stabilize? These questions motivate the discussion of stability in simulation in chapter 6.

5.6 Parameter Variation Conclusion

The robot simulation described in chapter 4 was created with relative simplicity in order to highlight critical design parameters while still maintaining sufficient accuracy to predict the effects of changing those parameters. This chapter describes how the simulation was used to investigate how changing the robots' parameters affects the their behavior. The main finding of this analysis are:

- The analysis of the robot's energetics shows that the most significant sources of

loss come from the excessive leg drag and pneumatic venting of air. While the robot's sprawled leg angles and high frequency running also reduce efficiency, these aspects of the design are less egregious and aid in creating fast and stable motion.

- The parameter variation study indicates the shape and relative effect of altering the robot's configuration. The study also highlights the five most significant parameters to tune for increasing performance.

- The leg angle investigation showed the range of configurations for fast, stable locomotion. This substantiated the applicability of findings from one legged models. The results also suggest that increasing the leg's sprawl angle dramatically affects stability.

- Investigation into terrain effects show that robot's stride period and mean leg angles should be altered for optimal running on changing slopes. Changing the leg posture is, however, a more effective approach than tuning the valve actuation frequency.

- The simulation was successfully used to redesign and configure the robot with a significant (1/3 body mass) load which resulted in a doubling of its speed.

In conclusion, this study has shown that detailed dynamic models can be a useful tool in understanding the motion of running, hexapedal robots. The complex model has confirmed findings from simple, more theoretical, models, as well as adding insight in areas that these simple models cannot address. Furthermore the practicle utility of the the simulation as a design tool has been validated by the simulatin-based tuning which resulted in the robot running twice as fast as had been achieved by emprical efforts alone.

Chapter 6

Stability

The simulation described in chapter 4 has been developed and used to understand some steady-state behaviors of the robot including energetics, parameter sensitivities, and the effect of changing terrain. It has also been used to tune the robot's design to maximize its forward running speed on flat ground.

The investigations in chapter 5 have shown that stability and optimal speed are tightly related for the *Sprawl* robots. Since the *Sprawl* robots' stability is largely a function of their structure and posture, understanding how changing these parameters affect stability is critical.

Thus far a simple binary definition of stability has been used–either the robot converges to a steady state gait on smooth terrain or it does not. Stability on rough terrain, however, is more difficult to measure. The question of how surface variations affect running has not yet been broached.

This chapter describes four different criteria for measuring aspects of stability that are applicable to a simulation of a robot running. Each of these criteria are used to investigate how changing the self-stabilizing posture (hip impedance and leg angles) affects the stability of the robot. By comparing the results from these four techniques a picture of how changing the robot's posture affects running over rough terrain begins to emerge.

6.1 Stability Measures

The stability of a robot running over rough terrain is a difficult property to quantify. At the most fundamental level, stability implies that the robot can continue to run in the commanded direction. Beyond this, it is desirable to have a discrete measure, so that the effect of design changes can be concretely evaluated. The rich nature of real surfaces, the need for repeatability, and practical limitations of modeling software all complicate the construction of viable, quantifiable measures of stability. Traditionally two approaches have been taken to measuring stability, experimental tests and theoretical measures.

6.1.1 Experimental Tests

A logical and useful test of a robot's performance over rough terrain is an obstacle course. Both *Rhex* [92] and *Tekken* [32] have published performance data for experimental tests on obstacle courses. However, the run-to-run variability of any such track makes any attempt to quantify how a particular design change or controller implementation affects performance imprecise. Generally only statistical statements about the probability of success can be made.

More significantly, the complexity and variation of real terrain requires fully-functional physical robots that are environmentally robust and ready to test. This makes rapid design explorations and changes early in the design cycle impossible.

It would be ideal to have a measure, or set of measures, that can be easily implemented on a simulation of a robot, and that scale well from one robot design to another. These measures should give insight into how changing the design or control scheme of a robot will affect the quality of the robot's motion over rough terrain, or the limit to the severity of terrain that can be traversed.

6.1.2 Theoretical Stability Measures

As summarized in chapter 2, there have been many measures for stability created for walking and running robots over the years. None of them, however, is wholly

adequate for predicting successful running for a complex system over rough terrain. Standard static and dynamic stability margins are commonly violated by running systems due to their high speeds and airborne phases. The other general approach to analyzing system stability, return map eigenvalue analysis, has thus far only been successfully applied to very simple models of robotic systems.

This chapter discusses four distinct scalar values or measures of performance. Each of these measures can easily be implemented on a steady state simulation of a robot running on a smooth surface. The measures are length independent, and thus can as easily be applied to a horse sized robot as an ant sized robot. Additionally, each can be used to test the effect of varying both physical and control parameters–an essential requirement for analyzing the *Sprawl* robots.

The sprawled fore-aft leg posture and the passive compliance in the legs are chosen as parameters to investigate, as they are the characteristic features of *Sprawlita's* self-stabilizing posture. Tuning these parameters not only effects the speed and maneuverability of the robot (as discussed in chapters 3 and 5), but also its ability to reject disturbances and passively stabilize its motion.

The four measures examined in this chapter are:

- Size of the parameter space that results in felicitous running on flat terrain
- The band of slopes that can be traversed in steady-state running
- Speed of recovery from a perturbation during running
- An adapted version of the 'Wide Stability Margin.'

Although each of these measures is applied to running on smooth surfaces, when taken together they consider many of the effects that result from running on rough terrain. A comparison of these measures serves to more fully illustrate how the configuration of stance parameters affects the robots stability.

6.2 Stability Margins

Most classical stability margins discussed in chapter 2 do not apply to a running robot with airborne phases. One exception is the recently proposed Wide Stability Margin (WSM) as used on *Tekken* [32]. As shown in figure 6.1, this measure maps the ground projection of each foot and the center of mass. Although this measure was developed to analyze walking, it can also be applied to running robots with flight phases. However, the WSM is analogous to the static stability margin, as it takes no account of the system dynamics. In general, and as acknowledged by [32], this method could be refined by substituting the ZMP for the ground projection of the center of mass.

6.2.1 Effect of Posture on Stability Margin

For the purposes of this investigation, an approximate WSM is used, which as shown in figure 6.1 simply measures the distance between the center of mass and front edge of the support polygon in the sagittal plane. This makes for a simple computation, but as shown in figure 6.2 it is adequite for predicting the occurrence of fore-aft nose diving it is adequate.

As shown in figure 6.2, the boundary of stable configurations as defined by the WSM has a good correlation with stability as defined by nose diving. While the WSM margin never actually goes to zero (as this would require the robot flipping forward–rather than nose diving), with a threshold of 33 mm, there is a strong alignment with nose diving. This makes sense, for in a nose dive, the front legs are both fully bent underneath the robot. This puts the center of mass of the robot as far forward relative to the front feet as possible.

Figure 6.2(b) shows how decreasing the magnitude of the mean leg angle (moving to the right of the plot) increases the size of the stability margin, which is proportional to the size of the circle at each configuration. This is expected as it moves the nominal location of the feet further away from the center of mass. The angle of the rear leg angle also makes a difference, as it affects the nominal body orientation and amount of pitching during a stride. Unfortunately these results simply tell us that greater

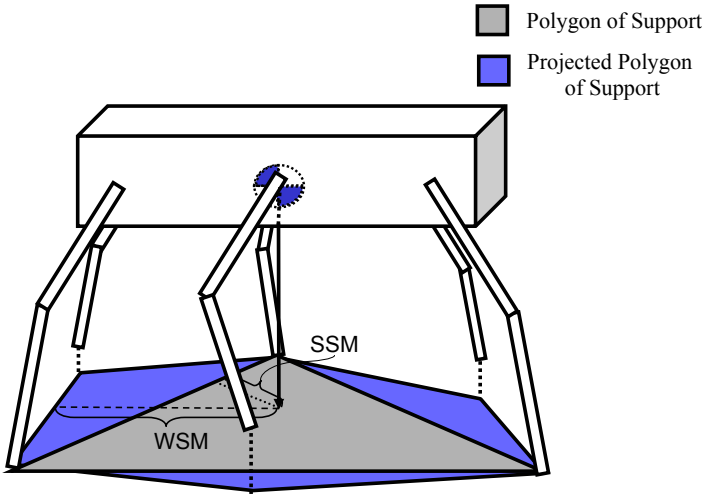

Figure 6.1: Diagram showing how the WSM is calculated and how the 33 mm threshold relates to the geometry.

stability in terms of WSM accompanies going slower.

As shown in figure 6.3, for configurations that nose dive, the WSM decreases over a number of strides until contact is made. The robot resets itself and then begins to fall forward again. The gradual nature of this instability suggests that if the maximum rotation of the front leg angles were sensed, the onset of instability could be detected, and the nominal orientation could be altered to right the robot. There are, in fact, two or three stride periods between when the threshold is crossed and contact is made, ample time to implement such a stabilizing reflex.

This section has shown that the WSM adaptation of the traditional stabilty margin is a good predictor of configurations that will crash and could be used at run time to moniter stability. A disadvantage of this measure is that it does not give insight into how either the size of the stable range or how changing leg configurations within the stable region affects the robot's ability to handle rough terrain.

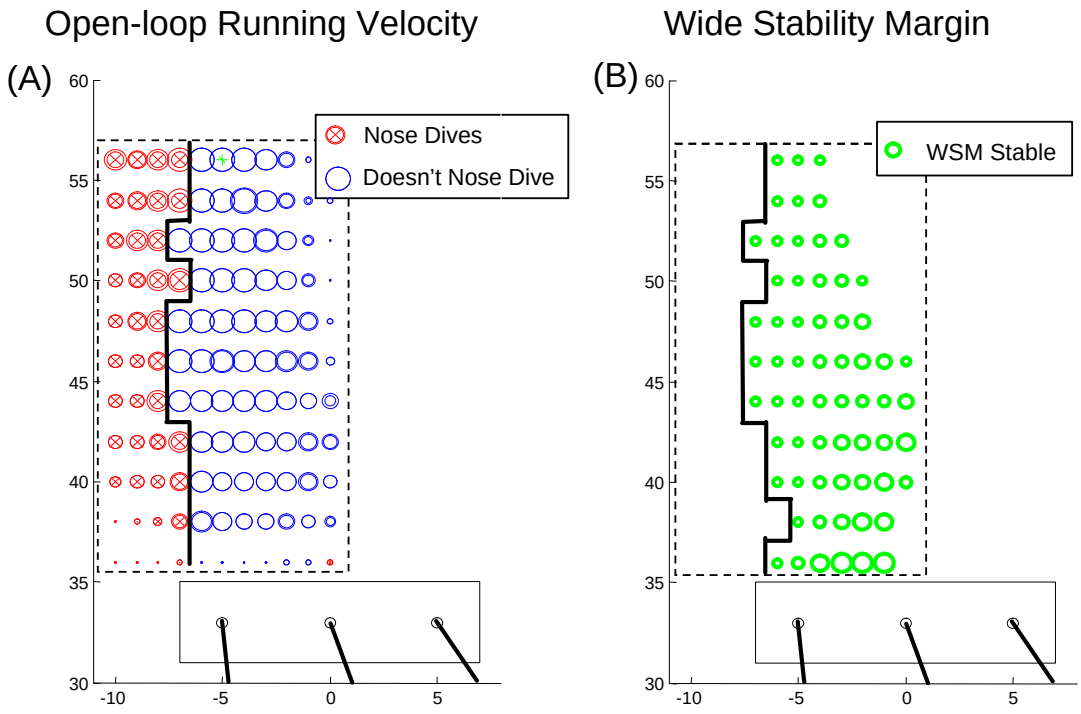

Figure 6.2: Effect of leg angle on simplified WSM. The dark line represent the boarder of instability as defined by 'nose diving' and the WSM respectively. The size of the circle represents the open-loop forward velocity for (a) and the magnitude of the WSM (b).

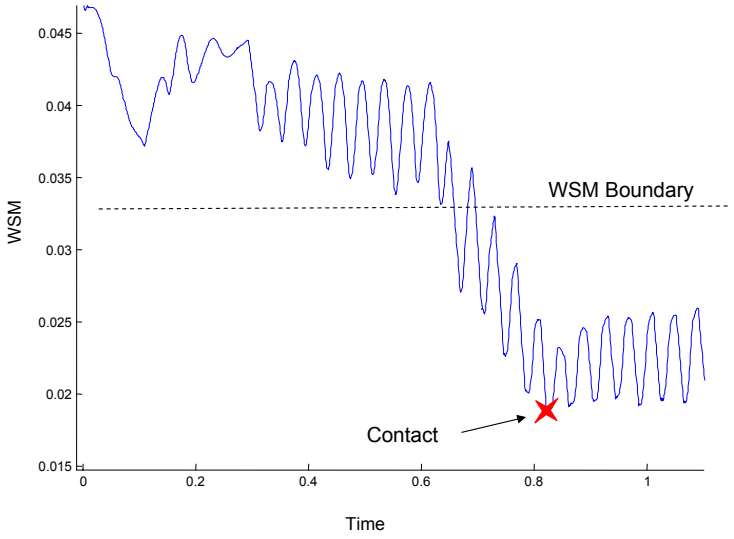

Figure 6.3: Typical decline in the WSM for an unstable configuration

6.3 Size of the Configuration Space

The next measure of stability considered is the percentage of configurations tested that result in felicitous locomotion. Configurations in this sense refer to leg angles and hip impedance, specifically, how changing the hip stiffness affects the size of the leg intersection space. The implied assumption is that increasing the size of the stable configuration space increases the range of rough terrain that can be traversed.

To investigate this, tests were run with hip stiffness from 0.050 Nm to 0.250 Nm and the range of leg configurations that resulted in fast, stable running was evaluated. The optimal configuration from the parameter tuning exercise described in section 5.5 for *Outdoor Sprawl* was used for this study. Hip damping was increased proportionally with stiffness for these trials.

Figure 6.4(a-c) shows the set of stable configurations for the minimum, the newly selected optimal, and the maximum stiffness. The shaded region on the left of each plot represents the unstable nose diving set of configurations. As in figure 5.11, the size of each circle is proportional to the model's velocity at that point. As the stiffness increases, this boundary shifts and tilts forward relative to the body of the robot. The

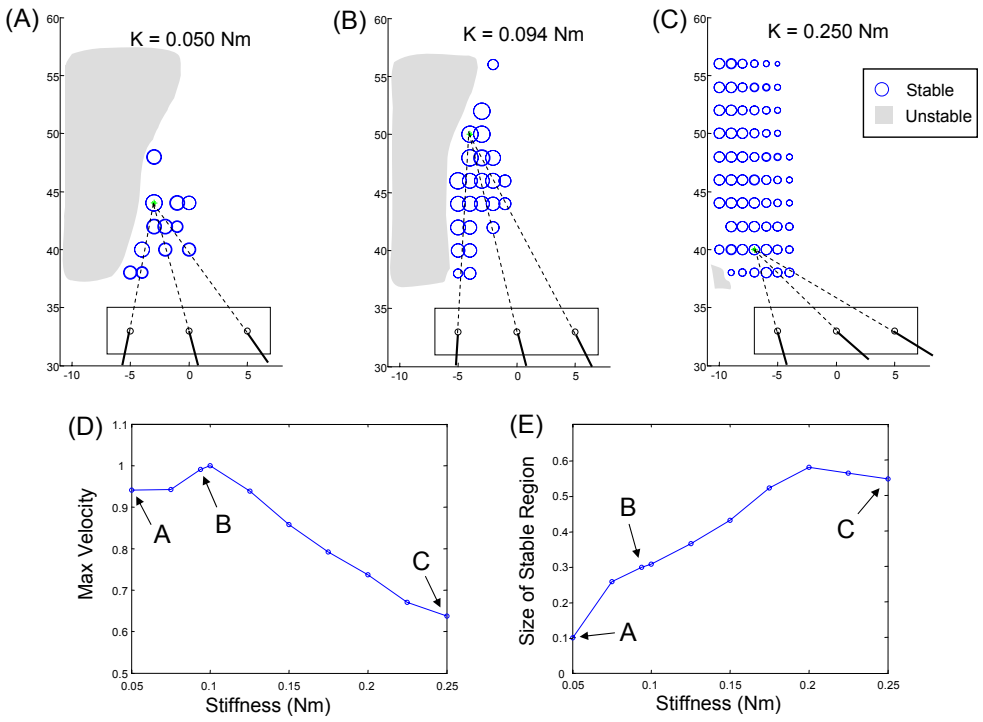

Figure 6.4: Effect of altering hip stiffness on velocity for a range of leg angles: (a) For the softest hips tested, (b) For optimal stiffness selected in section 5.5, and (c) for the stiff value tested. (d) shows the peak velocity for all configurations at each level of stiffness tested. (e) shows the fraction of the tested configurations at each stiffness that resulted in fast, period-1 running.

setting with the maximum velocity is indicated by the dashed lines. For the cases with the softer legs, this point occurs right on the boundary of stable configurations. This agrees with the prediction made by simple hopping models performed previously [21].

Figure 6.4(d) indicates how the maximum velocity changes with stiffness. As the stiffness increases, each leg rotates less, shortening the stride length, which results in slower running. As shown in (a-c) above, as the stiffness of the hips decreases the leg angles have to shift to stabilize the robot. At the softest levels the front feet are placed in front of the hips, resulting in negative work and slowing of the robot.

Figure 6.4(e) shows how the size of the stable region increases with hip stiffness. The size is calculated as the percentage of test configurations that result in fast and stable period-1 running. For large values of stiffness (k), there is a remarkably large set of configurations that result in desirable running patterns. These values would be even higher for the largest hip stiffness if the test area were shifted forward (to the left).

Figure 6.4(a) shows that, especially for comparatively soft legs, the postures that result in stable running are those where the orientation between the front and rear legs (or fore-aft sprawl angle) is large (i.e. more sprawled). For a parallel leg orientation (as used by almost all multi-legged running robots), the leg intersection point would be at infinity. The simulation, however, indicates that for this hip stiffness, as the legs become more parallel and the intersection point rises further above the body, the robot becomes less stable.

In addition to changing the size and shape of the stable region, modifying the hip impedance alters the leg configuration that results in maximum running speed. As the hip flexures are made stiffer, the mean leg angle increases (moves to the left) to compensate for the increased energy absorbed by the hips. As the legs move away from the 'ideal' stiffness $(k) = 0.10\ Nm$, the sprawl angle increases.

Using the size of the felicitous running region as a measure of stability allows the evaluation of the coupling between leg angles and hip stiffness. The simulation results show that increasing the hip impedance increases stability at the cost of speed, and suggests an advantageous design point with stiffness ($k = 0.10\ Nm$). This measure,

however, does not indicate how leg configuration within the felicitous region affects stability.

6.4 Slope Invariance

A third measure of how well a robot can run on rough terrain is its steady state ability to traverse a range of slopes, an approach taken by [83, 98]. A possible justification for this approach for certain frequencies of terrain features is given below.

Motivation

One of the fundamental differences between wheeled and legged terrestrial locomotion is the intermittent nature of ground contacts for a legged runner. As long as the swing foot does not make contact with the ground during retraction, the nature of the surface between foot falls is irrelevant to the running robot or animal. As shown schematically in figure 6.5(a), a continuous surface becomes a discrete set of foot holds. To a robot with the foot fall patten shown by the dots, the terrains shown in figures 6.5(b) and (c) are essentially identical. The primary effect of the change in terrain is experienced as an instantaneous slope for the robot. The robot's intermittent footfalls effectively digitally differentiate the continuously varying surface. Although the figure is two dimensional, the concept is directly extensible to a tripod gait over three dimensional terrain. The only difference is that in three dimensions there is a lateral as well as for-aft slope to be considered.

For surface variations at frequencies much larger or smaller than the length of the robot, the rate of change of the instantaneous slope is small, and it seems reasonable to conjecture that there is a monotonic, if nonlinear, mapping between the difficulty of traversing this range of slopes (figure 6.5(d)), and the ability of a robot to traverse a band of continuous slopes in a steady-state manner (figure 6.5(e)). If this is true, then measuring the range of 'characteristic slopes' that a given configuration of a robot can successfully navigate, may be a good indicator as to its robustness to rough terrain.

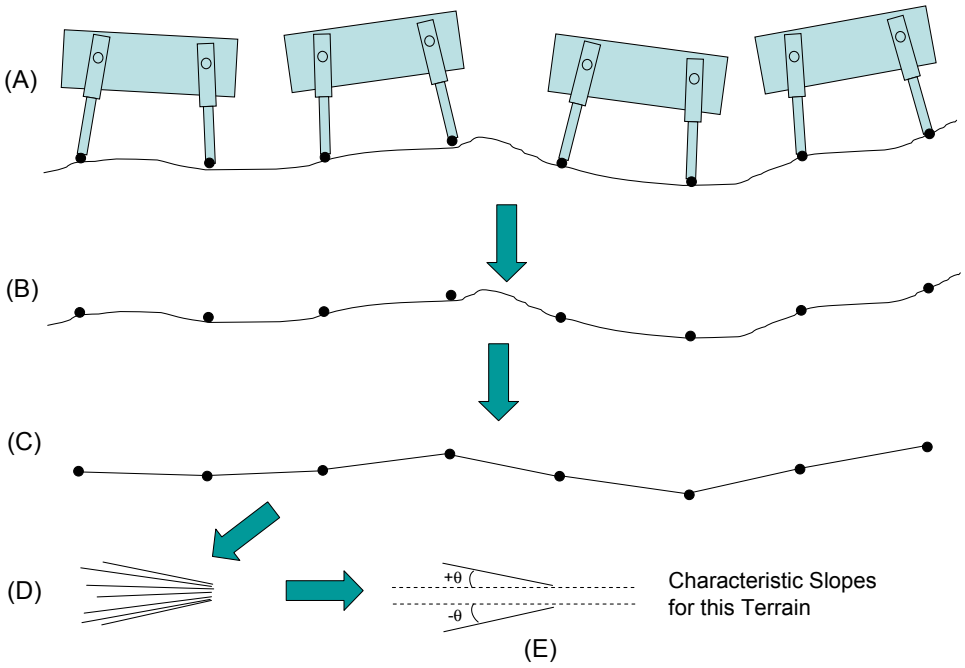

Figure 6.5: How intermittent foot contact digitally differentiates rough terrain, and the concept of a 'characteristic slopes' for a given terrain

Effect of Leg Configuration

In order to determine how changing leg orientation affects the range of characteristic slopes that a given robot can handle, a series of simulations were run. For these simulations the 'optimal' hip stiffness found in section 5.5 was used, and for each of the stable configurations on flat ground the robot was run on slopes up to $\pm$ 20 *degrees* with 2 *degree* gradations. To ensure directional stability orientation constraints were added to the simulation resulting in a slightly larger region of stable running, as shown in figure 6.6. As before, the steady state velocity and presence of 'nose dives' were examined to determine which trials resulted in good running. Figure 6.6(a) shows the steady-state velocity on level ground for each configuration. Figure 6.6(b) shows the band of slopes that was achievable for each configuration. In each case this is a plus/minus band. In other words, to rate a 6, the simulation was able to run well for each inclination between a +6 and a -6 *degree* slope.

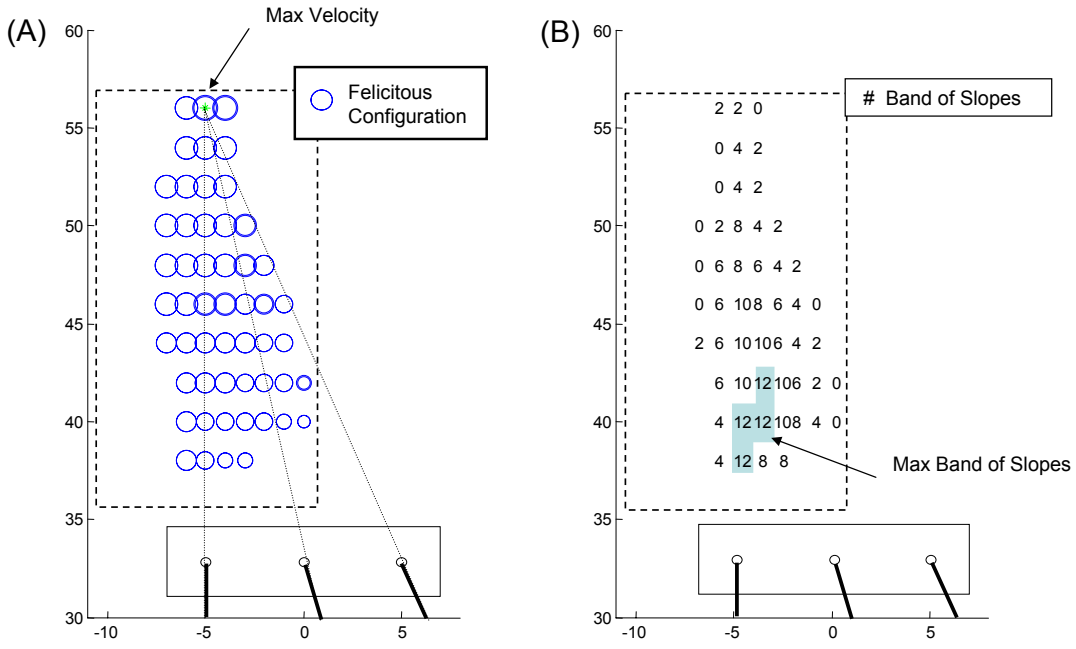

Figure 6.6: Effect of leg angle on bands of slope

Figure 6.6(b) shows that operation in the middle of the parameter space increases

the slope invariance. The most impressive finding, however, is that increasing the sprawl angle (moving down the vertical axis) dramatically increases the band of slopes that can be handled. Although the maximum speed occurs at a narrower sprawl angle, increasing the sprawl angle significantly improves the robot's invariance to slopes.

Discussion

Although configurations with a greater sprawl angle do better according to this measure, the difference might simply be due to the increased size of the polygon of support, rather than the differential leg function or antagonistic leg thrusting. To test this, as shown in figure 6.7, the footprint of a sprawled configuration was duplicated by shifting the location of the rear hip. For the less sprawled configuration, however, as shown in figure 6.7(b), this change did not increase the traversable band of slopes. Thus, it appears that the increase in slope invariance comes from the opposing lines of action of the legs.

In conclusion, slope invariance is a promising way of evaluating stability over rough terrain with steady-state simulations, as it is a measure of the size of the basin of attraction for height variations in terrain. This stability measure also highlights how increasing sprawl angles affects performance, and delineates the trade-off between speed and slope invariance. The weakness of this measure is that it does not capture the effects of impulses on the system.

6.5 Perturbation Response

Full *et al.* argue that analyzing the system response to perturbations is the next step in understand dynamic running [36]. For simple systems like hopping monopods and passive walkers perturbation analysis can be performed analytically via Floquet multipliers or eigenvalue analysis as describe in section 2.2.3 [57]. Models that exist in only one or two dimensions and have a single stance leg result in small state vectors and tractable dynamic equations of motion. For these simple models exact limit cycles can be found and used to analyze local convergence for true perturbations to the state vector. Additionally, perturbations in all directions can be analyzed simultaneously.

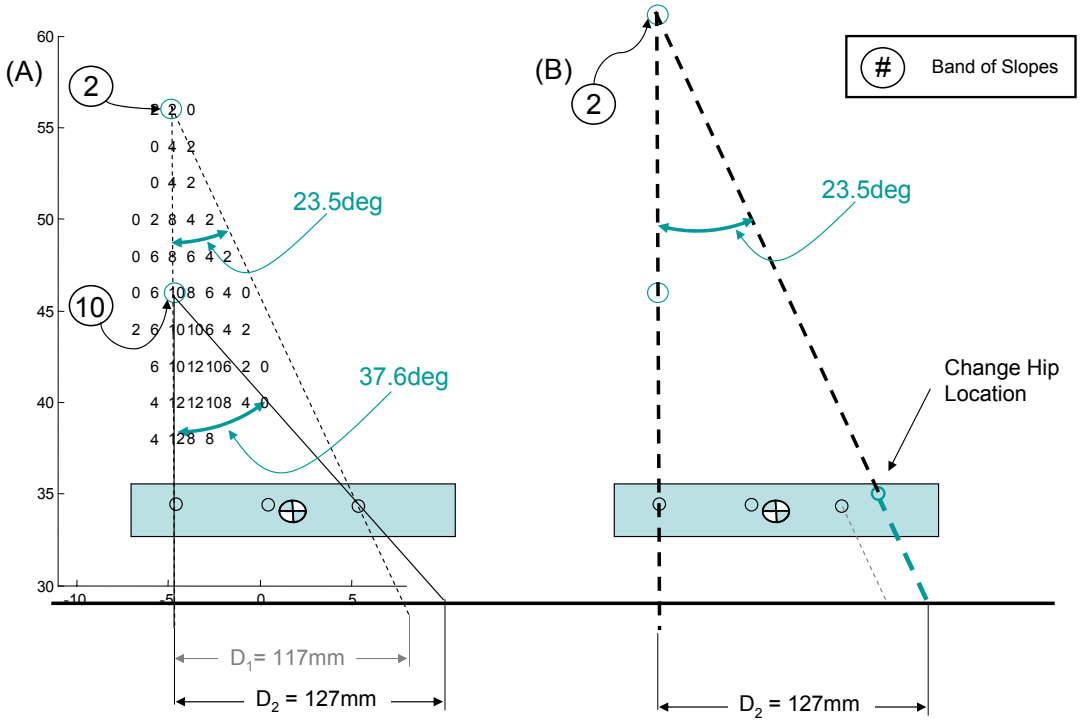

Figure 6.7: Effect of leg angle on bands of slope

However, calculating the size of the basin of attraction in N-dimensional space is still difficult.

On the other extreme of complexity are biological systems. *Sprawlita's* design was, in part, inspired by the results of clever perturbation studies on cockroaches which show that their passive structure is largely responsible for their stability to lateral perturbations [53]. These experiments were able to look at a single perturbation to a single type of animal. The resulting variations in the insects' stride pattern where then compared to 'normal' insect running to gain insights. A number of trials were necessary to gain statistical confidence in the results.

Having a full dynamic model of a running system places one in a position between these simple and complex cases. The simulation allows for applying precise and repeatable disturbance inputs into the model, but the nature of the simulation environment precludes applying perturbations to each position state of the system. In addition, the higher-order dynamics and the coupling in the model make the standard return-map linearization less meaningful as well as more difficult to perform and interpret.

The path taken in this thesis is two fold. First the response of a single configuration to a variety of disturbances is analyzed, and the resulting behavior in each direction of motion is observed. The coupling between the degrees of freedom is described, and the shape of the decaying-oscillations is mapped. Secondly, the effect of changing the stance parameters on the rate of recovery for two representative disturbances is observed.

6.5.1 Perturbation Response Behavior

For the first perturbation study, a nominal configuration of the tuned outdoor simulation is chosen in the middle of the stable region of leg angles which nearly optimizes forward velocity and slope invariance.

After achieving steady-state locomotion, the model is disturbed with impulses equal to approximately 15% of the forward momentum of the robot. A positive and negative impulse is applied at the center of mass of the body in three orthogonal

directions aligned with the orientation of the body. In addition, disturbance torques are applied about the same axes. All of the impulses are applied during an airborne phase.

A typical perturbation response plot is shown in figure 6.8. This shows the yaw rate response for a positive and negative applied yaw torque impulse applied at $t = 2.4$ *seconds*. As can be seen on the far left side of figure 6.8(a), the steady-state angular velocity normally oscillates during each stride. The effect of the perturbation decays and oscillates in a manner similar to an underdamped second-order system, but at a frequency about three times slower than the nominal oscillation. Figure 6.8(b) shows the same data, but strobed, or sampled, once per stride where each dot represents the body yaw rate at the beginning of a stride. For this trial the perturbation responses are symmetric, but this is not always the case. The higher order nature of the disturbance oscillation with its distinct frequency suggests using measures such as settling time and maximum overshoot, rather than simply the rate of decay from the first stride to the second, as is done in an eigenvalue analysis.

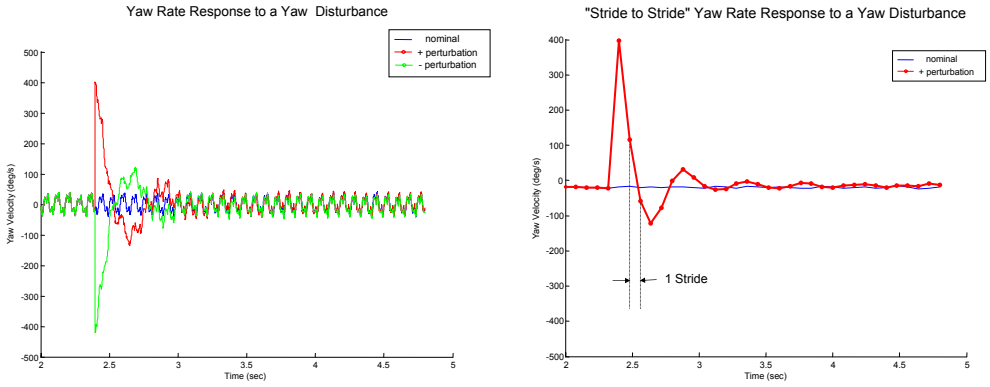

Figure 6.8: Effect of leg angle on bands of slope

Like its biological inspiration, *Sprawlita* demonstrates neutral stability for lateral motions and directional heading, but asymptotic stability in the other directions. The resulting change to the three body motions that should be stable (height, roll, and pitch) is observed. In the other three directions the robot's velocity should stabilize. As the velocity in each direction has large nominal oscillations, a filtered or strobed

value is used in these cases.

An examination of all possible combinations of inputs (12) and outputs(6) results in 72 distinct responses. To simplify the graphical representation, four outputs are chosen to focus on: roll, pitch, yaw rate, and forward velocity. Roll and pitch motions should naturally stabilize, but excursions beyond a certain amount will result in tipping and other forms of instability. Yaw rate and forward velocity are performance metrics of interest, in that poor response to either of these compromises locomotion and trajectory tracking. For each motion tracked, the four corresponding disturbance inputs are used, resulting in 16 plots.

Figure 6.9 shows the roll and pitch responses to all four inputs, and figure 6.10 shows the yaw rate and velocity responses to the same inputs. As can be seen in these figures, roll and yaw motions are strongly coupled. A disturbance in either of these directions also excites a pitching oscillation, but pitching disturbances do not excite changes in either the rolling or yawing motions. Disturbances in the fore-aft direction do not excite rotational motions, though any disturbance to an angular motion will slow the forward velocity.

Of the various directions, pitch disturbances settle at the slowest rate. All of the modes, however, stabilize regardless of the direction of disturbance, and they all reach a steady-state motion within one second. This is also the time required for the robot to reach its steady-state gait from the initial rest position.

From this analysis is would appear that roll and yaw are strongly linked and decay the fastest (have the lowest eigenvalues). Consequently, it seems logical to choose forward velocity and pitch as representative responses for evaluating the effect of changing configuration for the following reasons:

1. Any disturbance excites these modes.

2. Of all the rotational modes, pitch is the slowest to decay.

3. Changing the robots leg angles in the sagittal plane is most likely to affect pitch directly.

4. Pitch response relates to the planar slope invariance considered previously.

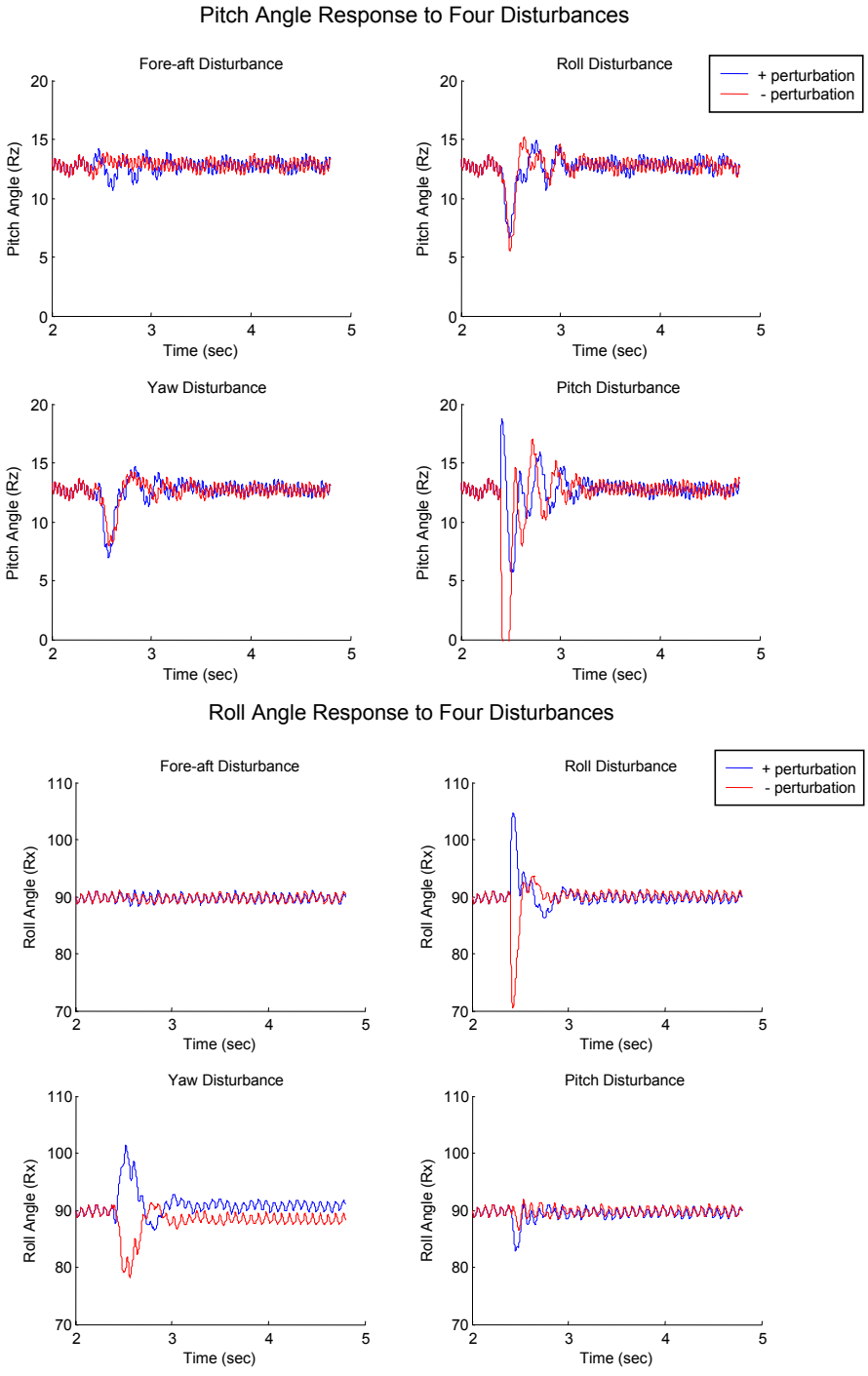

Figure 6.9: Perturbation response for Pitch and Roll

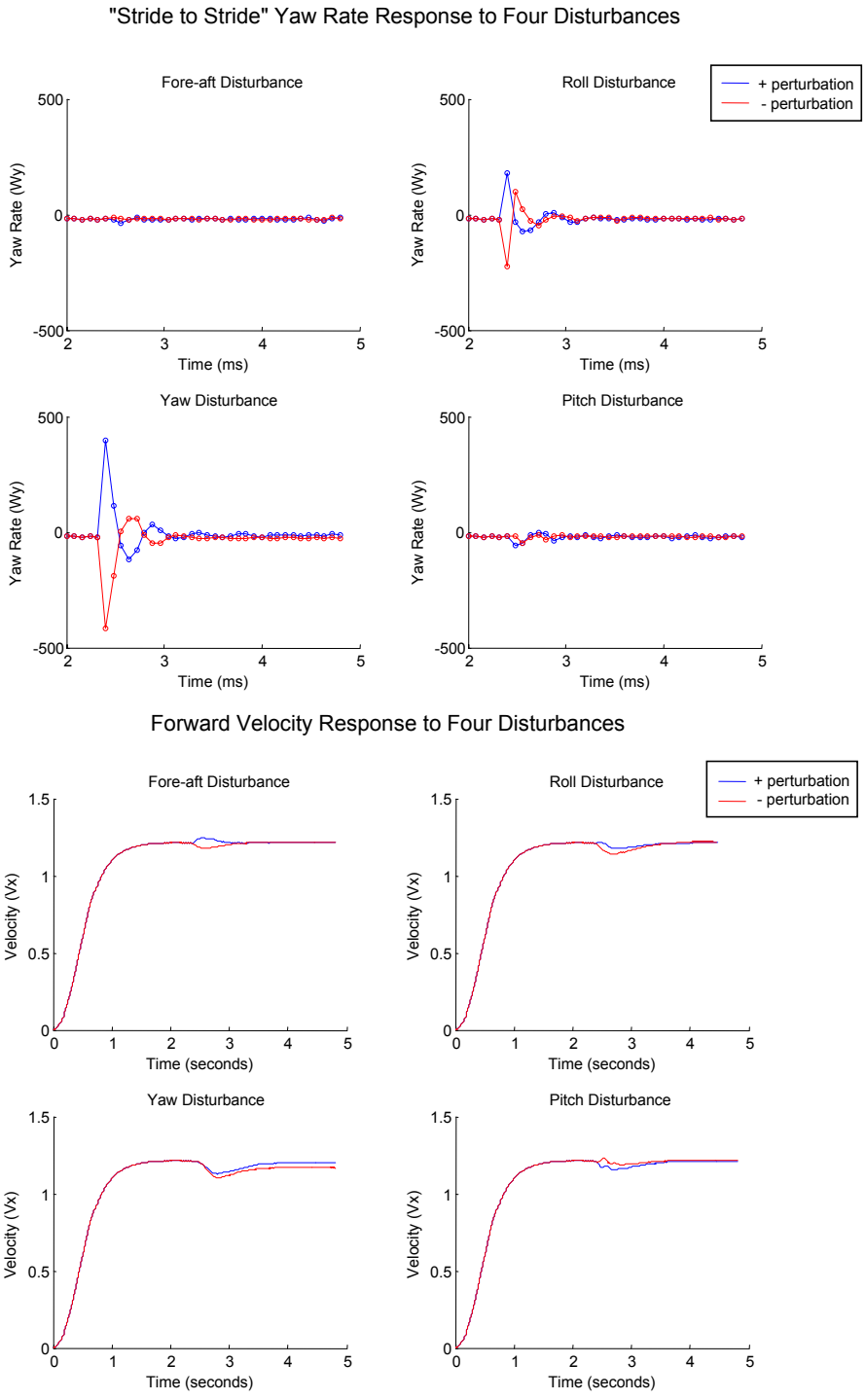

Figure 6.10: Perturbation response for yaw rate and velocity

5. Velocity is a performance variable of interest.

6.5.2 Configuration Dependant Response Rate

Figure 6.11 compares the pitch response to the speed response for a range of leg orientations. For each case the settling time is plotted, with the circle size being proportional to the number of strides required before the state has settled to its nominal value. The grey area highlights the region that converges the most quickly.

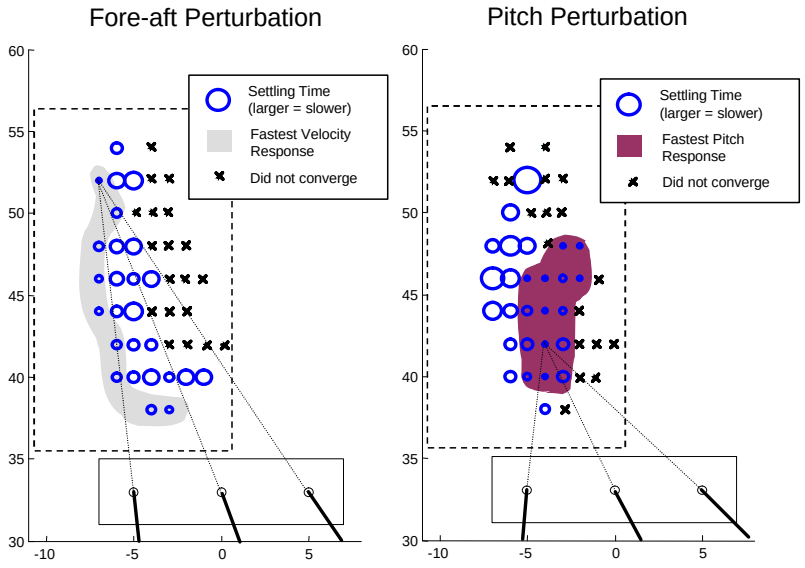

Figure 6.11: Effect of leg angle on perturbation settling time

As figure 6.11(a) shows, the region of fastest convergence for the fore-aft perturbation response lies on the border of unstable values. The region of the configuration space that results in the fastest running overlaps with this region. This may be due to stronger locking into the limit cycle, but these configurations also pose a greater danger of crashing due to configuration or alignment errors.

The pitch response to a pitching disturbance impulse is shown in figure 6.11(b). The region of fastest convergence occurs near the middle of the stable range. Values to the rear (right) of the stable region converge poorly for both types of disturbances. These values are not unstable in the sense of nose diving, but also do not show a

sharp period-1 gait locking. The pitch results agree well with the slope invariance tests of section 6.4. In both cases, the best performance is found in the center of the stable region.

Forward configurations (with the intersection point to the left) result in good fore-aft perturbation rejection. These configurations also have less body pitch and pitch oscillation in general, and a larger percentage of the leg thrust is horizontal. The central leg configurations, on the other hand, have larger nominal body pitches and larger oscillation in body pitch with each stride. These configurations are better able to quickly absorb the effects of sudden pitching torques applied to the body, as might result from a bump, pit, or change in ground slope.

Even though pure fore-aft disturbances are perhaps rare, the dependance of the forward velocity response on rotational disturbances as described in section 6.5.1 suggests that figure 6.11(a) may be a representative result in terms of speed for a range of perturbations. For surfaces with small disturbances that do converge the fore-aft response plot may be a good indicator of the resulting loss of speed, i.e. leg configurations that result in rapid velocity perturbation recovery may also mitigate the decrease in velocity while running over a given stretch of rough, but passable terrain.

The slow settling time and strong dependance of the pitching response on other types of disturbances suggests that figure 6.11b may be an indicator for predicting the effect of leg configuration on how rough a terrain the robot can successfully traverse.

6.6 Stability Measure Comparison

The four different measures described in this chapter all contribute to our understanding of how posture affects stability. The first measure, WSM, is an extension of the 'stability margins' applied extensively to walking robots. While it is an excellent predictor of configurations that lead to nose-diving, and could be used to implement a stumbling reflex or slope-adaptation algorithm, it does not tell us anything useful about how changing configurations within the stable regions affects performance. It simply implies that going slower increases stability.

The second measure, the size of the stable region, gives a good indication of how hip stiffness interacts with leg angles. It clearly shows the trade off between maximum possible speed and the size of the configuration space for changing hip stiffnesses. It also indicates a design 'sweet spot' for maximizing both. The third measure, slope invariance, gives an indication of how altering the leg orientation impacts the ability of the model to handle slopes. It gives evidence that increasing the leg sprawl angle increases stability.

The perturbation test study demonstrates the coupling between the motions of the robot and indicates how well the robot may respond to impulses and impacts encountered while running. It also indicates that configurations on the boundary of instability (more negative mean leg angles) have faster responses to fore-aft perturbations, but for rotational disturbances a more central leg placement is desirable.

Figure 6.12 graphically overlays the results from these four measures. The size of the circles at each configuration is proportional to the WSM for that setting. For fast operation on smooth terrain the leg configurations shown by the dotted lines that result in the maximum velocity would be recommended. For operation on unknown or rough terrain however, a more sprawled leg configuration coinciding with the intersection of the fastest pitch recovery and slope invariance regions would be suggested.

Although the connection between each of these measures and the effect of real terrain has not yet been ascertained, the composite effect from looking at these different measures provides an idea of how changing the robot's stance parameters will affect its stability. Though far from definitive, these measures provide a first step to capturing these complex interactions in a simulation environment in a manner that could be used as a design tool early in the plan/build/test cycle.

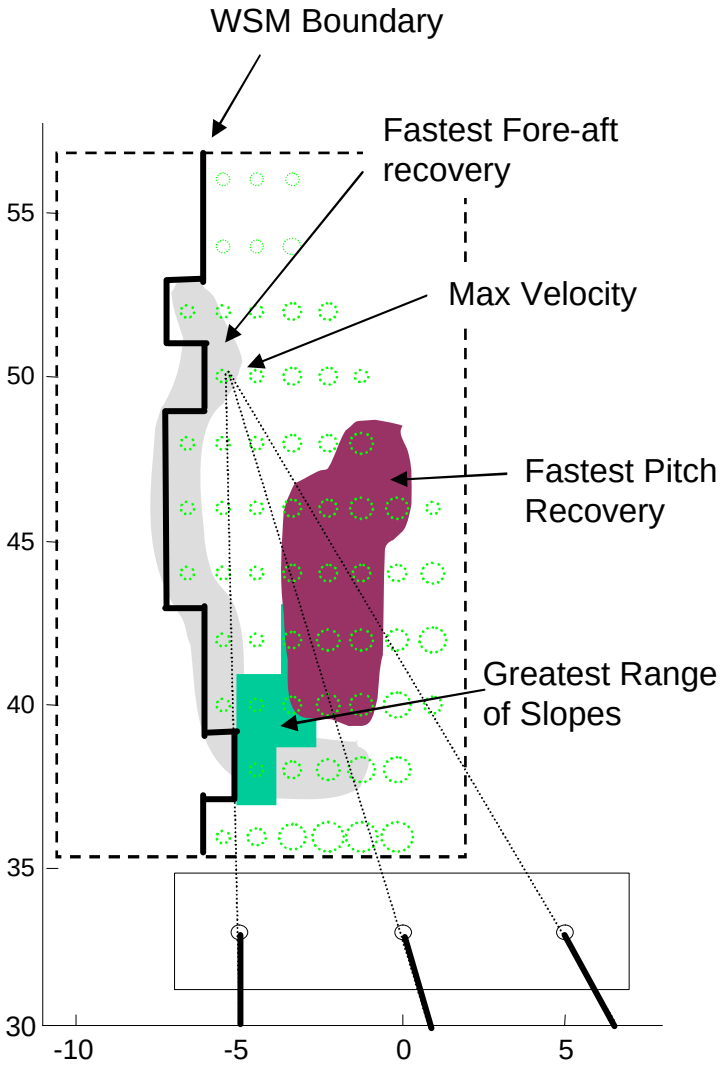

Figure 6.12: Comparison of the effect of leg posture for different stability measures. The circles represent the magnitude of the WSM for each of the stable configurations.

Chapter 7

Conclusions and Future Work

Before the research described in this thesis was begun, the only robots to run at speeds of body-lengths per second were the hopping robots developed under Raibert direction. These robots relied on leg symmetry, long airborne phases, knowledge of the terrain, and multiple sensor driven feed-back loops to run. Recent research into insect locomotion has inspired a number of robots, including the *Sprawl* robots described in this paper, as well as the *Scout* [29] and *Whegs* [85] and *Rhex* [3] robots, which can run as fast as the hopping robots, but can also handle unpredictable rough terrain. A large part of the success of these robots can be attributed to their simplicity and the judicial use of passive compliance in their legs.

Of these robots, the *Sprawl* robots are unique in that they use thrusting legs, passive compliant hips, and are *completely* open loop in their control. The resulting leg trajectories are consequently a function of the dynamic interaction with the substrate. Without the compliant hips, the robots would not be able to move. Consequently, the appropriate tuning of the physical properties of the legs is not only essential to perturbation rejection and running on rough terrain, but is requisite for any locomotion at all.

7.1 Contributions

One of the encouraging findings of this thesis is that there is a large region of the leg design space that results in forward locomotion, and that many of these configurations result in fast, self-stabilizing running. By appropriately tuning the leg structure we not only generate locomotion, but dynamic trajectories with a large basin of attraction.

Easily underappreciated is the fact that this basin of attraction includes the rest state of the robot–where all of the actuators are off, and the robot is lying on its belly. Being able to start from this lowest energy state has not only removed the necessity of specifying start-up control sequences, but more importantly allows for recovery from a wide variety of crashes and falls. The only way that this could be better were if the robot could reverse its legs and run on its back.

The development of the dynamic simulation of the robot has enabled a rapid virtual examination of the leg parameter space. This tool along with physical testing has shown the relative importance and effect of the various leg parameters on speed, and has allowed for the identification and mapping of critical parameters. To the extent that physical testing was possible, the relative magnitudes and shapes of simulation parameter studies agree with those tests in indicating the relative importance of design elements on performance.

The simulation findings also agree with those from simple one-legged models in predicting how changing the open-loop activation frequency affects the robots' speed and efficiency. The analysis further indicates the relative energetic cost and benefits of *Sprawl's* characteristic design decisions such as sprawled posture.

The tuning of these parameters on the simulation resulted in significant increases in the robot's running velocity. The application of these design changes back onto the physical robot resulted in similar increases in performance, providing confirmation of the model's predictive ability.

If a true optimization of the robot's speed were desired, the simulation would provide a meaningful approximation upon which to implement any one of a number of optimization schemes. Of greater interest than numerically calculating how to

implement incremental increases in speed is the intuition gained by studying the simulation as to the roles of elements such as leg inertia, hip damping, and stride frequency on the nature of the gait.

Of critical importance for running outdoors is the ability of the robot to reject disturbances and handle slopes and rough terrain. Defining stability for running outdoors is, however, a difficult task. Although a number of stability margins and measures have been proposed over the years, there exists no satisfactory metric to measure stability under such conditions.

One of the contributions of this thesis is the comparison of multiple measures of stability for a running robot. All of these measures can be applied to a simulation of the robot, thereby enabling a large number of inexpensive tests to be run. The fact that these measures are not restricted to fully functional physical robots means that any design changes suggested by their use can be implemented early on in the design/build/test cycle. And while none of the measures alone is a wholly acceptable representative of rough terrain stability, taken in aggregate, they produce a much clearer picture of a system's behavior.

The main advantage to these simulation based measures is that they allow an investigation into how changing the physical design affects the resulting robot performance. For a completely open-loop design such as the one used in the *Sprawl* robots, this is essential for evaluating how the changing the mechanical design affects the self-stabilizing properties of the legs.

One of the most interesting findings of the stability study on the *Sprawl* robots is that the use of a significant fore-aft leg sprawl improves the stability of the robot. Simply by configuring the legs with different nominal orientations, the legs take on different roles, produce different forces on the robot, and tend to aid in stabilization.

Other fast running robots' front and rear legs are not only physically identical, but operate with the same control and function in mind, resulting in similar ground reaction forces and a horizontal torso. The sprawled posture and significant body pitching found in the *Sprawl* robots are novel and, as the current study shows, aid significantly to the robots' stability.

7.2 Future Work

There are several avenues of future work from the current study, from the direct application of the simulation-based tuning approach to other robots to broad theoretical questions about the nature of stability when running over rough terrain, and how to appropriately tune the passively self-stabilizing posture of robots.

A very concrete potential application of the methodology described in this thesis is provided by *iSprawl*, the most recent incarnation of the *Sprawl* family of robots. *iSprawl* is a fully-autonomous, electrically driven version of the robot [55]. It uses a crank-rocker mechanism to convert the rotary output of the drive motor to a linear motion. Specially designed push-pull cables transmit the thrust to each leg in an alternating tripod gait. This robot is capable of running at 2.3 m/s or 15 $bodylengths/second$, making it currently the fastest legged robot for its size in the world. It was able to achieve a 50% speed increase by the addition of passive compliance in the shaft direction of each leg. The optimal magnitude of both this axial and the hip flexure remain, however, unknown. The application of the simulation tuning method described in chapter 5, should result in a significant further improvement in both speed and stability.

A second straightforward extension of the thesis is to look at the effect of changing rotational and axial leg compliance for a range of postures on the size of the stable region for the WSM, Slope Invariance, and Perturbation Response measures discussed in chapter 6. The shape and size of the stable region may change, giving further insight on how the passive structural elements affect stability.

Another area of future work involves improving and combining the stability measures suggested in chapter 6. The Wide Stability Margin could be augmented by including the effects of momentum and acceleration to create a stability margin that is useful for a running robot. If this augmented margin included the effects of the system dynamics, the system velocity, and ground conditions such as slope it could be used as an input for a feed-back stabilization scheme, or single measure of performance for design purposes.

In addition, the perturbation analysis can be extended to measure the size of

the basin of attraction, in addition to the rate of recovery. This, as yet, untapped possibility is one of the great advantages of this technique.

The slope invariance measure is currently only sensitive to the effect of low-frequency terrain changes, and only measures changes in the fore-aft direction. A more explicit connection between slope invariance and the effect of rough terrain can be created by including roll angles and by considering impulses. For an alternating tripod gait the extension to three dimensional terrain changes is straightforward. The intermittent nature of legged locomotion inherently bypasses high-frequency terrain features, but disturbances on the order of the length of the body of the robot may be significant. Some of the effect of this sort of terrain could be captured by looking at impulses applied in tandem with slope changes, while other effects will require a more specific and detailed model. For each of the theoretical measures of performance discussed in chapter 6, rigorous physical testing is required to illuminate the strength of connection between simulation results and the effect of real terrain.

This investigation into the dynamics of the *Sprawl* robots has shown the leg specialization and significant leg compliance and damping can lead to self-stabilizing running over rough terrain. The robots have demonstrated this, and the simulation has shown size and shape of this basin of attraction and how changing the robot's posture affects these. The larger questions of why this is the case, and how to successfully abstract these principles and apply them to other platforms remains the subject of future research. Some suggestions have been raised by the current study, but the complex nature of the coupled, non-linear dynamics of the system has thus far precluded the abstraction of more general and useful analytical tools.

Appendix A

Model Calibration

This section describes the physical tests used to calibrate the ADAMS model elements to their physical counterparts. Due to the nature of the modeling assumptions in the formulation of the simulation, the required accuracy of these tests is low. Nevertheless the procedures described here were followed to achieve reasonable accuracy with a low number of tests.

All of data for the motion/displacement tests was taken via high speed digital video. A MotionScope camera using RedLake software captured images at 250 frames/second. Approximately 6 mm diameter reflective markers were placed on the test platform and were tracked by the camera. Video processing was done with custom software that produced X,Y coordinates in MATLAB. Accuracy was typically better than 0.1mm. Force data was taken by a JR3 3 axis force/torque sensor at a sample rate of 1kHz. Force resolution was at least of 0.1N.

Three different tests are described in this section, the stiffness and damping of Sprawlita's rotational leg flexures, the ground contact stiffness and damping, and the frictional properties of the foot/treadmill interaction.

A.1 Sprawlita Hip Flexure Tests

Stiffness was measured by recording with high-speed digital camera the leg response to step deflections. Three reflective markers were added to the robot leg, One of which

was located on the effective center of rotation. The rotation of the line formed by the other two markers was used to calculate the angular response of the leg. Deflections of magnitudes typical during running were applied to the leg from both directions. Figure A.1 shows the test set up and a typical response in Cartesian coordinates.

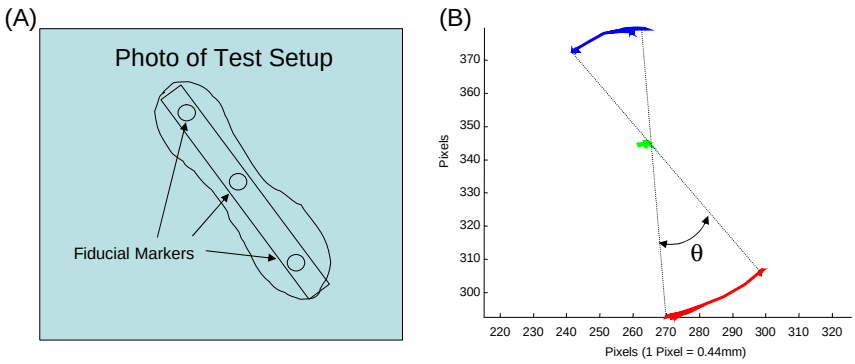

Figure A.1: (A) Picture of the hip flexure test set up indicating the locations of the markers, and (B) a typical picture of the motion of the markers in Cartesian space.

Figure A.2 shows the six trajectories that were averaged to generate figure 4.2b. Each one is overlaid with the resulting second order model trajectory.

A.2 Surface Friction Tests

The friction properties of the foot/treadmill interaction were modeled by a static and dynamic coefficient. In order to measure these a static version of the robot with a single tripod of legs rigidly attached to the body was built. This platform had the same rubber feet that were used on the treadmill, and approximately the same geometry. The platform was placed on the treadmill and attached via a cable to the JR3 force sensor, located directly behind it, as shown in figure A.3.

The treadmill was then turned on and the force profile was recorded. For each trial the recorded force ramped up to a peak and then dropped to a steady value as the treadmill moved under the stationary platform. The peak value was used to calculate the static friction, and the steady-state force value was used to calculate

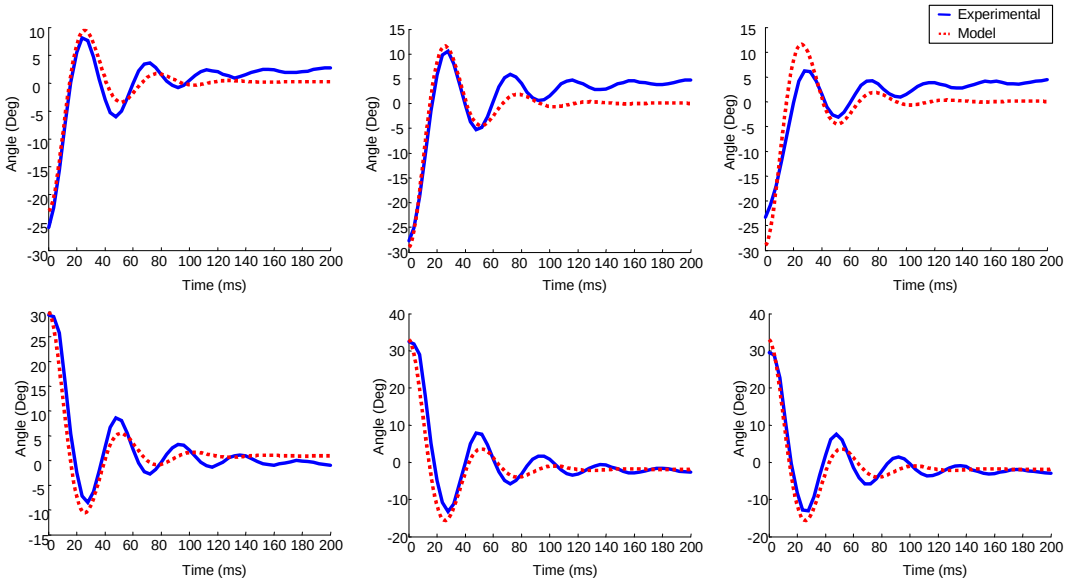

Figure A.2: Six step responses.

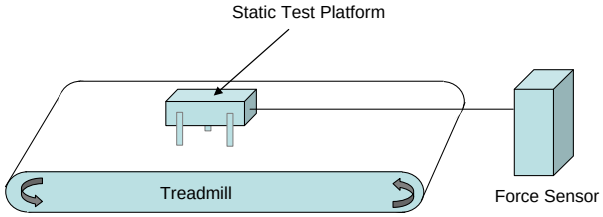

Figure A.3: Figure showing the surface friction test set up

the dynamic friction. Trials were run with a mass equivalent to *Sprawlita* (307g) and with 200g and 500g added. The results are shown in table A.1.

Trial	μ_S	μ_D
307-1	1.06	0.95
307-2	1.10	0.94
307-3	1.08	0.94
507-1	1.08	0.88
507-2	1.05	0.89
507-3	1.01	0.87
807-1	0.89	0.82
807-2	0.91	0.83
807-3	0.95	0.83

Table A.1: Friction test values

These results were comparable to earlier friction tests that looked at the necessary loading for incipient slip of a smooth section of polyurethane on the treadmill. The static values listed here were slightly higher than the earlier tests, presumably due to the interaction of the feet and the small conical depressions in the treadmill surface.

Although only three trials were run at each setting, the variance was low enough that an averaged value of the results was found to be acceptable. The addition of the mass to the body raised the center of mass of the platform above the attachment point of the cable. Similar eccentricities in the polyurethane tests resulted in more dramatic decreases in the measured coefficient of friction, even for the same test mass. Consequently, only the mean values for the unaltered test configuration were used in the ADAMS simulation.

A.3 Ground Contact Tests

The treadmill/foot effective stiffness was tested by examining the static deflection of the rigid test platform described in section A.2. The height of the center of mass of the test platform was recorded with the digital camera and reflective markers before and after a known mass was added to the body. The added test masses ranged from 500g to 2.5kg. Table A.2 shows the resulting stiffness for each test.

Trial	Stiffness N/m
200-1	9.41
200-2	5.54
200-3	5.54
500-2	8.82
500-3	4.45
1000-1	5.24
1000-2	6.32
1000-3	6.77
1500-1	6.85
1500-2	4.66
1500-3	4.89

Table A.2: Ground stiffness test values

The measured foot/surface interaction stiffness was relatively variable, but not overly non-linear, consequently the mean value of 6.26x10^4 N/m was used in the simulation.

To measure the effective damping of the surface the same test platform was dropped from about 35mm above the surface and the resulting penetration and bounce were measured with the high-speed digital camera. The resulting heights and penetration values are given in table A.3

Trial	bounce height (%)	Damping Ns/m
307-1	1.06	0.95
307-2	1.10	0.94
307-3	1.08	0.94
507-1	1.08	0.88
507-2	1.05	0.89
507-3	1.01	0.87
807-1	0.89	0.82
807-2	0.91	0.83
807-3	0.95	0.83

Table A.3: Ground damping test values

[something about how the value was calculated, and standard deviation . . .]

Accuracy in measuring the resulting height was decreased by the pitching and

rolling of the platform upon rebounding from the surface. Out of plane rotations were not accounted for in the marker processing software.

As shown in the terrain adaptation section the model is not very sensitive to small changes in stiffness and damping near these nominal values.

Bibliography

[1] Mojtaba Ahmadi and Martin Buehler. Stable control of a simulated one-legged running robot with hip and leg compliance. In *IEEE Transactions on Robotics and Automation*, volume 13, pages 96–104, 1997.

[2] R. McN Alexander. Three uses for springs in legged locomotion. *International Journal of Robotics Research*, 9(2):53–61, 1990.

[3] R. Altendorfer, N. Moore, H. Komsuoglu, M. Buehler, Jr. Brown H. B, D. McMordie, U. Saranli, R. Full, and D. E. Koditschek. Rhex: A biologically inspired hexapod runner. *Autonomous Robots*, 11(3):207–213, 2001.

[4] R Altendorfer, U Saranli, H Komsuoglu, D Koditschek, HB Brown, M Buehler, N Moore, D McMordie, and R Full. Evidence for spring loaded inverted pendulum running in a hexapod robot. In *EXPERIMENTAL ROBOTICS VII*, volume 271, pages 291–302. SPRINGER-VERLAG BERLIN, 2001.

[5] C. Angle. *Genghis: A Six-Legged Autonomous Walking Robot*. Sb, Massachusetts Institute of Technology, 189.

[6] C. Angle. *Design of an Artificial Creature*. PhD thesis, Masssachusetts Institute of Technology, 1991.

[7] F. Asano, M. Hashimoto, N. Kamamichi, and M. Yamakita. Extended virtual passive dynamic walking and virtual passivity-mimicking control laws. In *Proceedings - IEEE International Conference on Robotics and Automation*, volume 3, pages 3139–3144, 2001.

[8] S. A. Bailey, J. G. Cham, M. R. Cutkosky, and R. Full. Biomimetic robotic mechanisms via shape deoposition manufacturing. In J Hollerbach and D. E. Koditschek, editors, *International Symposium for Robitics Research (ISRR2000)*, London, 2000.

[9] S. A. Bailey, J. G. Cham, M. R. Cutkosky, and R. J. Full. Comparing the locomotion dynamics of the cockroach and a shape deposition manufactured biomimetic hexapod. In *Experimental Robotics Vii*, volume 271, pages 239–248, 2001.

[10] JE Bares and DS Wettergreen. Dante ii: technical description, results, and lessons learned. *International Journal of Robotics Research*, 18(7):621–49, 1999.

[11] Matthew D. Berkemeier. Modeling the dynamics of quadrupedal running. *International Journal of Robotics Research*, 17(9):971–985, 1998.

[12] K. Berns, R. Dillmann, and S. Piekenbrock. Neural networks for the control of a six-legged walking machine. *Robotics and Autonomous Systems*, 14(2-3):233–244, 1995.

[13] M Binnard and MR Cutkosky. Design by composition for layered manufacturing. *JOURNAL OF MECHANICAL DESIGN*, 122(1):91–101, 2000.

[14] M. B. Binnard. *Design of a Small Pneumatic Walking Robot*. Sm, Massachusetts Institute of Technology, 1995.

[15] R. Blickhan and R. J. Full. Similarity in multilegged locomotion: Bounding like a monopod. *JOurnal of Comparative Physiology*, 173(5):509–517, 1993.

[16] G BOX and S BISGAARD. Statistical tools for improving designs. *MECHANICAL ENGINEERING*, 110(1):32–40, 1988.

[17] B. Brown and G. Zeglin. The bow legged hopping robot. In *IEEE International Conference on Robotics and Automation*, pages 781–786, New York, NY, 1998.

[18] I.E. Brown and G.E. Loeb. A reductionist approach to creating and using neuromusculoskeletal models. In J.M. Winters and P.E. Crago, editors, *Biomechanics and Neural Control of Posture and Movement*, pages 148–163. Springer-Verlag, 2000.

[19] M. Buehler, D. E. Koditschek, and P. J. Kindlmann. Planning and control of a juggling robot. *International Journal of Robotics Research*, 13(2):101–118, 1994.

[20] G. A. Cavagna, N. C. Heglund, and Taylor C. R. Mechanical work in terrestrial locomotion: Two basic mechanisms for minimizing energy expenditure. *American Journal of Physiology*, 233, 1977.

[21] J. G. Cham. *On Stability and Performance in Open-loop Running*. PhD thesis, Stanford University, 2002.

[22] J. G. Cham, S. A. Bailey, and M. R. Cutkosky. Robust dynamic locomotion through feedforward-preflex interaction. In *ASME IMECE Proceedings*, Orlando, Flordia, 2000.

[23] J. G. Cham and M. R. Cutkosky. Adapting work through actuator phasing in running. In *Intl. Symp on Adaptive Motion of Animals and Machines (AMAM2003)*, Kyoto, Japan, 2003.

[24] J. G. Cham, J. Karpick, J. E. Clark, and M. R. Cutkosky. Stride period adaptation for a biomimetic running hexapod. In *International Symposium of Robotics Research*, Lorne Victoria, Australia, 2001.

[25] C. Chevallereau, G. Abba, Y. Aoustin, F. Plestan, E.R. Westervelt, C. Canudas-de Wit, and J.W. Grizzle. Rabbit: A testbed for advanced control theory (preprint). *IEEE Control Systems Magazine*, 2002.

[26] W. Chun. The walking beam: a planetary rover. *Martin Marietta Astronautics Group Journal*, 1:32–39, 1990.

[27] J. E. Clark, J. G. Cham, S. A. Bailey, E. M. Froehlich, P. K. Nahata, R. J. Full, and M. R. Cutkosky. Biomimetic design and fabrication of a hexapedal running robot. In *Proceedings - IEEE International Conference on Robotics and Automation*, volume 4, pages 3643–3649, 2001.

[28] H. Cruse. What mechanisms coordinate leg movement in walking arthropods? *Trends in Neurosciences*, 13:15–21, 1990.

[29] M. De Lasa and M. Buehler. Dynamic compliant quadruped walking. In *Proceedings IEEE International Conference on Robotics and Automation*, volume 3, pages 3153–3158, 2001.

[30] K. S. Espenschied, R. D. Quinn, R. D. Beer, and Hillel Chiel. Biologically based distributed control and local reflexes improve rough terrain locomotion in a hexapod robot. *Robotics and Autonomous Systems*, 18(1-2):59–64, 1996.

[31] K. S. Espenschied, R. D. Quinn, H. J. Chiel, and R. D. Beer. Leg coordination mechanisms in stick insect applied to hexapod robot locomotion. *Adaptive Behavior*, 1(4):455–468, 1993.

[32] Y. Fukuoka, H. Kimuar, and A. H. Cohen. Adaptive dynamics walking of a quadruped robot on irregular terrain based on biological concepts. *International Journal of Robotics Research*, 22(3-4):187–202, 2003.

[33] R Full, K Autumn, J. I. Chung, and AN Ahn. Rapid negotiation of rough terrain by the death-head cockroach. *American Zoologist*, 38(81A), 1998.

[34] R. J. Full, R. Blickhan, and L. H. Ting. Leg design in hexapedal runners. *Journal of Experimental Biology*, 158(UL):369–390, 1991.

[35] RJ Full and DE Koditschek. Templates and anchors: Neuromechanical hypotheses of legged locomotion on land. *Journal of Experimental Biology*, 202(23):3325–3332, 1999.

[36] RJ Full, T Kubow, J Schmitt, P Holmes, and D Koditschek. Quantifying dynamic stability and maneuverability in legged locomotion. *INTEGRATIVE AND COMPARATIVE BIOLOGY*, 42(1):149–157, 2002.

[37] RJ FULL and MS TU. Mechanics of a rapid running insect - 2-legged, 4-legged and 6-legged locomotion. *JOURNAL OF EXPERIMENTAL BIOLOGY*, 156(AR):215–231, 1991.

[38] J. C. Gallagher, R. D. Beer, K. S. Espenschied, and R. D. Quinn. Application of evolved locomotion controllers to a hexapod robot. *Robotics and Autonomous Systems*, 19(1):95–103, 1996.

[39] E. Garcia, J. Estremera, and P. Gonzalez de Santos. A comparative study of stability margins for walking machines. *Robotica*, 20(6):595–606, 2002.

[40] M Garcia, A Chatterjee, A Ruina, and M Coleman. The simplest walking model: Stability, complexity, and scaling. *JOURNAL OF BIOMECHANICAL ENGINEERING-TRANSACTIONS OF THE ASME*, 120(2):281–288, 1998.

[41] M Garcia, AD Kuo, AM Peattie, PC Wang, and RJ Full. Damping and size: Insights and biological inspiration. In *International Symposium on Adaptive Motion of Animals and Machines*, Montreal, Canada, 2000.

[42] A Goswami, B Thuilot, and B Espiau. A study of the passive gait of a compass-like biped robot: Symmetry and chaos. *INTERNATIONAL JOURNAL OF ROBOTICS RESEARCH*, 17(12):1282–1301, 1998.

[43] Ambarish Goswami. Postural stability of biped robots and the foot-rotation indicator (fri) point. *International Journal of Robotics Research*, 18(6):523–533, 1999.

[44] Jesse W. Grizzle, Gabriel Abba, and Franck Plestan. Asymptotically stable walking for biped robots: Analysis via systems with impulse effects. *IEEE Transactions on Automatic Control*, 46(1):51–64, 2001.

[45] K. Hirai, M. Hirose, H. Haikawa, and Takenaka T. The development of the honda humanoid robot. In *IEEE International Conference on Robotics and Automation*, 1998.

[46] S. Hirose, H. Tsukagoshi, and K. Yoneda. Normalized energy stability maring: Generalized stability criterion for walking vehicles. In *Climbing and Walking Robots (CLAWAR 1998)*, pages 71–76, Brussels, 1998.

[47] S. Hirose, K. Yoneda, and H. Tsukagoshi. Titan vii: Quadruped walking and manipulating robot on a steep slope. In *Proceedings - IEEE International Conference on Robotics and Automation*, Albuquerque, New Mexico, 1997.

[48] J. Hodgins and M. H. Raibert. Biped gymnastics. *International Journal of Robotics Research*, 9(2):115–132, 1990.

[49] N. Hogan. Impedance control: an approach to manipulation. i. theory. *Transactions of the ASME. Journal of Dynamic Systems, Measurement and Control*, 107(1):1–7, 1985.

[50] Larry L. Howell. *Compliant Mechanisms*. Wiley, New York, 2001.

[51] Jianjuen Hu, Jerry Pratt, and Gill Pratt. Stable adaptive control of a bipedal walking robot with cmac neural networks. In *Proceedings - IEEE International Conference on Robotics and Automation*, volume 2, pages 1050–1056, 1999.

[52] DL Jindrich and RJ Full. Many-legged maneuverability: Dynamics of turning in hexapods. *Journal of Experimental Biology*, 202(12):1603–1623, 1999.

[53] DL Jindrich and RJ Full. Dynamic stabilization of rapid hexapedal locomotion. *JOURNAL OF EXPERIMENTAL BIOLOGY*, 205(18):2803–2823, 2002.

[54] D. Kang, Y. Lee, S. Lee, Y. Hong, and Z. Bien. A study on an adaptive gait for a quadruped walking robot under external forces. In *IEEE Interternational Conference on Robotics and Automation*, pages 2777–2782, Albuquerque, NM, 1997.

[55] S Kim, J. E. Clark, and M. R. Cutkosky. isprawl: Autonomy, and the effects of power transmission. In *International Conference on Climbing and Walking Robots (CLAWAR)*, volume 7. Professional Engineering Publishing, Madrid, Spain, 2004.

[56] Bernhard Klaassen, Ralf Linnemann, Dirk Spenneberg, and Frank Kirchner. Biomimetic walking robot scorpion: Control and modeling. In *Proceedings of the ASME Design Engineering Technical Conference*, volume 5, pages 1105–1112, 2002.

[57] D Kodistchek and M Buehler. Analysis of a simplified hopping robot. *International Journal of Robotics Research*, 10(6):587–605, 1991.

[58] H. Komsuoglu, D. McMordie, U. Saranli, N. Moore, M. Buehler, and D. E. Koditschek. Proprioception based behavioral advances in a hexapod robot. In *Proceedings - IEEE International Conference on Robotics and Automation*, volume 4, pages 3650–3655, 2001.

[59] TM Kubow and RJ Full. The role of the mechanical system in control: a hypothesis of self-stabilization in hexapedal runners. *Philosophical Transactions of the Royal Society of London Series B-Biological Sciences*, 354(1385):849–861, 1999.

[60] V KUMAR and KJ WALDRON. Force distribution in walking vehicles. *JOURNAL OF MECHANICAL DESIGN*, 112(1):90–99, 1990.

[61] A. D. Kuo. Stabilization of lateral motion in passive dynamic walking. *International Journal of Robotics Research*, 18(9):917–930, 1999.

[62] C. Locke. Pushing the envelope: Space telerobotics at carnegie mellon university. *IEEE Expert*, 5(3):2–6, 1990.

[63] D. W. Marhefka, D. E. Orin, J. P. Schmiedeler, and K. J. Waldron. Intelligent control of quadruped gallops. *IEEE/ASME Transactions on Mechatronics*, 8(4):446–456, 2003.

[64] A. J. McClung, J. G. Cham, and M. R. Cutkosky. Dynamic maneuvering of a biologically inspired hexapedal robot. In *ASME IMECE Proceedings*, 2004.

[65] Tad McGeer. Passive dynamic walking. *International Journal of Robotics Research*, 9(2):62–82, 1990.

[66] R. B. McGhee and A. A. Frank. On the stability properties of quadruped creeping gaits. *Mathematical Bioscience*, 3:331–351, 1968.

[67] T. A. McMahon. Mechanics of locomotion. *International Journal of Robotics Research*, 3(2):4–28, 1984.

[68] T. A MCMahon and G. C. Cheng. Mechanics of running. how does stiffness couple with speed? *Journal of Biomechanics*, 23(1):65–78, 1990.

[69] K. Meijer and R. J. Full. Stabilizing properties of invertebrate skeletal muscle. *American Zoologist*, 39, 1999.

[70] R. Merz, Prinz. F. B., K. Ramaswami, M. Terk, and L. E. Weiss. Shape deposition manufacturing. In *Proceedings of the Solid Freeform Fabrication Symposium*, University of Texas at Austin, 1994.

[71] D. A. Messuri and C. A. Klein. Automatic body regulation for maintaining stability of a legged vehicle during rough-terrain locomotion. *IEEE Journal of Robotics and Automation*, RA-1(3):132–141, 1985.

[72] K. D. Mombaur. *Stability Optimization of Open-loop Controlled Walking Robots*. PhD thesis, Universitaet Heidelberg, 2001.

[73] E. Z. Moore, D. Campbell, F. Grimminger, and M. Buehler. Reliable stair climbing in the simple hexapod 'rhex'. In *Proceedings - IEEE International Conference on Robotics and Automation*, volume 3, pages 2222–2227, 2002.

[74] Adam Morecki and Kenneth J. Waldron. *Human and machine locomotion*. Springer, Wien ; New York, 1997.

[75] R. S. Mosher. Versatile walking truck. In *ASME - Transportation Eng Conference*, Washington D.C., 1968.

[76] J. G. Nichol, L. R. Palmer, and K. J. Waldron. Design of a leg system for quadruped gallop. In Tian Huang, editor, *World Congress in Mechanism adn Machine Science*, Tianjin, China, 2003. China Machinery Press.

[77] H. Ohta, M. Yamakita, and K. Furuta. From passive to active dynamic walking. *International Journal of Robust and Nonlinear Control*, 11(3):287–303, 2001.

[78] K Ono and R Takahashi. Self-excited walking of a biped mechanism. *International Journal of Robotics Research*, 20(12):953–966, 2001.

[79] D. E. Orin. *Interactive Control of a Six-Legged Vehicle with optimization of both stability and energy*. PhD thesis, The Ohio State University, 1976.

[80] K. Osuka, Y. Saruta, and K. Kirihara. Development and control of new legged robot quartet iii - from active walking to passive walking. In *IEEE International Conference on Intelligent Robots and Systems*, volume 2, pages 991–995, 2000.

[81] F. Pfeiffer, J. Eltze, and Weidemann, editors. *The TUM Walking Machine*. Intelligent Automation and Soft Computing 2. TSI Press, Albuquerque, NM, 1994.

[82] I. Poulakakis, J. A. Smith, and M. Buehler. On the dynamics of bounding and extensions towards the half-bound and the gallop gaits. In *International Symposium on Adaptive motion of Animals and Machines (AMAM)*, Kyoto, Japan, 2003.

[83] Jerry Pratt, Chee-Meng Chew, Ann Torres, Peter Dilworth, and Gill Pratt. Virtual model control: an intuitive approach for bipedal locomotion. *International Journal of Robotics Research*, 20(2):129–143, 2001.

[84] Jerry Pratt and Gill Pratt. Intuitive control of a planar bipedal walking robot. In *Proceedings - IEEE International Conference on Robotics and Automation*, volume 3, pages 2014–2021, 1998.

[85] RD Quinn, GM Nelson, RJ Bachmann, DA Kingsley, JT Offi, TJ Allen, and RE Ritzmann. Parallel complementary strategies for implementing biological principles into mobile robots. *International Journal of Robotics Research*, 22(3/4):169–86, 2003.

[86] M. H. Raibert. Trotting, pacing, and bounding by a quadruped robot. *Journal of Biomechanics*, 1991.

[87] Marc H. Raibert. *Legged robots that balance*. MIT Press series in artificial intelligence. MIT Press, Cambridge, Mass., 1986.

[88] Robert Ringrose. Self-stabilizing running. In *Proceedings - IEEE International Conference on Robotics and Automation*, volume 1, pages 487–493, 1997.

[89] M. E. Rosheim. *Robot Evolution: The development of Anthrobotics*. Wiley-Interscience, New York, NY, 1994.

[90] U. Saranli. *Dynamic Locomotion with a Hexapod Robot*. PhD thesis, The University of Michigan, 2002.

[91] Uluc Saranli, Martin Buehler, and Daniel E. Koditschek. Design, modeling and preliminary control of a compliant hexapod robot. In *Proceedings - IEEE International Conference on Robotics and Automation*, volume 3, pages 2589–2596, 2000.

[92] Uluc Saranli, Martin Buehler, and Daniel E. Koditschek. Rhex: A simple and highly mobile hexapod robot. *International Journal of Robotics Research*, 20(7):616–631, 2001.

[93] Uluc Saranli and Daniel E. Koditschek. Back flips with a hexapedal robot. In *Proceedings - IEEE International Conference on Robotics and Automation*, volume 3, pages 2209–2215, 2002.

[94] S. Sastry. *Nonlinear Systems: Analysis, Stability and Control*. Springer Verlag, 1999.

[95] S. Schaal, D. Sternad, and C. G. Atkeson. One-handed juggling: A dynamic approach to a rhythmic movement task. *Journal of Motor Behavior*, 28(2):165–183, 1996.

[96] J Schmitt and P Holmes. Mechanical models for insect locomotion: Dynamics and stability in the horizontal plane i. theory. *Biological Cybernetics*, 83(6):501–515, 2000.

[97] Shin-Min Song and Kenneth J. Waldron. *Machines that walk : the adaptive suspension vehicle*. MIT Press series in artificial intelligence. MIT Press, Cambridge, Mass., 1989.

[98] G. Taga. A model of the neuro-musculo-skeletal system for human locomotion ii. real-time adaptability under various constraints. *Biological Cybernetics*, 73(2):113–121, 1995.

[99] LH TING, R BLICKHAN, and RJ FULL. Dynamic and static stability in hexapedal runners. *JOURNAL OF EXPERIMENTAL BIOLOGY*, 197:251–269, 1994.

[100] S. Vogel. Better bent than broken. *Discover*, 16(5):62–67, May 1995.

[101] M. Vukobratovic, A. A. Frank, and D. Juricic. On the stability of biped locomotin. *IEEE Trans Bio-Med Eng*, 17(1):25–36, 1970.

[102] KJ Waldron. Force and motion management in legged locomotion. *IEEE Journal of Robotics and Automation*, RA/2(4):214–20, 1986.

[103] E. R. Westervelt and J. W. Grizzle. Design of asymptotically stable walking for a 5-link planar biped walker via optimization. In *Proceedings IEEE International Conference on Robotics and Automation*, volume 3, pages 3117–3122, 2002.

[104] E. R. Westervelt, J. W. Grizzle, and D. E. Koditschek. Hybrid zero dynamics of planar biped walkers. In *IEEE Transactions on Automatic Control*, volume 48, pages 42–56, 2003.

[105] X. Xu, W. Cheng, DM Dudek, M. Hatanaka, M. R. Cutkosky, and RJ Full. Material modeling for shape deposition manufacturing of biomimetic componentsd, September 10-14 2000.

[106] C. Zhang and S. Song. Gaits and geometry of a walking chiar for the disabled. *Journal of Terramechanics*, 26(3):211–233, 1989.

[107] F Zonfrilli, G. Oriolo, and D. Nardi. A biped locomotion strategy for the quadruped robot sony ers-210. In *IEEE International Conference on Robotics and Automation*, pages 2768–2774, 2002.